# AMMONIUM RICH WASTEWATER TREATMENT AND VALUE ADDITION USING MICROALGAE-BACTERIAL CONSORTIA IN PHOTO-ACTIVATED SYSTEMS

*A Thesis*

*Submitted in partial fulfilment of the requirements for*

*the award of the degree of*

**DOCTOR OF PHILOSOPHY**

*by*

**ARUN S**

**DEPARTMENT OF BIOSCIENCES AND BIOENGINEERING**

**INDIAN INSTITUTE OF TECHNOLOGY GUWAHATI**

**GUWAHATI-781039, ASSAM, INDIA**

**JUNE 2021**

*Dedicated to my family*

# INDIAN INSTITUTE OF TECHNOLOGY GUWAHATI

## DEPARTMENT OF BIOSCIENCES AND BIOENGINEERING

## DECLARATION

I, here declare that the content embodied in this thesis entitled **‘‘Ammonium rich wastewater treatment and value addition using microalgae-bacterial consortia in photo-activated systems’’** is the result of investigations carried out by me at Department of Biosciences and Bioengineering, Indian Institute of Technology Guwahati, Guwahati, India, under the supervision of Prof. Kannan Pakshirajan.

In keeping with the general practice of reporting scientific observations, due acknowledgements have been made wherever the work described is based on the findings other investigations

Date: **Arun S**

Place: IIT Guwahati

**INDIAN INSTITUTE OF TECHNOLOGY GUWAHATI**

**DEPARTMENT OF BIOSCIENCES AND BIOENGINEERING**

# CERTIFICATE

It is certified that the work described in this entitled **''Ammonium rich wastewater treatment and value addition using microalgae-bacterial consortia in photo-activated systems''** by **Arun S** for the award of degree of Doctor of Philosophy is an authentic record of the results obtained from the research work carried out under the supervision in the Department of Biosciences and Bioengineering, Indian Institute of Technology Guwahati, Guwahati, India, and this work has not been submitted either in whole or in part elsewhere for a degree.

Date:

Place: IIT Guwahati

_____

(Signature of Thesis Supervisor)

**Prof. Kannan Pakshirajan**

Professor

Department of Biosciences and Bioengineering

Indian Institute of Technology Guwahati

Guwahati-781039, Assam, India

# ACKNOWLEDGEMENTS

*First and foremost, I would like to thank Lord Jesus Christ for giving me the strength, knowledge, ability and opportunity to undertake this work and to preserve and complete it satisfactory. Without his blessings, this achievement would not have been possible.*

*In this journey towards this degree, I have found a teacher, an inspiration, a role model and a pillar of support in my supervisor, Prof. Kannan Pakshirajan, Department of Biosciences and Bioengineering IIT Guwahati. Without his able guidance, this thesis would have not been possible and I shall eternally be grateful to him for his assistance.*

*I take this opportunity to express my gratitude to my Doctoral committee members, Prof. G. Pugazhenthi, Dr. Senthilkumar Sivaprakasam and Dr. Soumen Kumar Maiti for their constructive criticism and precious suggestions throughout his work.*

*I extend my gratitude to the Department of Biosciences and Bioengineering, Centre for the Environment, Department of Chemical Engineering, Centre for Energy and Central Instruments Facility, IIT Guwahati for providing technical and instrumental support to this work. I also take this opportunity to thank all the non-teaching staff and teaching assistants who helped in different instrumentations. I would gratefully acknowledge the fellowship provided to me by UGC during all these years and Government of India for funding this work.*

*I am grateful to all my former, current lab mates and my friends Dr. Vibha Sinha, Dr. Madhavi Singh, Dr. M. Gopi Kiran, Dr. Arindam Sinha Roy, Dr. Lalit Goswami, Dr. Arvind Kumar Shakya, Dr. M.M. Tejas Namboodiri, Madu Purnima, Surjith Ramasamy, Dr. Arul Manikandan, Anil kumar, Muthuvel, Krishna Kumar, Tanushree Paul, Manoj Kumar, Dipak Kumar Kanaujiya, Sudeshna Saikia, Dr. V. Divyabaskaran, Bharat Bhushan Negi, Ajay Kumar*

***P V, SVG Kumari, Kakali priyam Goswami and Selvanayagai for their help and support during my research work. At last but not the least, I am thankful to my family and friends for their patience, understanding and encouragement. This would not have been possible without their unwavering and unconditional love and support given to me at all times for which I shall ever remain indebted.***

**June 2021** **Arun S**

**IIT Guwahati**

CONTENTS

**Page No.**

## List of Figures

## List of Tables

**Abbreviations**

BNR: Biological nitrogen removal

ARWW: Ammonium rich wastewater

AOB: Ammonia oxidizing bacteria

NOB: Nitrite oxidizing bacteria

MUD: Methanol utilizing denitrifier

SNR: shortcut nitrogen removal

PSBR: Photo-sequencing batch reactor

PBR: Photobioreactor

Anammox: Anaerobic ammonium oxidation

WWTP: Wastewater treatment plants

SVI: Sludge volume index

TSS: Total suspended solids

VSS: Volatile suspended solids

ADL: Anaerobic digestion liquor

HRT: Hydraulic retention time

SRT: Sludge retention time

AMO: Ammonia monooxygenase

NIR: Nitrite reductase

NOR: Nitrite oxidoreductase

NR: Nitrate reductase

STP: Sewage treatment plants

GC: Gas Chromatography

FID: Flame ionization detector

SOUR: Specific oxygen uptake rate

SOPR: Specific oxygen production rate

DALI: Daily average light intensity

MFC: Microbial fuel cell

MPMFC: Membrane photosynthetic microbial fuel cell

PMFC: Photosynthetic microbial fuel cell

CV: Cyclic voltammetry

SNAD-MFC: Shortcut nitrification and autotrophic denitrification (anoxic cathode) MFC

IEM: Ion exchange membrane

FESEM: Field emission scanning electron microscopy

SBR: Sequencing batch reactor

DO: DO concentration

**Nomenclature**

$b_{AOB}$: Respiration rate constant for AOB

$Y_{AOB}$: Aerobic yield of AOB

$b_A$: Algae decay

$K_{IA}$: Half saturation constant for algae growth on I

$\mu_{max, A}$: Maximum specific growth rate of algae

k: Ammonium removal rate

$\mu_{max, AOB}$: Maximum specific growth rate of AOB

$\mu_{max, NOB}$: Maximum specific growth rate of AOB

$S_{o2}$: Saturation concentration for $O_2$ in water

$b_H$: Aerobic endogenous respiration rate for heterotrophs

$b_{NOB}$: Respiration rate constant for NOB

$\mathbf{Y_{NH_4}}$: Algal growth yield on ammonium

$\mathbf{Y_{O_2}}$: Oxygen production yield by algae

$\mathbf{K_{NH_4,A}}$: Saturation constant for ammonium

$\mathbf{K_{O_2,AOB}}$: Saturation constant for $\mathbf{S_{O_2}}$

I: Light intensity

$X_A$: Biomass concentration

$\mathbf{i_{N,BM}}$: N content of bacterial biomass

$\mathbf{K_{O_2,NOB}}$: Saturation constant for $S_{O_2}$ for NOB

$\boldsymbol{\eta_H}$: Anoxic reduction factor for heterotrophs

$K_{NH_4,H}$: Saturation constant for $S_{NH_4}$ for heterotrophs

$K_L a_{o2}$: Mass transfer coefficient of $O_2$

# Chapter 1

# Introduction

## 1.1 Introduction

Environmental pollution and energy crisis are emphasized to be one of the major global problems in the recent years. Over the past centuries, rapid increase in urbanization and industrial revolution has resulted in severe environmental pollution, health problems and energy crisis (Thomas et al., 2017; Sarvajith et al., 2018; Wang at al., 2016). Therefore, greatest challenge for the researchers is to find the alternative methods to reduce environmental pollution and sustainable energy production. Hence, bioelectricity production and processes using sustainable resources by mitigating nitrogen pollution have gained recent interest. This study, therefore, focused on biological nitrogen removal by microalgae-bacterial consortia and its applications in microbial fuel cell for bioelectricity production.

Although ammonia is toxic to many aquatic life, it is an excellent substrate for ammonia oxidizing bacteria and microalgae, such as *Nitrosomonas*, *Chlorella sp.*, *Chlamydomonas*, *Stichococcus*, *Ankistrodesmus* and *Scenedesmus sp.* etc. The conventional method for ammonium removal is activated sludge process, which utilizes aeration for oxidation of ammonium via nitrification and denitrification (Wang et al., 2015; Karya et al., 2013). The oxidation (nitrification) and reduction (denitrification) reactions are the basis for most of the domestic and industrial wastewater treatment of ammonium by conventional activated sludge process (Wang et al., 2015; Karya et al., 2013). Although the conventional process serves as a potential method with high removal rate, the process has its own disadvantages such as very high operating cost due to mechanical aeration, external carbon source addition for nitrification and denitrification, restricted choice of ammonium uptake by bacterial biomass, high energy requirement due to continuous

aeration, etc. (Manser et al. 2016; Wang et al., 2015). Due to these disadvantages, cost-effective and sustainable methods for ammonium removal from wastewater are the needs of the hour.

Also, from economic and environmental point of view, ammonium removal by microalgae-bacterial consortia are of great interest. Over the last decade various microalgae-bacterial consortia capable of efficient ammonium removal have been reported (Karya et al., 2013). These microalgae-bacterial consortia are not only able to grow autotrophically on ammonium but also offer advantages in term of high N affinity, anoxic zone for denitrification, algal photosynthesis, shortcut nitrogen removal, well settled biomass with high settling velocity and energy production (Wang et al., 2105). Among these advantages, microalgal photosynthesis is attractive as it potentially provides $O_2$ for nitrification and bioelectricity production (Wang et al., 2013; Wang et al., 2015). As oxygen production by microalgae is high, ammonium removal using oxygen produced by microalgal photosynthesis does not need any external aeration. On the other hand, use of oxygen in microbial fuel cell where $O_2$ and electron combines to produce bioelectricity makes its application more innovative (Wang et al., 2013). However, microbial fuel cell is not economic as compared with other renewable energy resources due to high electrode cost, reduced MFC performance and doubtful reliability.

Another less explored application of biological nitrogen removal is ammonium removal by microalgae-bacterial consortia, where $O_2$ produced from the microalgae can directly be utilized as electron acceptor by ammonium oxidizing bacteria (AOB) and nitrite oxidizing bacteria (NOB). Ammonium rich wastewater generated by different industries, such as food processing industry, fertilizer industry, tannery, dairy, etc. are generally high in ammonium content (Manser et al., 2016; Wang et al., 2015). Hence, an efficient method is necessary to enable the complete treatment of ammonium rich wastewater. Over the past decade, a lot of research has been undertaken to

establish an efficient and sustainable method for treatment of ammonium rich wastewater (Akizuki et al., 2020). Many types of microalgae-bacterial consortia including microalgae-nitrifier, microalgae-nitrifier-denitrifier and microalgae-AOB-anammox consortia have been examined for ammonium removal (Akizuki et al., 2020; Karya et al., 2013; Manser et al., 2016; Wang et al., 2015). Ammonium removal efficiency for the reactor system operating with the consortium depends on the type of bacteria, microalgae and their interaction with each under different operating conditions. Besides, their use may result in reduction of ammonium removal efficiency and this would require an additional treatment (Wang et al., 2020).

Successful application of BNR by microalgae-bacterial consortia implies the need to minimize undesired $NO_3$ production by NOB (Wang et al., 2015). For practical applications, therefore, oxygen production combined with nitrification process, such as for BNR by microalgae-bacterial consortia, might result in maximal utilization of oxygen, provided the AOB can outcompete the NOB (Wang et al., 2015). Only problem with this method seems to be $O_2$ availability at a high ammonium concentration. However, several consortia of microalgae and bacteria have been recently reported to use ammonium as the substrate for BNR without any external aeration (Karya et al., 2013; Wang et al., 2015; Manser et al., 2016).

Most of these microalgae-bacterial consortia (AOB and NOB) are light sensitive (Manser et al., 2016; Wang et al., 2015) and, therefore, optimum light intensity is required to maintain suitable environmental condition, which makes the process more efficient and its commercialization Moreover, it is reported that microalgae-bacterial consortia compared to pure AOB and NOB culture are better in terms of ammonium removal and light inhibition to AOB and NOB. The poor settleability of algal biomass is also a major concern as it limits its harvesting efficiency.

Hence, there is a need to explore microalgae-bacterial consortia capable of ammonium removal, which can oxidize ammonium as well as reduce nitrite or nitrate present in wastewater utilizing the *in-situ* produced $O_2$. Also, the effect of different process parameters, such as initial ammonium concentration, pH, light intensity, etc. on ammonium removal using microalgae-bacterial consortia and energy production in MFC should be evaluated in detail. The ammonium removal enhancement strategies also need to be looked into for achieving a high process efficiency (ammonium uptake by microalgae and ammonium removal by BNR). Moreover, to study the scale up potential of this process, suitable photobioreactor system with optimum process conditions needs to be evaluated.

### 1.2 Aim and objectives

This study was aimed at biological nitrogen removal by microalgae-bacteria consortia using a photo-sequencing batch reactor and its application in microbial fuel cell.

In order to accomplish this aim, the following objectives were framed:

i. Process parameter optimization and kinetic modelling of shortcut nitrogen removal by microalgae-bacterial consortium

ii. Effect of light intensity on nitrification by microalgae-nitrifying bacteria consortium in a photosequencing batch reactor

iii. Effect of different nitrogen sources on nitrification by microalgae-nitrifying bacteria consortium

iv. Shortcut nitrogen removal and bioelectricity production using an integrated membrane photosynthetic microbial fuel cell

## 1.3 Organization of thesis

The present work has been divided into seven chapters. The first chapter gives a general introduction, aim and objectives of this work. Chapter 2 presents the available literature on biological nitrogen removal by microalgae-bacterial consortia and characterization of microalgae-bacterial consortia, conventional methods for biological nitrogen removal and different applications of microalgae-bacterial biomass, photobioreactor design for ammonium removal, effect of various process parameters, methods to enhance microalgae-bacterial biomass harvesting. In Chapter 3, details on screening of microalgae-bacterial consortia for efficient ammonium removal, elucidation of ammonium removal pathway, effect of various process parameters (pH, DO and ammonium concentration) on ammonium removal in photo sequencing batch reactor, analysis of the microalgae biomass are reported. Effect of light intensity on ammonium removal by microalgae-bacterial consortia in a photosequencing batch reactor and $O_2$ requirement for nitrification, $O_2$ production by microalgae, and its effect on ammonium removal are detailed in Chapter 4. In Chapter 5, the effect of different nitrogen sources on ammonium removal, PSBR performance and data validation on ammonium removal pathway are described. Chapter 6 presents the results of the shortcut nitrogen removal and bioelectricity production by microalgae-bacterial consortia using an integrated microbial fuel cell. The effect of different nitrogen source and light/dark period on MFC performance are also discussed in this chapter. Chapter 7 draws summary and suitable conclusions based on the previous chapters. This chapter also provides some useful recommendations for future research in the relevant area.

# Chapter 2

# Literature review

## 2.1 Microalgae-bacterial consortia for biological nitrogen removal (BNR)

### 2.1.1 Microalgae-bacterial microbiome

The mechanism of biological nitrogen removal (BNR) from ammonium rich wastewater (ARWW) using microalgae-bacterial processes is analogous to that employed in the activated sludge process, but in the absence of external aeration (Fig. 2.1). Microalgae such as *Chlorella sp.*, *Chlamydomonas sp, Stichococcus sp*, *Ankistrodesmus sp* and *Scenedesmus sp.* along with the bacteria *Nitrosomonas* (ammonia oxidizing bacteria ), *Nitrobacter sp* (nitrite oxidizing bacteria), denitrifying bacteria or anammox bacteria have been used to effectively remove nitrogen from high strength $NH_4^+$ wastewater (De Godos et al., 2009; Karya et al., 2013; Wang et al., 2015; Rada-Ariza et al., 2017; Munoz and Guieysse, 2006; Manser et al., 2015; Van der steen et al., 2015).

Consortia of microalgae with AOB, NOB, denitrifiers and anammox bacteria can play an important role during the biological removal of ammonium, nitrite and nitrate from wastewater in photobioreactors (PBR). An increase in the removal of ammonium, nitrite and nitrate (Table 2.1) is achieved due to $O_2$ produced through algal photosynthesis during the light period (high DO level), followed by nitrite or nitrate reduction during the dark period (low DO level) by denitrifiers and anammox (Fig. 2.1). The oxygen production by algal photosynthesis is attractive as it reduces the operation cost and overcomes the disadvantages with mechanical aeration and poor biomass settling in a conventional activated sludge process. Microalgal-bacterial consortia can support anoxic reduction (de-nitrification) of nitrite and nitrate (Karya et al., 2013; De Godos et al., 2014). However, denitrifiers and anammox bacteria in the microalgae-bacterial consortia are sensitive to high light intensities and DO levels, thereby affecting the process efficiency (Caicedo et al., 2000).

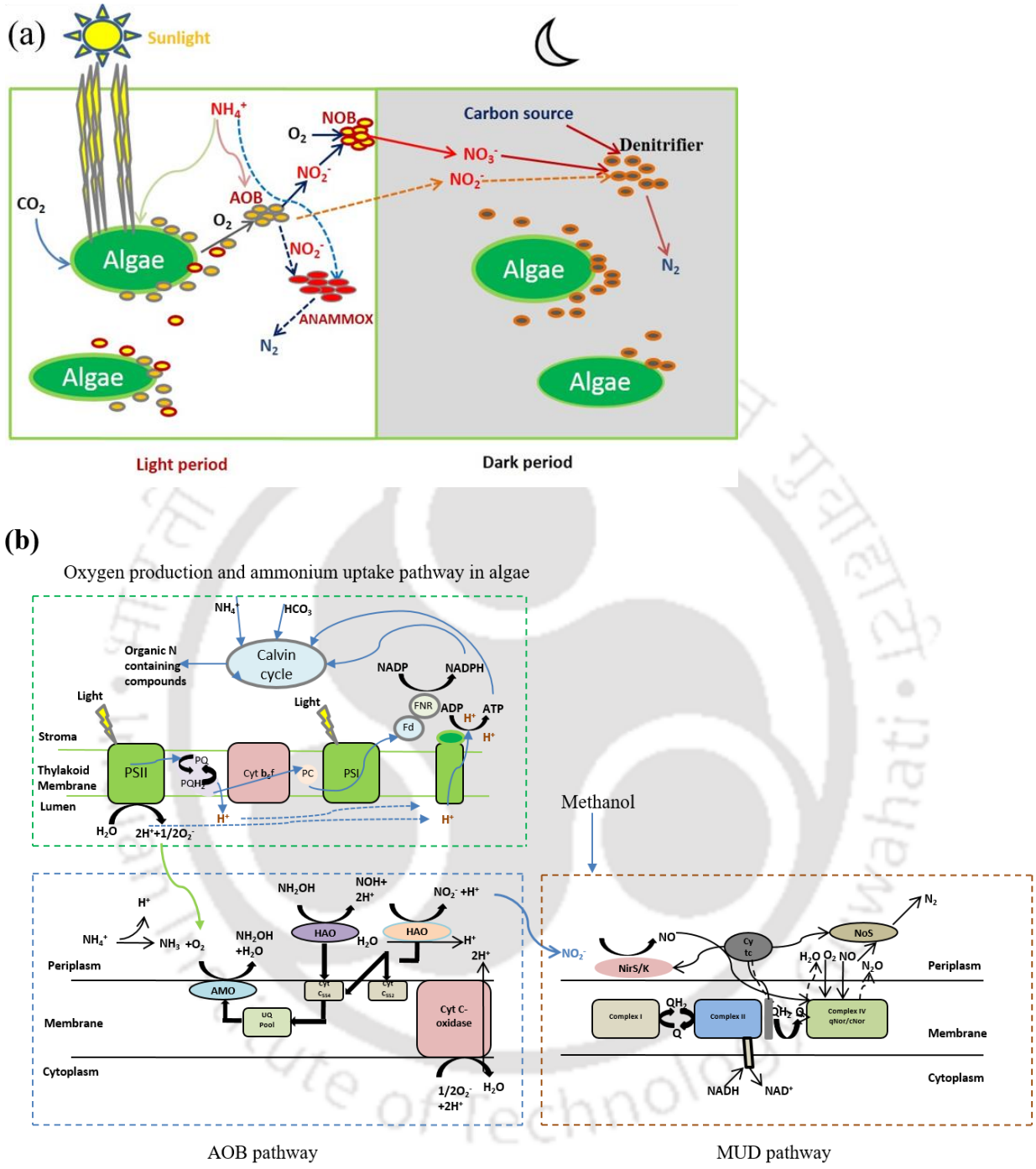


**Fig. 2.1** Mechanism (a) and pathway (b) involved in BNR by microalgae-bacterial (AOB and denitrifier) consortia

**Table 2.1** Major applications of various microalgal-bacterial consortia in BNR process

| Consortia | Application | Salient results | References |
|---|---|---|---|
| Microalgae-AOB-NOB consortium. | Removal of ammonium from synthetic wastewater containing 50 mg $NH_4^+$ -N/L | ➢ Maximum nitrification rate of 7.7 mg $NH_4^+$ -N/L h without mechanical aeration<br>➢ Ammonium removal by:<br>1. (81-85%) Nitrification<br>2. (19 -15%)Ammonium uptake by algae<br>➢ Oxygen production rate by algae - 0.46 kg/$m^3$ | Karya et al., 2013 |
| Microalgae-AOB-denitrifier consortium | Removal of ammonium from anaerobically digested swine waste concentrate containing 297 mg $NH_4^+$ -N/L | ➢ Maximum nitrification rate of g $NH_4^+$ -N/L h without mechanical aeration<br>1. Ammonium removal by: Denitrification (81.7%), Biomass uptake (18.3%)<br>➢ Algal photosynthesis<br>1. Volumetric oxygen production: 193 mg/L. d | Wang et al., 2015 |
| Algae-nitrifying bacterial consortia and anammox granules | Removal of ammonium from high strength ammonium wastewater (anaerobic digestion) | ➢ Photosequencing batch reactor phase (Algae-AOB consortia)<br>1. Ammonium removal rate of 4.3 mg of N/L. h<br>➢ Algammox phase<br>1. Maximum nitrification rate of 7.0 mg $NH_4^+$ -N/L. h<br>2. Nitrite reduction by anammox (82%) | Manser et al., 2016 |
| Microalgal-AOB-NOB consortium | Removal of ammonium from synthetic wastewater | ➢ Ammonium removal rates<br>1. 100± 18 mg $NH_4^+$ -N/L. d (microalgae-bacterial consortia)<br>2. 44 ± 16 mg $NH_4^+$ -N/L d (only microalgae) | Rada-Ariza et al., 2017 |
| Microalgal-AOB-NOB consortium | Synthetic wastewater | ➢ Total ammonium removal rate of 2.3 mg $NH_4^+$ -N/L. h<br>➢ Algal photosynthesis: 82% oxygen output<br>➢ Oxygen diffusion through mixed surface: 18% | Van der Steen et al., 2015 |

### 2.1.2 Ammonium oxidation through algal photosynthesis

Ammonium removal by microalgae was compared to that by using microalgae-bacterial (nitrifier) consortia for treating synthetic wastewater in a flat panel photo-bioreactor (Rada-Ariza et al., 2017). Ammonium was completely oxidized by the AOB and anammox, followed by reduction of nitrite or nitrate due to denitrification or uptake by microalgae under light and dark periods by consortia of microalgae-AOB-NOB-denitrifier/anammox with an excess of oxygen production as per the reactions presented in Table 2.2.

The microalgae-bacterial (nitrifier) consortia were capable of converting ammonium at a maximum rate of 7.7 mg $NH_4^+$-N L. h in an open PBR, which is comparable to an oxygenation capacity of 0.43 kg/$m^3$·d (Karya et al., 2013). The value is close to that observed using a high rate algal ponds (HRAP) (0.3-0.38 kg/$m^3$·d) (Grima et al., 1999) and slightly lower than that in an optimized PBR process (up to 8.3 kg/$m^3$·d) (Hu et al., 1996). Similarly, 132.7 mg/L. d of N was removed in a PSBR cultured with *Scedesmus* sp. and an AOB culture, which was more than the 50 mg/L of N removal obtained by Karya et al. (2013) using a photobioreactor or 7.0 mg/L·h of N removal obtained by Manser et al. (2015) using a photosequencing batch reactor (PSBR). These experiments demonstrated the potential benefits of microalgal-bacterial consortia in photo-bioreactors for the removal of ammonium rich wastewater. Conversely, certain limitations are known in microalgae-bacterial consortia, including sensitivity to varying concentrations of ammonium (Tam et al.,1996), high light intensity (Manser et al., 2015) and microalgae grow at a higher rate (Table 2.3) than AOB, NOB and denitrifiers (except anammox). Therefore, special care must be provided in choosing the microbial consortia and optimizing the process parameters.

**Table 2.2.** Nitrogen uptake by microalgae-bacterial consortia for BNR

| Process | | Metabolism | Stoichiometric equation | Reference |
|---|---|---|---|---|
| 1. Algae-nitrifier consortia for nitrification | Microalgal photosynthesis and ammonium uptake | Oxygen production by algae | $CO_2 + H_2O + \lambda_{photon} \rightarrow CH_2O + O_2$ | Karya et al., 2013 |
| | | Ammonium uptake by algae | $16NH_4^+ + 106CO_2 + 236H_2O + HPO_4^{2-} \rightarrow C_{106}H_{181}O_{45}N_{16}P + 118O_2 + 17\ H_2O + 14H^+$ | |
| | Nitrification | Ammonium oxidation by nitrifier | $NH_4^+ + 1.32NO_2^- + 1.98HCO_3^- + 0.98H_2O \rightarrow 0.021C_5H_7NO_2 + 0.98NO_3^- + 2.02H_2O + 1.88H_2CO_3$ | |
| 2. Shortcut nitrogen removal by algae-bacterial consortia | Microalgal photosynthesis and ammonium uptake | Oxygen production and ammonium uptake by algae | $CO_2 + H_2O + \lambda_{photon} \rightarrow CH_2O + O_2$<br>$NH_4^+ + 7.6CO_2 + 17.7H_2O \rightarrow C_{7.6}H_{8.1}O_{2.5}N + 7.6O_2 + 15.2\ H_2O + H^+$ | Wang et al., 2015] |
| | Nitritation | Ammonium oxidation by autotrophic AOB | $NH_4^+ + 1.24O_2 + 0.16CO_2 + 0.04HCO_3^- \rightarrow 0.04C_5H_7O_2N + 0.96NO_2^- + 0.96\ H_2O + 1.92H^+$ | |
| | Denitritation | Heterotrophic denitritation | $5CH_3COO^- + 8NO_2^- + 11H^+ \leftrightarrow 4N_2 + 5CO_2 + 10H_2$ | |
| 3. Algae-bacterial consortia for nitrification and denitrification | Microalgal photosynthesis and ammonium uptake | Oxygen production and ammonium uptake by algae | $CO_2 + H_2O + \lambda_{photon} \rightarrow CH_2O + O_2$<br>$NH_4^+ + 7.6CO_2 + 17.7H_2O \rightarrow C_{7.6}H_{8.1}O_{2.5}N + 7.6O_2 + 15.2\ H_2O + H^+$ | De Godos et al., 2009 |

| | | | | |
|---|---|---|---|---|
| | Nitrification | Ammonium and nitrite oxidation by autotrophic AOB and NOB | $NH_4^+ + 1.32NO_2^- + 1.98HCO_3^- + 0.98H_2O \rightarrow 0.021C_5H_7NO_2 + 0.98NO_3^- + 2.02H_2O + 1.88H_2CO_3$ | |
| | Denitritation | Heterotrophic denitrification | $5CH_3COO^- + 8NO_3^- + 13H^+ \leftrightarrow 4N_2 + 10CO_2 + 14H_2O$ | |
| 4. Algal anaerobic ammonium oxidation (ALGAMMOX) | Nitritation | Ammonium and nitrite oxidation by autotrophic AOB | $NH_4^+ + 1.24O_2 + 0.16CO_2 + 0.04HCO_3^- \rightarrow 0.04C_5H_7O_2N + 0.96NO_2^- + 0.96\ H_2O + 1.92H^+$ | Manser et al., 2015 |
| | Denitritation | Heterotrophic denitritation | $5CH_3COO^- + 8NO_2^- + 11H^+ \leftrightarrow 4N_2 + 5CO_2 + 10H_2O$ | |
| | Denitrification | Anaerobic ammonium oxidation (Anammox) | $NH_4^+ + 1.3NO_2^- + .04HCO_3^- + 0.1H^+ \rightarrow N_2 + 0.3NO_3^- + 0.1CH_2O_{0.5}N_{0.15} + 2H_2O$ | |

**Table 2.3:** Kinetic parameters and stoichiometric yield coefficient involved in BNR.

| Organisms | ($\mu_{max}$) $d^{-1}$ | | | $K_{donor}$ | | | $K_{acceptor}$ | | | Yield coefficient | | | References |
|---|---|---|---|---|---|---|---|---|---|---|---|---|---|
| | Min | Medium | max | Min | Medium | Max | Min | Medium | Max | Min | Medium | Max | |
| **AOB** | 0.28 | 0.735 | 2.2 | **g N $m^{-3}$** | | | **g $O_2$ $m^{-3}$** | | | **g COD/g N** | | | Blackburne et al., 2007; Plattes et al., 2007 |
| | | | | | | | | | | 0.15 | 0.165 | 0.18 | |
| | | | | 0.07 | 0.295 | 4.59 | 0.03 | 0.74 | 3 | **g VSS/g N** | | | |
| | | | | | | | | | | 0.05 | 0.072 | 0.29 | |
| **NOB** | 0.14 | 0.75 | 5.41 | **g N $m^{-3}$** | | | **g $O_2$ $m^{-3}$** | | | **g COD/g N** | | | Delgado Vela et al., 2015; Plattes et al., 2007 |
| | | | | 0.11 | 0.5 | 7.6 | 0.06 | 0.435 | 5.81 | 0.041 | 0.0605 | 0.08 | |
| | | | | | | | | | | **g VSS/g N** | | | |
| | | | | | | | | | | 0.02 | 0.084 | 0.14 | |
| **Denitrifier** | 0.69 | 5.4 | 12 | **g COD $m^{-3}$** | | | **g $NO_3^-$ $m^{-3}$** | | | **g COD/g COD** | | | Gujer et al., 1999; Iacopozzi et al., 2007 |
| | | | | 2 | 20 | 20 | 0.2 | 0.5 | 0.5 | 0.4 | 0.645 | 0.8 | |
| **Anammox bacteria** | 0.0073 | 0.1175 | 0.23 | **g N $m^{-3}$** | | | **g N $m^{-3}$** | | | **g COD/g N** | | | Delgado Vela et al., 2015; Pérez et al., 2014 |
| | | | | 0.03 | 7.42 | 36.45 | 0.002 | 2 | 21 | 0.048 | 0.159 | 0.17 | |
| **Microalgal-bacterial consortium** | 0.1 | 2 | 10.32* | **$K_{NH_4}$ (g N $m^{-3}$)** | | | **$K_{NO_3}$ (g N $m^{-3}$)** | | | **g COD/g N** | | | Delgado Vela et al., 2015; Pérez et al., 2014 |
| | | | | 0.0001 | 3.01 | 31.5 | 0.001 | 7.625 | 31.5 | 11.91* | 13.88* | 15.84* | |

**Maximum specific growth rate - $\mu_{max}$, half-saturation constants for electron donor - $K_{donor}$, and acceptor - $K_{acceptor}$)**, * Represents microalgal consortium

### 2.1.3 Oxidation of ammonium and nitrite through algal photosynthesis

External aeration accounts for more than 45%-75% of the total energy consumed in a conventional activated sludge process (Karya et al., 2015; Stenstrom and Rosso, 2008). Microalgal-bacterial consortia can thus significantly reduce the energy requirements for ammonium removal from wastewater by photosynthetic activity of microalgae for supplying the required $O_2$ to the AOB and NOB as depicted in Fig. 2.1. This symbiotic (microalgae, AOB, NOB, denitrifiers and anammox bacteria) relation can be applied for sustainable removal of nitrogenous pollutants from wastewater, which is further advantageous due to the reduced risk of ammonia release, commonly observed in algae based wastewater treatment processes due to the slow ammonium uptake by algae (Tam et al., 1996; Azoz and Goldman, 1982; Guo et al., 2016). For example, microalgae-bacterial (nitrifier) consortia were successfully used for the oxidation of synthetic wastewater by Karya et al. (2013). Similarly, microalgae-bacterial consortia were able to support ammonium oxidation by AOB, NOB and nitrite reduction by denitrifiers without any additional oxygen supply and with external addition of acetate as an organic carbon source for denitrification (Karya et al., 2013; Wang et al., 2015; Van der Steen et al., 2015; De Godos et al., 2014).

### 2.1.4 Ammonium oxidation coupled to denitrification

Microalgal-bacterial based methods are interesting as oxidation of nitrogen containing compounds reduces the oxygen concentration that is favorable for denitrification. For example, the total amount of oxygen consumed per mole of ammonium oxidized is reduced from 1.32 g $O_2$ in the nitrification process by microalgae-nitrifier consortia to 1.24 g $O_2$ in a short cut nitrogen removal process by mixed cultures of microalgae and AOB, which is attributed to the successful inhibition of NOB activity due to the low DO concentration in microalgal-bacterial consortium (Karya et al.

2013; Wang et al., 2015; Manser et al., 2015). The values were the same (1.24 g $O_2$) for the algammox (microalgae-AOB and anammox) process at a HRT of 4 d (Manser et al., 2015).

Microalgal-bacterial consortia contribute to denitritation/denitrification by creating anoxic zones in microalgae-bacterial flocs (Wang et al., 2015; Manser et al., 2015; De Godos et al., 2014). Wang et al. (2015) reported ammonium removal rates of 4.7 mg $L^{-1}$ $h^{-1}$ by nitritation and denitritation (108.5 mg $NH_4^+$-N $d^{-1}$) using consortia of microalgae-bacteria under light and dark conditions, which is close to the 5 mg $L^{-1}$ N $d^{-1}$ removal achieved using microalgae-AOB and anammox consortia (Manser et al., 2016). The applicability of ammonium removal by microalgae-bacterial consortia at a high $NH_4^+$ concentration (above 300 mg $NH_4^+$-N /L) remains a concern, which needs to be addressed further.

## 2.2 Complete nitrogen removal using microalgae and AOB-NOB-Denitrifiers-Anammox

### 2.2.1 Microalgae and nitrogen removing bacteria

The interactions among microalgae, nitrifiers and denitrifiers are not limited to a simple $CO_2/O_2$ and $NH_4^+/NO_2^-/NO_3^-$ exchange, but they can either have a positive or negative effect on nitrification or nitritation processes during the light period depending on several factors. For example, interaction of microalgae and bacteria leads to a decrease or increase in the pH in case of $HCO_3^-$ or $CO_2$ as the carbon source. Moreover, interaction of microalgae and bacteria is known to increase the dissolved oxygen (DO) production (Fig. 2.2). Besides, interaction of microalgae and bacteria can lead to the production of extra cellular polymeric substances (EPS), excretion of inhibitory metabolites, pH increase and reduction in DO concentration during the dark period (Munoz and Guieysse, 2006; Karya et al., 2015; Wang et al., 2015; Manser et al., 2016).

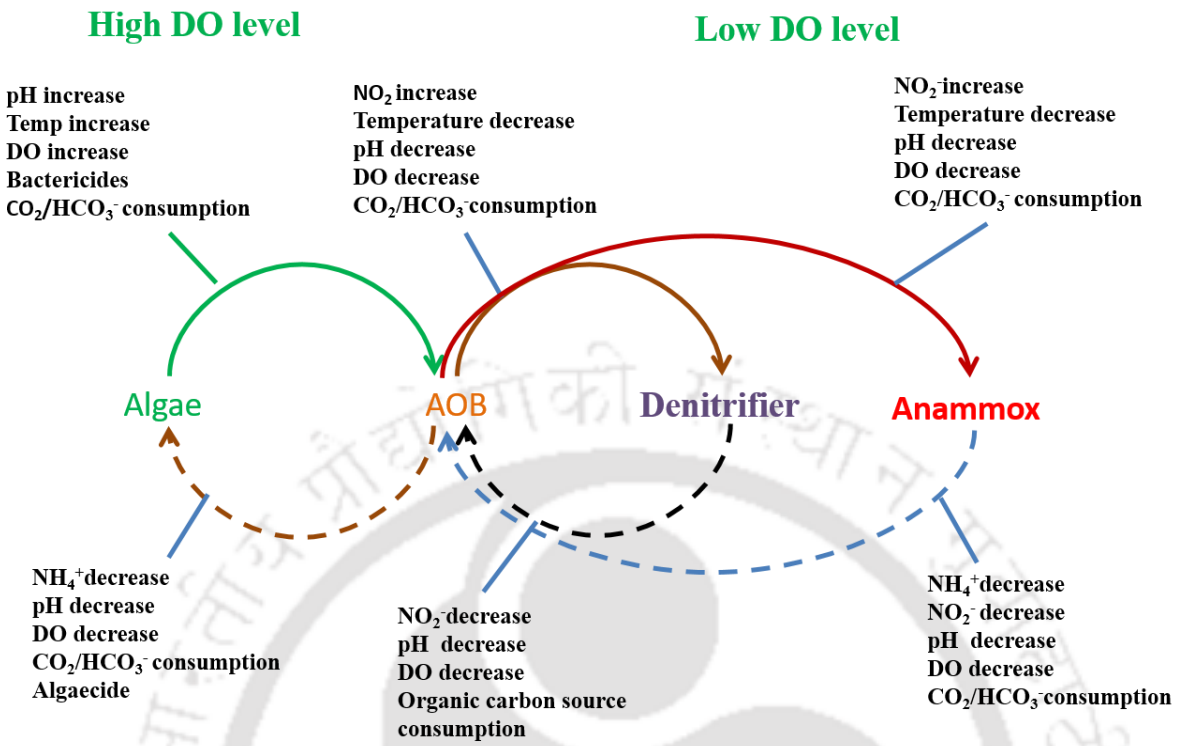


**Fig. 2.2** Interactions among microalgae, AOB, NOB, denitrifier and anammox bacteria for BNR

The creation of anoxic zones inside the microalgae-bacterial flocs leads to enhancement in denitrification or anammox activity by decreasing the DO level during the dark period. Wang et al. (2015) observed complete nitrogen removal by microalgae-bacterial consortia with externally added acetate. Likewise, AOB growth enhances anammox metabolism for ammonium oxidation by decreasing the DO level in the system, which inhibits anammox even at a DO level as low as 1.5. mg/L $O_2$ (Manser et al., 2016; Egli et al., 2001). Wang et al. (2015) also reported that AOB activity enhanced ammonium oxidation during the light period and reduction of nitrite or nitrate by denitrifiers during the dark period. Recent studies suggest that AOB and denitrifiers (Wang et al., 2015; Manser et al., 2016) attach to the surface of other microorganisms as revealed by FESEM images (Fig. 2.3).

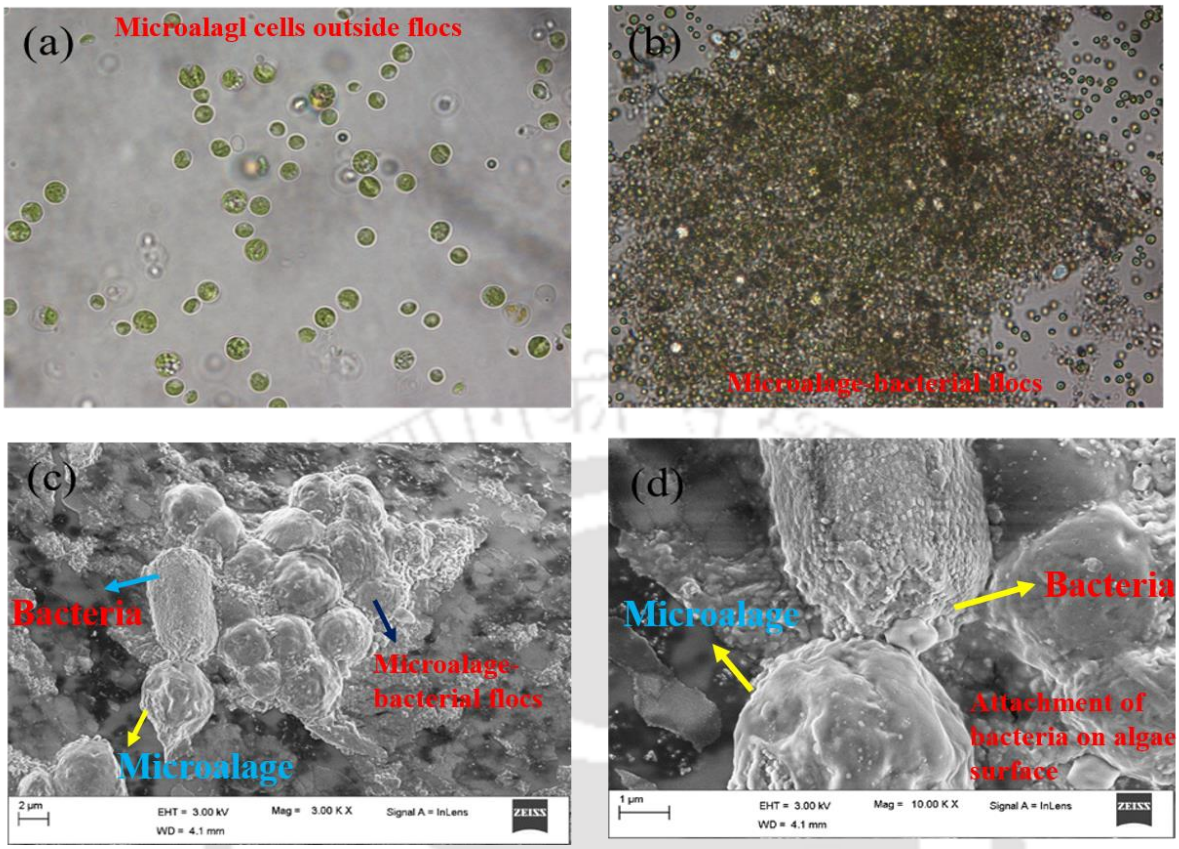


**Fig. 2.3** Microscopic (a - microalgal cells outside flocs and b - algae bacterial floc) and FESEM images showing interaction between microalgae and AOB (c) and attachment of bacteria on microalgae (d)

### 2.2.2. Inoculation

The symbiotic activity of microalgal-bacterial consortia affects the removal rate of nitrogen and hence, it is important to select the right combination of microalgae, AOB, NOB, denitrifiers and anammox (anoxic) in such systems. Slow growing anammox bacteria and microalgae are hardly used in continuous microalgae-bacteria based BNR systems (Manser at al., 2016). Some denitrifier species, e.g. *Paracoccus versutus* KS293, *Pseudomonas stutzeri* X31, *Enterobacter cloacae* HNR, *Pseudomonas tolaasii* Y-11, *Acinetobacter* sp. HA2, *Pseudomonas stutzeri* ZF31 or *Acinetobacter junii* YB are also highly resistant to DO (Guo et al., 2016; He et al., 2016; Huang et al., 2015; Ji et al., 2014; Ren et al., 2014; Zhang et al., 2019; Yao et al., 2013).

For an effective start-up of microalgae-bacterial consortia (nitrifier/denitrifier and anammox) in a PSBR for BNR from domestic wastewater, proper mixing of microalgae, nitrifiers and denitrifiers with the wastewater is important as it allows DO assimilation by AOB and NOB as well as formation of algae-bacterial flocs (Karya et al., 2013; Wang et al., 2015; Manser et al., 2016) or granules (Zhang et al., 2019; Zhang et al., 2020). Activated sludge or raw anaerobically digestated swine waste concentrate mixed with algae can be utilized as the inoculum. A different approach (only algae-AOB phase for reduction in DO concentration below 0.17 mg/L to support anammox activity) is used for anammox as a DO level above 1.5 mg/L $O_2$ inhibits the growth of anammox bacteria. The same strategy could be applied for treating high strength ammonium wastewater (COD/TN ratio), as it enables AOB, anammox bacteria and algae to interact with each other during the process.

### 2.3 Effect of environmental factors on BNR by microalgal-bacterial consortia

#### 2.3.1 Light supply

Light intensity (sunlight) significantly changes during the entire day and during the entire year. Maximum photosynthesis rate increases with a light intensity up to 400–1100 μmol photons/$m^2$ s in HRAPs. Microalgae-bacterial (AOB, NOB) activity increases with light intensity up to 500 μmol/$m^2$·s, above which nitrifying bacteria (Vergara et al., 2016) and photosynthetic activities (200–400 μE/$m^2$·s) become saturated in photobioreactors (Sutherland et al., 2015). Photoinhibition is, therefore, common during the mid-day period when light intensity can reach up to 4000 $\mu Em^{-2}s^{-1}$ (Vergara et al., 2016). Proper design of photobioreactor can thus protect the microalgal cells from damage by increasing the photoperiod, uniform distribution of light irradiation in a PBR (or PSBR and FPPB) or by flashing light (intermittent light exposure) (Degen et al., 2001; Laws et al., 1983).

Microalgal photosynthesis ceases in periods of low light intensity, which commonly leads to the formation of anoxic conditions in a PSBR. Nevertheless, photosynthesis and nitrogen removal usually continue once light is accessible again for microalgae. HRAPs can consequently handle variations in natural light intensity by, for example, increasing the hydraulic retention time (HRT) (Sutherland et al., 2015). A long HRT during periods of low light intensities is essential to prevent accumulation of nitrogen compounds and their inhibition. In a PSBR cultured with microalgal-bacterial consortia consisting of *Stichococcus* (1.1%), *Chlorella* spp. (95.2%), *C. sorokiniana* – *Comamonas* sp *and Chlamydomonas* (3.1%), oxygen production, ammonium removal and biomass concentration decreased when the dark period was extended for 12 d, but the performance was restored each time when illumination was provided (Wang et al., 2015). Storage of ammonium rich wastewater during the dark period could, therefore, improve the nitrogen removal efficiency by denitrification or denitritation using microalgal-bacterial consortia in PSBR.

### 2.3.2 Dissolved oxygen (DO) concentration

High DO levels support the growth of AOB and NOB, but inhibit the growth of denitrifiers. Moreover, it induces photo-oxidative loss in photosynthetic cells and, thus, increases the nitrogen removal efficiency by nitrification and decreases nitrite or nitrate removal by denitrification (Karya et al., 2013; Rada-Ariza et al., 2017). For example, Karya et al. (2013) reported 100 % nitrogen removal by nitrifiers at a DO level in the range 0.3-2.4 mg/L. However, Rada-Ariza et al. (2017) reported denitrification inhibition at high DO levels (above oxygen saturation).

Oxygen super-saturation in PBRs developed for microalgae cultures can reach a maximum of 400%, which adversely affects the growth of microalgae (Munoz and Guieysse, 2006). For example, Matsumoto et al. (1996) observed a 98% reduction in oxygen production rate when the DO was increased from 0 to 29 mg/L. Oxygen super-saturation is, however, not a major issue for

nitrogen removal owing to continuous oxygen utilization by AOB and NOB. For example, the DO level continuously increased to 0.31 mg/L during the light period and maintained at a very low level (≈0.19 mg $L^{-1}$) during the dark period for ammonium removal using a PSBR (Wang et al., 2015). However, the DO rapidly decreased following the complete oxidation of ammonium which is advantageous for denitrifiers or anammox bacteria (Wang et al., 2015; Manser et al., 2016). Further study are warranted to optimize the DO concentration for shortcut nitrogen removal or simultaneous nitrification and denitrification.

### 2.3.3 Temperature

The productivity of microalgal-bacteria based systems usually decreases at low (<16 ºC) temperatures (González-Fernández et al., 2011). Ammonium removal efficiency by using a mixed culture of *Chlorella vulgaris*, *Chlamydomonas reindhardtii* and *Scenedesmus obliquus* was enhanced when the temperature was increased from 15 to 23°C (González-Fernández et al., 2016). However, De Godos et al. (2009) revealed that a cold-adapted microalgal-bacterial consortium was applicable for nitrogen removal at an average temperature of 7°C during the months from January to May (Period I). Similarly, a pilot-scale HRAP was capable of supporting 96% ammonium removal during Period II (late June to early August) with an average temperature of 17 °C and an average light intensity below 7062 (± 81) W h/$m^2$. These studies show that the BNR with cold-adapted microalgal-bacterial biomass in HRAPs is feasible, despite the decrease in activities of microalgae and bacteria with temperature.

High temperatures at high biomass concentrations and a high light intensity results from convection of a large portion of the sunlight into heat (temperature up to 45 °C) by algae, which affects the photosynthetic activity and cellular metabolism in most species (Nwoba et al., 2019). In order to improve the light utilization efficiency by a stable microalgal-bacterial biomass,

temperature control by heat exchangers has been suggested which escalates the cost further (Nwoba et al., 2019).

### 2.3.4 pH

Microalgae, nitrifiers, denitrifiers and anammox bacteria are inhibited by the combined influence of high pH, temperature and high ammonia concentrations as well as by the uncoupling of ammonia oxidation from photosynthesis (Azov and Goldman, 1982). For example, Przytocka-Jusiak, (1976) observed complete inhibition of *C. vulgaris* growth at ammonia concentrations above 700 mg/L N and pH 8. Similarly, Abeliovich and Azov, (1976) reported inhibition of *S. obliquus* and the $IC_{50}$ value amounted to 50 mg/L total ammonia at pH over 8 in high rate sewage oxidation ponds. Konig et al. (1987) observed no significant effect on the growth of *Chlorella* and *Euglena* at 10 mM of ammonia and pH 9.0. (Table 2.4).

Nitrifier, denitrifier and anammox bacteria are sensitive to high ammonium concentrations as $NH_4^+$ is capable of diffusing through the membrane and reduce the intracellular pH, thereby interfering with the trans-membrane pH gradient necessary for ATP synthesis by AOB (Vadivelu et al., 2007). It also causes a direct inhibitory effect from free ammonia (FA) on nitrite oxidoreductase, which is required in the electron transport in NOB (Vadivelu et al., 2006), Vadivelu et al. (2006) observed no significant effect on growth of a *Nitrosomonas* culture at 16 mg/L $NH_3$-N and pH in the range 6.9-7.3. However, *Nitrobacter* (NOB) is completely inhibited (100%) at 2.5-25 mg/L $NH_3$-N and pH 8.5 (Balmelle et al., 1992). Similarly, anammox bacteria was inhibited by a total ammonia concentration of 40 mg/L at a pH in the range 7-8 in a moving bed biofilm bioreactor (Jaroszynski et al., 2012), whereas no inhibitory effect on anammox was observed even at 1500 mg/L $NH_3$-N at a pH above 8 in a lab-scale upflow fixed-bed reactor (Aktan et al., 2012)

**Table 2.4. Ammonia inhibition of microalgae and bacteria (AOB, NOB and anammox)**

| Microorganism | Ammonia concentration (mg/L $NH_3$-N) | Optimum pH and temperature | Inhibition on cell growth | Reference |
|---|---|---|---|---|
| *C. vulgaris* | 330,700 | 8.0-9.0 | 50% , Complete inhibition | Przytocka-Jusiak, 1976 |
| *S. obliquus* | 16.8 | 8-9.0 | 50% inhibition | Azov, Y. and Goldman, 1982 |
| *Chlorella and Euglena* | 560 | 9.0 | No ammonia toxicity | Konig et al., 1987 |
| *Nephroselmis pyriformis* | 0.0328 | 8.0 | 50% inhibition | Källqvist, T. and Svenson, A., 2003 |
| *S. obliquus* | 50 | >8.0 | Complete inhibition | Abeliovich and Azov, 1976. |
| *Nitrosomonas* Culture | 16 | 6.9-7.3 | No inhibiton | Vadivelu et al., 2006 |
| *Nitrobactor* | 1-9 | 7.3 | 12% inhibition, at 4-9 mg/L $NH_3$-N concentration (Free ammonia) | Vadivelu et al., 2007 |
| *Nitrobacter* | 2.5 -25 | 8.5 | 100% inhibition | Balmelle et al., 1992 |
| NOB | 9 | 8.1 and 21˚C | Complete inhibition | Rols et al., 1994 |
| AOB | 70 | 7 and 40˚C | Initiated inhibition at 70 mg/L $NH_3$-N | Hellinga et al., 1999 |
| AOB | 300 | 8 and 35˚C | Inhibition at 300 mg/L $NH_3$-N | Van Hulle et al., 2007 |
| AOB | 25 | 8.1 and >25 ˚C | 40% reduction in $NH_3$ oxidation rate at 25 mg/L $NH_3$-N | Balmelle et al., 1992 |
| Anammox | 40 | 7-8 and 30-37 ˚C | $IC_{50}$ (50%) | Jaroszynski et al., 2012 |
| Anammox | 1500 | 8 and 34 ˚C | No inhibitory effect | Aktan et al., 2010 |

It is hard to separate the direct effect of pH on algal-bacterial consortia from collateral effects like variations in the $HCO_3^-/CO_3^{2-}/CO_2$, phosphorus and $NH_4^+/NH_3$ equilibria (Abeliovich and Azov, 1976; Przytocka-Jusiak, 1976; Rols et al., 1994). The pH also affects phosphate and ammonia removal through phosphate precipitation at a high pH (9–11) and ammonia volatilization at pH 9.9 (Craggs et al., 2003). (Table 2. 4). However, it is comparatively easy to maintain the pH in

microalgae-bacterial systems, because the nitritation process produces $H^+$ ions and algal photosynthesis produces $OH^-$ ions during the light period.

In a PSBR for nitrogen removal from anaerobically digested swine manure concentrate by microalgal-AOB consortia, the wastewater pH decreased up to 7.1 during the light period; whereas a small increase in pH occurred during the dark period (Wang et al. 2015). The pH ranges 7-7.5, which is beneficial for nitrification, is necessary to enhance the nitrogen removal efficiency (Antoniou et al., 1990) as complete inhibition of nitrification at a high pH (8-9.5) (advantageous for the killing of pathogens) is generally observed in HRAPs (Craggs et al., 2003; Alcántara et al., 2015). This is attributed to a quicker release of $H^+$ in nitrification/nitritation than that of hydroxide ions through microalgal photosynthesis. A small increase in pH was observed during the dark period (anoxic), owing to hydroxide ions and alkalinity produced during denitritation.

### 2.3.5 Inhibitory effects of heavy metals

Heavy metals are strong inhibitors of $NH_4^+$ oxidation, $NO_2^-$ oxidation, $NO_3^-$ reduction and anaerobic ammonium oxidation and microalgal photosynthesis. The inhibitory concentrations vary depending on the type of microorganism (AOB, NOB, denitrifier, anammox or activated sludge) (You et al., 2009; Hu et al., 2002; Bi et al.,2014; Sakadevan et al., 1999). The specific ammonia utilization rate (SAUR) in activated sludge was inhibited at 40 mg/L of Pb, >5 mg/L of Ni and > 20 mg/L of Cd (You et al., 2009).

Pure cultures of nitrifiers (*Nitrosomonas* and *Nitrobactor sp.*) are also sensitive to heavy metals. In a continuous flow stirred tank reactor 50% inhibition of nitrification occurred due to 5 mg/L Cu and 94% inhibition of ammonia oxidation due to 250 mg/L Ni [76]. *Nitrosomonas* was inhibited equally or more than *Nitrobactor* sp, whereas *Nitrosomonas europaea* is less tolerant (90% of inhibition of ammonia oxidation) to 1µM $CdCl_2$, 6µM $HgCl_2$, or 8µM $CuCl_2$ (Park et al., 2008),

but the culture is more sensitive than activated sludge (Madoni et al., 1999). Therefore, anammox bacteria are expected to be more inhibited by heavy metals than AOB, NOB or denitrifiers. For example, inhibition was observed at 11.52 (± 0.49) mg/L for Ag, 11.16 (± 0.42) mg/L for Cd and 60.35 (± 2.47) mg/L for Hg (Park and Ely, 2008). Partial inhibition (50% inhibition) of anammox growth has been observed at 4.2 mg/L for Cu, 11.12 mg/L for Cd, 7.6 mg/L for Zn and 48.6 mg/L for Ni (Bi et al., 2014; Park and Ely., 2008)

### 2.4 Application of microalgal–bacterial consortia in bio-refineries

Biomass can be utilized for different applications (Table 2.5), but microalgal-bacterial biomass grown on wastewater is rarely applicable for food products or value added chemicals owing to the high-grade demand of such products. Microalgae-bacterial biomass can be used as fertilizer only if it is free from heavy metals, recalcitrant compounds as well as pathogens. Therefore, the best choice for the utilization of the microalgal–bacterial biomass is hydrocarbon fuel production by hydrothermal liquefaction or biogas production by anaerobic digestion (Fig. 2.4). This is a highly significant production route of hydrocarbon fuels and methane, compared to conventional activated sludge processes by which approximately 50% of carbon dioxide is released in the environment. For example, Chen et al. (2014) examined that the highest bio-oil yield (49%) with a maximum heating value of 33.3 MJ/Kg originated from a consortium of microalgae and bacteria used for wastewater treatment. A high methane yield of more than 0.53 $m^3$/kg VS was obtained by anaerobic digestion of algal biomass as compared with 0.35 $m^3$/kg VS using substrates like maize silage and field grass (Prajapati et al., 2013). Moreover, the biogas produced by anaerobic digestion of the microalgae can be reused directly in a PBR to remove the $CO_2$ present (biogas commonly contains approximately 40% $CO_2$ and 60% $CH_4$) for algal cultivation (Mandeno et al.,

2005). This further enables complete sequestration of $CO_2$ and enhances the energy efficiency ($CH_4$ enrichment) of the process.

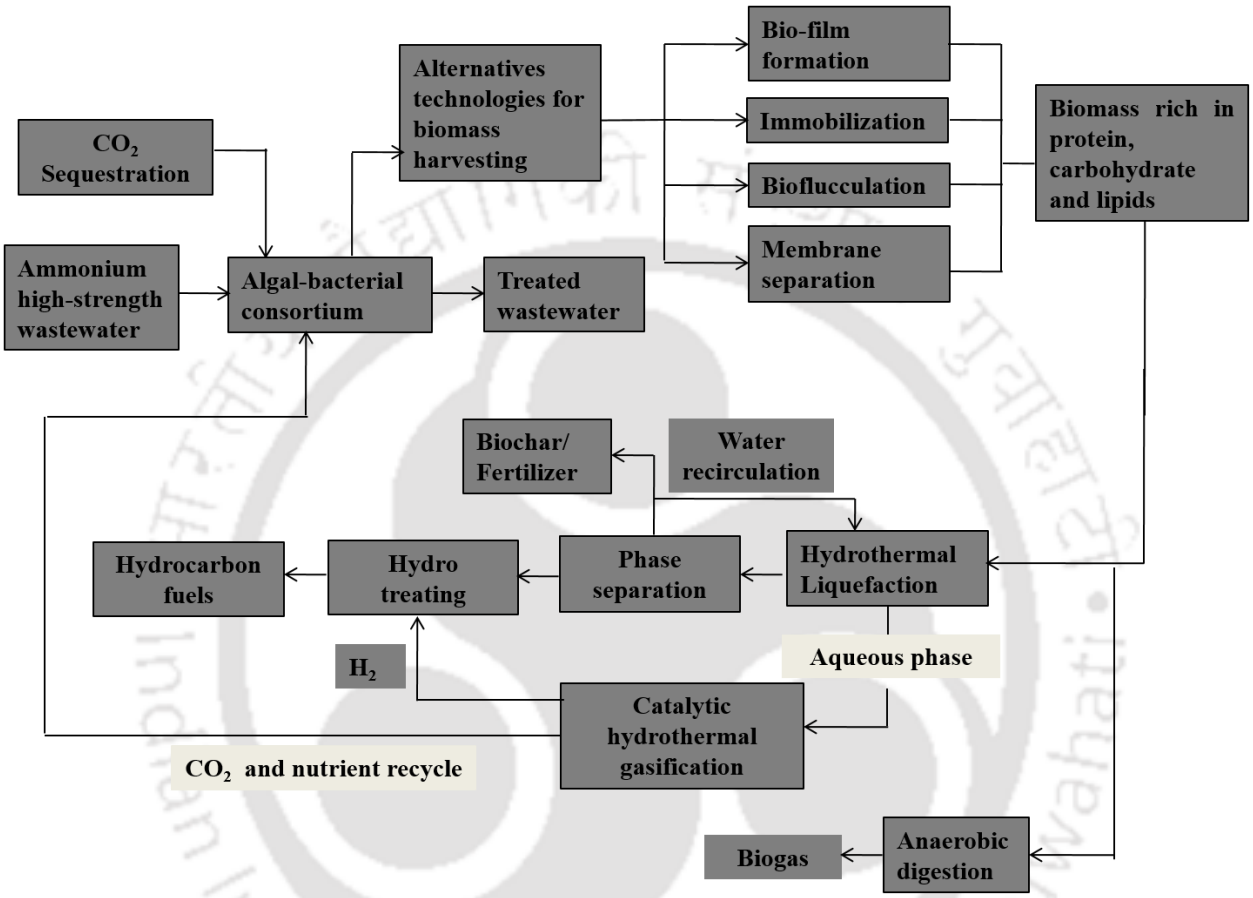


**Fig. 2.4.** Process flow diagram showing ammonium removal from wastewater and resource recovery

**Table 2.5. Valorization of microalgae–bacterial biomass**

| Uses | Remarks | References |
|---|---|---|
| Bioethanol production | Bioethanol can be produced by saccharification of algal biomass which contain 38% of starch granules | Matsumoto et al., 2003 |
| Biodiesel production | Transesterication for the production of fatty acid methyl esters from triglycerides with alcohol in the presence of a catalyst | Cuellar-Bermudez et al., 2014 |

| | | |
|---|---|---|
| Electricity generation | Sediment-type microbial fuel cell (MFC) for the generation of electricity by the symbiotic relation between microalgae and heterotrophic bacteria | Wang et al., 2015 |
| Biohydrogen production | Biophotolysis of water with algae and cyanobacteria<br>Photodecomposition of organic materials through photosynthetic bacteria.<br>Fermentative $H_2$ production from organic materials<br>Hybrid methods by fermentative and photosynthetic bacteria | Das and Veziroğlu, 2001. |
| Biogas | Anaerobic digestion or algal anaerobic digestion of algal biomass tomethane and carbon dioxide | Prajapati et al., 2013 |
| Biopolymer | Polyhydroxyalkanoates production by PHA accumulation microorganism | Fradinho et al., 2013 |
| Hydrocanbon fuels | Hydrothermal liquefaction of algal biomass | Chen et al., 2014 |
| Pigments | Astaxanthin, chlorophyll, zeaxanthin, lutein, *β*-carotene, or phycocyanin production by algae | Chew et al.,2019 |
| Fertilizer | Algae contain large portions of N and P, and hence, biomass from wastewater treatment signifies an attractive inexpensive fertilizer. | Ramanan et al., 2016 |
| Animal feed | *Dunaliella, Thalassiosiraweiss flogii, Tetraselmis, Isochrysis, Nannochloropsis or Chaetoceros* are used as food source for shrimp or shellfish | Hemaiswarya et al., 2011 |

## 2.5 Microalgae-bacterial consortia harvesting

Harvesting of biomass is essential to meet the effluent standards and avoid cell washout in sequencing batch as well as in continuous operation modes for real time wastewater treatment systems (Karya et al., 2013; Rada-Azira et al., 2017). However, none of the commercially available methods, including centrifugation and filtration, are cost-effective and feasible for large-scale harvesting of microalgae (Munoz and Guieysse., 2006; Udom et al., 2013). Wastewater treatment ponds are, often characterized by poor biomass settling, which is very difficult in the case of HRAPs (Munoz and Guieysse., 2006).

Microalgal flocculation following gravity settling is the best harvesting technique, applied in open pond systems due to the large wastewater volumes being treated and the low concentration

of the biomass produced (Nurdogan and Oswald., 1996). Microalgal bacterial flocs are aggregates composed of microalgae and bacteria which assist the microalgae to settle quicker than microalgae alone (Ummalyma et al., 2017). Bio-flocculation is mainly attributed to natural aggregation of biomass by extracellular polymeric substances (EPS) produced by microalgae (Fig. 2.5). Ummalyma et al. (2017) suggested that functional groups (charged) present in bio-flocculants benefit in accumulation of microalgae cells along with either electrostatic patch or charge neutralization, which aids in forming flocs. Zheng et al. (2012) reported that *B. subtilis* in γ-PGA is utilized for the flocculation of the microalgae *Phaeodactylum tricornutum* with a 97% efficiency. Both microalgae and bacteria are capable of producing EPS which is responsible for the floc formation. Fig. 2.5b and c show the bioflocculant characteristics of algae-bacterial consortia before and after bio-flocculation. Ummalyma et al. (2017) reported that bacteria of the genera *Terrimonas, Sphingobacterium and Flavobacterium* with microalgae produce flocs of 100 mm diameter with a high sedimentation and flocculation ability, which is comparable with those of *C. vulgaris* alone (20 mm). Wang et al. (2015) reported the EPS production using microalgae-bacterial consortia in PSBR for BNR which enabled the formation of microalgal-bacterial flocs in the size range 0.6 (±0.3) mm for easy biomass removal by gravity separation. Karya et al. (2013) observed an increase in the floc density during BNR using a photobioreactor with a maximum SVI (Sludge volume index) of 160 mL/g that resulted in a clear effluent with a low biomass concentration.

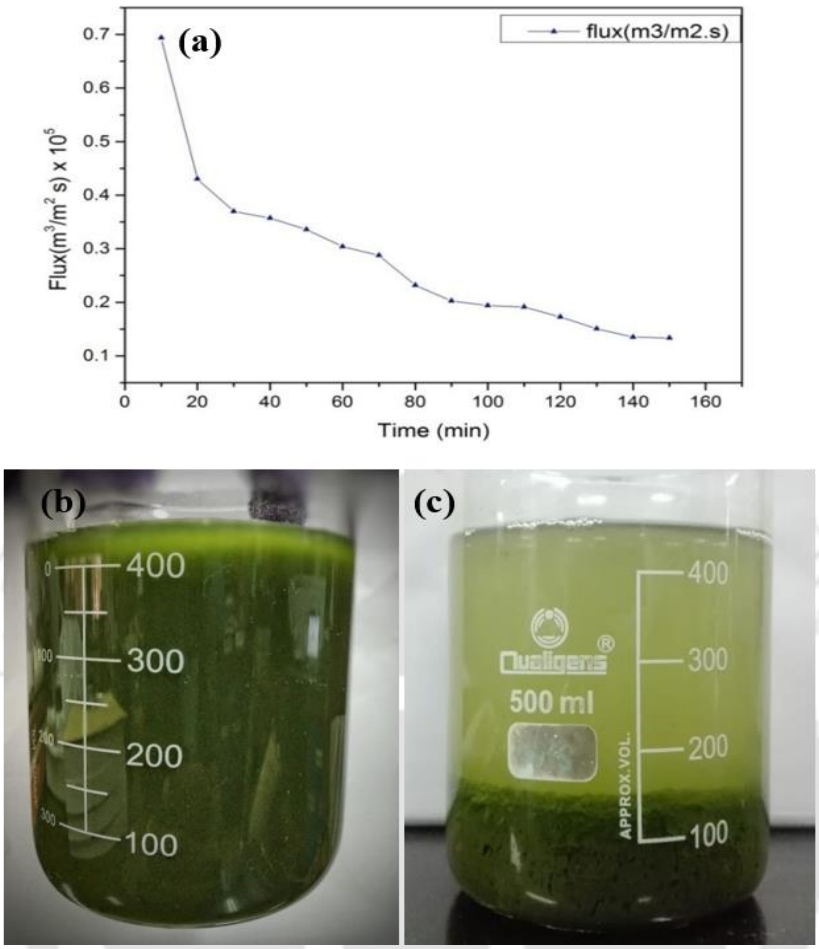


**Fig. 2.5** Evolution of permeate flux with time: (a) permeate, bio-flocculation of microalgae-bacterial biomass, (b) before settling and (c) after settling

Microalgae-bacterial immobilization is an effective means to retain biomass during wastewater treatment, (De-Bashan et al., 2002) and for which polymeric materials such as alginate (De-Bashan et al., 2002; Hernandez et al., 2009), agar, carrageenan or chitosan (De-Bashan and Bashan., 2010) can be used. Alginate matrices are weak in the presence of phosphate ions, lack long-term stability and are costly, which limit their application in wastewater treatment (De-Bashan and Bashan., 2010). Co-immobilization of *Chlorella vulgaris* with the microalgae growth-promoting bacterium *Azospirillum brasilense* in alginate beads is highly effective in removing nitrogen and phosphorous from synthetic wastewater (De-Bashan et al., 2002). Polyvinyl foams and chitosan are inexpensive

matrices that can be considered for different applications in wastewater treatment (Olguín, 2012). Chitosan-immobilized cells of *Scenedesmus* sp. are highly efficient for the treatment of wastewater containing nitrate and phosphate (Fierro et al., 2008).

Biofilm formation is another means to retain algal biomass which involves biomass growth on the surface of various substrates. Simultaneous production of algal biomass-free effluent and retention of algal biomass can be achieved using a biofilm photobioreactor (De Godos et al., 2009). A *Chlorella* sp. biofilm growing on polystyrene foam was used to treat dairy manure and achieved a high biomass yield of 25.65 $g/m^2$ with a maximum fatty acid yield of 2.31$g/m^2$ (Johnson and Wen., 2010). The biomass was recovered from the support by employing a simple scrapping mechanism. Another growth method for attached cultures is the rotating algal biofilm (RAB). Using RAB *in situ* mechanism for biomass harvesting resulted in a high biomass yield of 16.20 $g/m^2$ with cotton dust as the support material (Gross et al., 2013).

Membrane filtration (microfiltration (MF) and ultrafiltration (UF)) is another separation technique for harvesting microalgae from culture medium owing to its easy operation and high separation efficiency. Algal cells of C*hlorella vulgaris and* marine diatom *Phaeodactylum tricornutum* were recovered by submerged microfiltration together with centrifugation to obtain a final biomass concentration of 22% (w/v) (Bilad et al., 2012) The energy utilized to dewater *P. tricornutum* and *C. vulgaris* was 0.91 $kWh/m^3$ and 0.84 $kWh/m^3$, respectively. The energy requirement could be further reduced by using a magnetically induced membrane vibrating (MMV) system with a final biomass concentration of 25% (w/v) (Bilad et al., 2013). The energy utilized to recover *C. vulgaris and P. tricornutum* was, respectively, as low as 0.84 and 0.77 $kWh/m^3$, corresponding to 1.39 and 1.46 kWh/kg of the recovered biomass. In addition to the high cost of the membranes, pressure-driven UF and MF are subject to membrane fouling and are

relatively energy intensive (Table 2.6). Fig. 2.5(a) shows the evolution of the permeate flux with time using an inexpensive ceramic membrane (Purnima et al., 2020) for the separation of microalgal-bacterial consortia at an applied pressure of 345 kPa and a constant cross flow velocity of 40 L/h.

**Table 2.6.** Techniques used harvesting of microalgae-bacterial consortia

| Harvesting technique | Microorganism | Separation efficiency (%) | Advantages with respect to mechanical methods | Reference |
|---|---|---|---|---|
| 1. Bioflocculation | *Phaeodactylum tricornutum with B. subtilis* ($\gamma$ –PGA), *Scenedesmus* sp. with *Paenibacillus* sp and Marine microalga *Nannochloropsis with Solibacillus silvestris*[C] | 97 [A], 95[B] and 90[C] | Efficient, environment friendly, No lipid Cheap, sustainable and contamination free | Zheng et al., 2012; Kim et al., 2011; Wan et al., 2013 |
| 2. Membrane separation | *P. tricornutum*<br>*Chlorella vulgaris* | 85<br>100 | Energy efficient | Bilad et al., 2013 |
| 3. Biofilm formation | *Botryococcus braunii* | Biomass recovery -0.71 ($g/m^2$ d) | Low energy and water requirement Energy requirement reduced by 99.7% for dewatering | Ozkan et al., 2012 |
| 3.1 Rotating algal biofilm reactor | Mixed culture of *Diatoma Pediastrum* and *Chlorellasp.* | Biomass recovery - 31($g/m^2$ d) | Low energy and water requirement | Christenson and Sims., 2012 |
| 3.2 Rotating algal biofilm growth system | *Chlorella vulgaris* | Biomass recovery was (1.08 ± 0.14), (0.70 ± 0.19), (0.09 ± 0.08), and (0.08 ±0.06) for cotton - dust, rag, denim and corduroy | Easy harvest operations such as scrapping biomass from the attached surface | Gross et al., 2013 |
| 3.3 Algal biofilm membrane photobioreactor | *Chlorella vulgaris.* | Biomass production= 0.072 g $L^{-1}d^{-1}$ | Low cost for recovering, and dewatering process | Gao et al., 2015 |

## 2.6 Operation and design of photo-bioreactors for BNR

### 2.6.1 Photo-bioreactor operation

#### 2.6.1.1 Mixing in bioreactors

PBRs are operated as either plug-flow or mixed flow (CSTR) systems. Homogenous environment in a PBR are desirable during the removal of nitrogen as its allows uniform exposure to light and nutrients and lower the risk of sedimentation of the microalgae-bacterial consortia. Mixing also avoids the development of anoxic zones, which is disadvantageous for anoxic growth of denitrifiers and anammox bacteria and reduces mass transfer (oxygen mass transfer) limitations for nitrifiers (AOB, NOB) (Karya et al., 2013; Wang et al., 2015; Manser et al., 2016). Paddle wheels are frequently utilized for microalgal cultivation in HRAPs and open ponds as they are cost effective and provide good mixing. Wang et al. (2015) reported that 74% of $O_2$ was provided by microalgal photosynthesis and 26% was provided by mechanical aeration using paddle wheels for removing ammonium from anaerobically digested swine waste concentrate.

#### 2.6.1.2. Microalgae–bacterial biomass concentration

Light intensity is a main factor that determines the microalgae biomass concentration in PSBR, PBRs and FPPBR, which is expressed as the energy accumulated as biomass per unit of light utilized (Janssen et al., 2000). It thus affects the photosynthesis and nitrogen removal rates attained by the microalgal-bacterial consortia. Wang et al. (2015), for example, reported that an increase in light intensity from 74.2 (± 5.3) to 105 (± 7.2) μmol/$m^2$·s in a PSBR resulted in 28% enhancement in ammonium removal due to the increased biomass concentration (TSS) from 774 (±126) mg/L (Chlorophyll a-17.4 ± 3.6 mg/L) to 1229 (± 28) mg/L (Chlorophyll a-28.5 ± 2.5 mg/L). However, a decrease in the biomass (TSS) concentration from 1195 mg/L to 710 mg/L was observed when the microalgal-bacterial biomass was subjected to an extended dark period of 12 days. When the

biomass concentration (TSS) reached a steady state value of 1235 (± 125) mg/L, light supplied to the system was utilized to oxidize ammonium by AOB. A further increase in the TSS concentration caused mutual shading, which is advantageous to avoid inhibition of AOB and NOB by light intensity; the threshold light intensity limit for AOB and NOB is above 75 μmol $m^{-2}$ $s^{-1}$ (Manser et al., 2016). Too high TSS concentration also increases the microalgal dark respiration to occur (De Godos et al., 2014), resulting in a decreased DO availability to the AOB and NOB.

Prediction of the optimal biomass concentration in microalgal-bacterial consortia under natural illumination is highly problematic as the light intensity available on site greatly differs with time and region. At low light intensities, photo-limitation (insufficient light) conditions are helpful to keep the incidence of light/dark periods high, which results in maximum activities of microalgae, AOB and NOB. At light intensities above the saturation value, i.e. at light irradiation over 500 μmol/$m^2$·s, photo-inhibition can be utilized to keep the incidence of light/dark periods low, which results in maximum microalgal photosynthetic activity, but causes inhibition of AOB and NOB activity (Vergara et al., 2016; Wahidin et al., 2013). Moreover, the application of high microalgal concentrations to keep a high light/dark frequency needs efficient mixing without affecting the microalgal-bacterial (AOB and NOB) cells (Hu et al, 1996).

#### 2.6.1.3 Hydraulic retention time (HRT) and Sludge retention time (SRT)

HRAP are conventionally operated at an HRT of 2-6 d (Park et al., 2011) and almost the same values have been applied to PSBR, PBR and FPPBR (Karya et al., 2013; Wang et al., 2015; Rada-Ariza at al., 2017; Manser et al., 2017). Wang et al. (2015), for example, reported complete ammonium removal and low DO levels (because of nitritation) at an HRT and SRT of, respectively, 4 days and 8 days. Uncoupling of SRT and HRT avoids wash-out of slow growing AOB and produces well settled biomass. Furthermore, Rada-Ariza et al. (2017) reported

ammonium removal rates of microalgal-bacterial consortia in a FPSBPR at 100 (± 18) mg $NH_4^+$-N/L·d as compared with only 44 (± 16) mg $NH_4^+$-N/L·d using microalgae only at a HRT and SRT of, respectively, 2 and 3 days. When the HRT and SRT values were decreased from 4 to 2 d and 5 to 3.5 d, respectively, the nitrogen removal efficiency decreased as a result of washout of nitrifiers, showing that the process is limited by the nitrification rates. Complete nitrogen removal and improved biomass settling was, however, achieved at an HRT and SRT of, respectively, 2 and 8 days by sedimentation with improved settling properties and partial recycle of the biomass produced (Rada-Ariza et al. 2017).

### 2.6.2. Photo-bioreactor design

Microalgae-bacterial consortia can be cultivated in HRAPs (open type), FPPBR, PSBR or PBR as depicted in Fig. 2.5. As discussed earlier, nitrogen removal by microalgae-bacterial consortia is limited by DO level, which in turn depends on the light intensity. Therefore, in the absence of any economic concern, PBRs for treatment of nitrogen pollutants and PBRs for microalgal cultivation share the same main design considerations: efficient light utilization, effective mixing, good biomass settleability, scale-up, control over the nitrification and denitrification reaction during the light as well as dark period and light inhibition on the photosynthetic cells.

#### 2.6.2.1. Open bioreactors: High rate algal ponds (HRAPs)

Typical HRAPs used for nitrogen removal are shallow open raceway ponds with mechanical mixing by a paddle wheel (Park et al., 2011; Garcia et al., 2000). These are generally suited for treating industrial, municipal


**Fig. 2.6.** Schematic of (a) open pond (Montemezzani et al., 2016), (b) tubular photobioreactor (De Andrade et al., 2016) and (c) flat plate photobioreactor fed with $CO_2$ rich air (Lindblad et al., 2019) and agricultural wastewaters. HRAPs are specially developed to match microalgal growth and oxygen production for treating wastewater containing low ammonium and COD concentrations. HRAPs are 0.1-0.3 m deep open ponds and 2-3 m wide constructed in a raceway arrangement, and their size varies from 1000 to 5000 $m^2$ in large-scale applications (Grima et al., 1999; Abeliovich and Azov., 1976).

Under optimum conditions, HRAPs can remove TKN up to 80-86% during the months of January-May compared to only 54% during July-September with biomass productivities of 21-28 $g/m^2 \cdot d$ (DE Godos et al., 2009). This design also permits for nitrogen removal under continuous operation at an HRT of 2-10 days (De Godos et al., 2009). However, due to the demerits of the HRAPs such as large land requirement, difficulties in biomass harvesting, risk of contamination,

temperature dependence and limitation in availability of light, nutrients and $CO_2$, only a few full scale plants are currently in operation for biological nitrogen removal (Benemann, 1986 ; Shelef, 1982; García et al., 2006; Park and Craggs., 2010).

### 2.6.2.2. Closed photo-bioreactors

Closed photo-bioreactors offer a high oxygenation capacity (1.8-8.3 kg $O_2/m^3 \cdot d$) with high nitrogen removal efficiencies, low risk of pollutant volatilization, high photosynthetic efficiencies and good biomass settling properties as compared to HRAPs (Karya et al., 2013; Wang et al., 2015; Hu et al., 1996). Moreover, they can be constructed vertically to reduce land demand for microalgae cutivation (Pulz, 2001) and water loss due to evaporation which is highly important in HRAPs (Pulz, 2001). However, PSBR, FPPBR and PBRs are more costly to build due to the requirement of transparent materials, for example Plexiglas, PVC or glass, which are often problematic to operate at large scale (Fig. 2.5).

Photobioreactors are arranged in either vertical, inclined or horizontal configurations (Fig. 4 (a-c)) (Munoz et al., 2004; Ugwu et al., 2008). Table 2.7 compares the performance of these photobioreactors for treating nitrogen containing wastewater. Tubular PBRs (Fig. 2.5(b)) are useful for outdoor cultivation and easy to scale up by increasing the diameter of the tubes (Ugwu et al., 2008). They also exhibit efficient light distribution to cells by providing good mixing in the tubes (Ugwu et al., 2005) Therefore, oxygenation rates of up to 0.43 kg $O_2/m^3 \cdot d$ (up to 8 kg $O_2/m^3 \cdot d$) have been achieved in photobioreactors under sequencing batch mode (Karya et al.,2013). The rate is considerably higher than the oxygenation values in waste stabilization ponds or HRAP and it is similar to the maximum oxygenation rate of mechanical aerators (3 kg $O_2 \cdot m^{-3} d^{-1}$) (Munoz and Guieysse., 2006).

**Table 2.7.** Comparison of open and closed type photo-bioreactor with microalgal-bacterial consortia reported in the literature for BNR

| Reactor type | Light utilization efficiency | Maximum Oxygenation capacity | Design criteria and features | Reference |
|---|---|---|---|---|
| **HRAP** | Low | 0.3-0.38 kg $O_2$ $m^{-3}$ $d^{-1}$ | HRAP of 0.1–0.3 m deep ponds and 2–3 m wide | Grima et al., 1999 |
| **PSBR** | Very high | 0. 193 kg $O_2$ $m^{-3}$ $d^{-1}$ | Volume of 2 Land diameter 15 cm, height 12 cm | Wang et al., 2015 |
| **Algae-bacterial PBR** | Low | 0.46 kg $O_2$ $m^{-3}$ $d^{-1}$ | Volume of 1 L and diameter of 11.5 cm | Karya et al., 2013 |
| **Tubular biofilm photobioreactor** | High | 3.20 kg $O_2$ $m^{-3}$ $d^{-1}$ | Volume of 600-ml and 110-ml cylindrical glass settler (3 cm internal diameter) | Munoz et al., 2004 |
| **PBR** | High | 0.11-0.13 mg $O_2$ $m^{-3}$ $d^{-1}$ | Total working volume of 3.5 L | De Godos et al., 2010 |

Mechanical aeration in MFCs accounts for approximately 50% of the total operating cost (del Campo et al., 2015). Therefore, microalgae based MFCs can be more energy efficient due to algal photosynthesis in the cathodic compartment, which can provide $O_2$ for the cathodic reaction. This symbiotic relationship can also be used for sustainable development of MFCs by using produced excess algal biomass for the anodic reaction and $CO_2$ from the anodic compartment used as inorganic carbon source for algal growth, which is advantageous in terms of simultaneous $CO_2$ capture and electricity production (Wang et al., 2010; Wang et al., 2014).

Some previous studies reported successful use of algae in the cathodic compartment for power generation using MFCs**.** For example, an algae assisted cathode was successfully utilized for power production in MFCs with a maximum power density of 21 $mW.m^{-2}$; which was further improved to 38 $mW.m^{-2}$ with modification (carbon nanotube coating) of the cathode (Wang et al., 2014). Similarly, the growth of algae on the surface of the cathode supported oxygen production by algae via photosynthesis without any external aeration and with the addition of sodium carbonate as an

inorganic carbon source (Kakarla and Min, 2014). Wang et al. (2010) analyzed different algal concentrations (measured using optical density (OD), 0.21 (658 nm) and 0.85 (658 nm) for the removal of $CO_2$ in algal based MFCs and compared the electricity production values. Oxygen produced by algal photosynthesis was efficiently consumed (DO concentration decreased from 7.6 to 0.9 mg/L) showing that the produced $O_2$ during the light period was used as electron acceptor for the cathodic reaction with an excess of inorganic carbon source. Simultaneous use of algae in both anode (lipid extracted algal biomass used as electron donor) and cathode (oxygen produced by algal photosynthesis used as electron acceptor for cathodic reaction) in algae based MFCs yielded a maximum power density of 2.7 W $m^{-3}$ (Khandelwal, et al., 2018).

From the detailed literature review it is clear that only a few previous studies have reported on microalgal-bacteria consortia for 100% ($NH_4^+$-N) removal as most of these could only tolerate only< 84.8% (low $NH_4^+$-N concentration). Also, most of the microalgae-bacterial consortia used for BNR involves nitrification and denitrification in common and therefore would require large amount of aeration and energy to achieve complete nitrification during wastewater treatment operation. The poor uptake rate of ammonium by microalgae in wastewater treatment is another hurdle for its utilization by microalgae-bacterial consortia. Further, any effort to effectively scale up this method requires continuous operation using photosequencing batch reactor. Furthermore, suitable applications of microalgae-bacterial consortia such as pigments production, animal feed, BNR, photosynthetic microbial fuel cell, shortcut nitrogen removal, etc. could enhance its commercial feasibility.

# Chapter 3

## Process optimization and kinetic modelling of shortcut nitrogen removal by microalgae-bacterial consortium

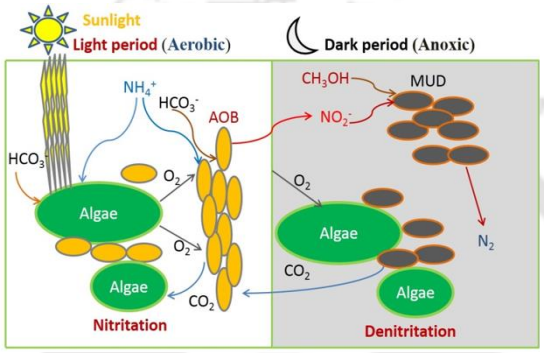


**Shortcut nitrogen removal**

Methanol addition

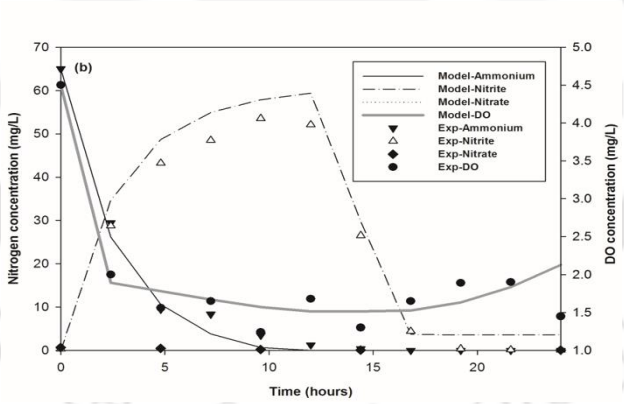

**ABSTRACT**

This study was aimed at process optimization and kinetic modelling of shortcut nitrogen removal by a mixed consortium of microalgae, enriched ammonia oxidizing bacteria (AOB) and methanol utilizing denitrifier (MUD) in a photo-sequencing batch reactor (PSBR). Alternating light and dark periods were followed to obtain complete biological nitrogen removal (BNR) without any external aeration and with the addition of methanol as the sole carbon source, respectively. The results showed that influent $NH_4^+$ was oxidized to $NO_2^-$ by AOB during the light periods at a rate of 8.09 mg $NH_4^+$-N $L^{-1}h^{-1}$. Subsequently, $NO_2^-$ was completely reduced during the dark period due to the action of MUD in the presence of methanol. The high activities of ammonia monooxygenase (AMO) and nitrite reductase (NIR) enzymes revealed the strong role of AOB and MUD for achieving shortcut nitrogen removal from the synthetic wastewater. The reduced activities of nitrate reductase (NR) and nitrite oxidoreductase (NOR) at a high concentration of DO, $NH_4^+$ and $NO_2^-$ in the system further confirmed the nitrogen removal pathway involved in the process. The biomass produced from these experiments showed good settling properties with a maximum sedimentation rate of 0.7 -1.8 m $h^{-1}$, a maximum sludge volume index (SVI) in the range 193 ml $g^{-1}$-256 ml $g^{-1}$and floc size of 0.2-1.2 mm. In order to describe the growth and interaction among the algae, AOB and MUD for nitrogen removal in the system, the experimental results were fitted to four metabolic models, which revealed a best fit of the experimental data due to the models based on algae-AOB and algae-AOB-MUD activities than with the other two models.

## 3.1 Introduction

Biological nitrogen removal (BNR) by nitrifying and denitrifying bacteria is a well-established method for the treatment of low strength ammonium wastewater (Carrera et al., 2003). However, in case of ammonium rich wastewater, which contains 200-2200 mg/L of total nitrogen, conventional BNR process requires significantly high amount of energy for its operation in wastewater treatment plants (WWTP) (Arnold et al., 2000; Bassin, 2018; Farazaki and Gikas, 2019; Ilies et al., 2001; Orhon et al., 2000; Ramaswami et al., 2019; Shiskowski et al., 1998). This is mainly because energy consumption by aeration accounts for 45%-75% of the total energy requirement (Stenstrom and Rosso, 2008). Moreover, an efficient and cost effective carbon source for BNR process is key to its success in WWTP (Manser et al., 2016). Furthermore, understanding the mechanism of actions involved in ammonium oxidation under high dissolved oxygen (DO) concentration condition and utilization of cheap organic carbon source for de-nitrification are critical for minimizing the process cost (Peng and Zhu, 2006).

There is an increase in evidence showing that microalgae play a major role in nutrient removal, which also produce high amount of oxygen during photosynthesis, in WWTP as well as in marine and terrestrial ecosystems (Munoz and Guieysse, 2006; Saranya and Shanthakumar, 2019). The high DO content due to microalgae is highly desirable than mechanical aeration for nitrification and oxidation of organic pollutants in WWTP (Chojnacka et al., 2005; Wang et al., 2015). Although high DO concentration is not required during complete BNR (nitrification and denitrification) process, other alternative processes are suggested to reduce the requirement of DO and organic carbon source for nitrogen removal which are: 1) simultaneous nitrification and de-nitrification, 2) shortcut nitrification and de-nitrification, 3) oxygen limited autotrophic nitrification-denitrification (OLAND),4) completely autotrophic nitrogen removal over nitrite

(CANON), 5) anaerobic ammonium oxidation (ANAMMOX) and aerobic deammonification process (Hippen et al., 1997; Mulder et al., 1995; Munch et al.,1996; Peng and Zhu, 2006; Sliekers et al., 2002; Windey et al., 2005). Among these different process, shortcut nitrification and de-nitrification using algae-bacterial consortium is highly promising due to less consumption of oxygen and organic carbon source (Zhu et al., 2008; Goncalves et al., 2017). In several studies involving microalgae-bacterial consortium, the $NH_4^+$oxidation pathway followed by ammonia oxidizing bacteria (AOB) has been identified as the key for complete nitrification with maximum $NH_4^+$conversion and without external aeration (Akizuki et al., 2019; Karya et al., 2013; Manser et al., 2016; Rada-Ariza et al., 2019; Wang et al., 2015). In this method, $O_2$produced by algae is utilized for $NH_4^+$oxidation by AOB under aerobic conditions to produce $NO_2^-$, which is subsequently converted to $N_2$ gas by de-nitrifier under anoxic condition (Manser et al., 2016; Meng et al., 2019; Wang et al., 2015). AOB has been suggested to play a key role in shortcut nitrogen removal by the oxidation of $NH_4^+$ to $NO_2^-$under light conditions, and in this nitritation process $NH_4^+$ acts as the electron donor. Increased $NO_3^-$ production under high DO concentration in algal-bacterial consortium is due to the activity of nitrite oxidizing bacteria (NOB), which can however be avoided under limiting DO concentration (Karya et al., 2013; Ma et al., 2015).

De-nitrification by methanol utilizing denitrifier (MUD) for $NO_3^-$/$NO_2^-$ reduction to $N_2$ has been reported in several studies and is highly advantageous over the anammox process due to high biomass growth rate and yield (Ni et al., 2010; Waki et al., 2013). Moreover, methanol as an organic carbon source for denitrification does not lead to $N_2O$ accumulation during nitrate reduction at a pH in the range 7.0-8.0. In addition, methanol can be utilized by denitrifying bacteria even in the absence of free molecular oxygen (anoxic condition) for its cellular activity (Pan et al., 2012). On the other hand, anammox based nitrogen removal process is applicable only for treating

wastewater with low or negligible organic carbon content. However, wastewater usually contains organic carbon and nitrogen; hence, simultaneous removal of organic carbon in the presence of high ammonium concentration (high COD/N ratio) is highly problematic in WWTP (Kumar and Lin, 2010). Therefore, this study aimed at simultaneous removal of high concentrations of nitrogenous and organic compounds in absence of external aeration by using a consortium of algae, AOB and MUD. The association among the different species for BNR are represented in equations 3.1−3.4. Equations 3.1 and 3.2 show oxygen production and ammonia uptake by algal biomass, respectively (Ezeet al., 2018; Manser et al., 2016).

$$CO_2 + H_2O + \lambda_{photon} \rightarrow CH_2O + O_2 \qquad (3.1)$$

$$16NH_4^+ + 92H_2O + HPO_4^{2-} + 106HCO_3^- \rightarrow C_{106}H_{263}O_{110}N_{16}P + 92OH^- + 106O_2 \qquad (3.2)$$

Equation 3.3 estimates the uptake and oxidation of ammonia to nitrite by autotrophic AOB (Manser et al., 2016).

$$NH_4^+ + 1.24O_2 + 0.16CO_2 + 0.04HCO_3^- \rightarrow 0.04C_5H_7O_2N + 0.96NO_2^- + 1.92H^+ \qquad (3.3)$$

Finally, equation 3.4 describes nitrite reduction to $N_2$ by MUD.

$$0.5CH_3OH + NO_2^- \rightarrow 0.5N_2 + 0.5CO_2 + 0.5H_2O + OH^- \qquad (3.4)$$

In a recent study on microalgae-bacterial consortium for BNR, it was observed that the $NH_4^+$ oxidation rate depended on high DO concentration whereas $NO_2^-$ reduction rate depended on low DO concentration (Manser et al., 2016; Wang et al., 2015), thus revealing a strong effect due to DO concentration on $NH_4^+$ oxidation rate and $NO_2^-$ reduction rate in this process. Hence, this study was further aimed at examining shortcut nitrogen removal from high COD/N ratio containing wastewater using a consortium of algae, AOB and MUD in a photo-sequencing batch reactor (PSBR) by alternating light and dark periods. The effect of DO concentration on $NH_4^+$oxidation

rate and de-nitrification rate, and the activities of key enzymes such as ammonium monooxygenase (AMO), nitrite oxidoreductase (NOR), nitrate reductase (NR) and nitrite reductase (NIR) were analyzed to gain insight into the shortcut BNR process. The experimental data was fitted to different metabolic models based on one or more mechanisms, such as algal photosynthesis, $NH_4^+$uptake by algae, $NH_4^+$oxidation by AOB, $NO_2^-$oxidation by NOB and $NO_2^-$reduction by MUD, to describe the bio-kinetics of nitrogen removal in the process.

## 3.2 Materials and methods

### 3.2.1 Microorganism and culture conditions

A 5L fermenter (BIOSTAT B plus, Sartorius, Germany) was used to enrich AOB in biomass obtained from a WWTP located at IIT Guwahati, Assam, India; the bioreactor was operated under sequencing mode as described in Law et al. (2012). The SBR was operated in identical cycles of 6 h each cycle comprised of 2.5 min feeding stage I, 65 min aerobic reaction stage I, 30 min settling, 10 min decanting, 92 min idle stage I, 2.5 min feeding stage II (aeration on), 65 min aerobic reaction stage II, 92 min idle stage II and 1.2 min wasting (aeration on). Photo-sequencing batch reactor operating cycles during the start-up phase and biological nitrogen removal phase is shown in Fig. 3.1. The sequencing batch reactor (SBR) was fed with synthetic wastewater containing 5.63 g/L of $NH_4HCO_3$, 0.064 g/L of $KH_2PO_4$, 0.064 g/L of $K_2HPO_4$ and 2ml of trace element solution. The pH was maintained at 7.0 throughout the experiment, and the system was operated over 4 months to achieve a stable performance in terms of complete oxidation of ammonium to nitrite.

For enriching MUD culture, the same SBR was inoculated with activated sludge from a sewage treatment plant (STP) in Mangalore, India, and operated in the same manner as described by Pan et al. (2012). The SBR was then fed with synthetic wastewater containing a mixture of solution I

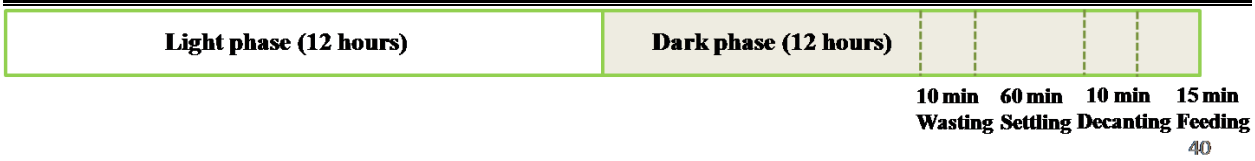


(a) Start-up phase (0 to 82 days)

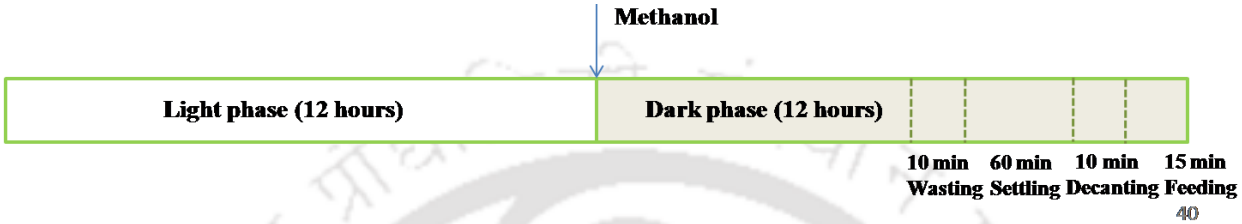


(b) Biological nitrogen removal phase (82to 151 days)

**Fig. 3.1** Photo-sequencing batch reactor operating cycles during the start-up phase and biological nitrogen removal phase

and II of volume 0.91 L and 0.09 L, respectively. Solution I contained 1.48 g /L of $NaNO_3$; 0.222 g/L of $MgSO_4 \cdot 7H_2O$;0.022 g/L of $CaCl_2 \cdot 2H_2O$; 0.192 g/L of $K_2HPO_4$; 0.314 g /L of $NH_4Cl$ and 2.2 ml of trace element solution, whereas solution II contained 7.4 ml/L of methanol. Sodium nitrate was initially used for enriching MUD in the consortium and not for BNR. The SBR system was operated over six months for complete removal of nitrate and methanol. The presence of MUD in the consortium was indicated by simultaneous utilization of methanol and denitrification in the experiments.

### 3.2.2 Algae isolation and identification

The microalgae used in this study was isolated from WWTP located at IIT Guwahati, Assam, and for which 5 ml of sample collected was inoculated into BG-11 medium containing 250ml Erlenmeyer flask followed by incubation at 25°C. 12 hr of light and 12 hr of dark period was maintained during the growth period. After 20 days of incubation, 5 ml of the algal culture was transferred into modified BG-11 medium containing a high concentration of ammonium (200 mg/L of $NH_4$-N) and methanol (7.4 ml/L). After two weeks of incubation, the culture was spread onto BG-11 agar plates; the single algal colonies obtained were sub-cultured using BG-11 media and the algal isolates were observed under an optical microscope (Model YS 100, Nikon, USA). The culture was further analyzed for 23S rRNA gene sequencing and homology of its partial 23S rRNA gene sequence was carried out using the bioinformatic tool basic local alignment search tool (BLAST) of National Center for Biotechnology Information (NCBI). The gene sequence was subsequently submitted to GenBank database and its accession number was obtained. The culture was finally identified as *Chlorella sorokiniana***.**

### 3.2.3 Nitrogen removal experiments

40 mL of the enriched *C. sorokiniana* culture and 5mL of the enriched AOB culture were taken in a 5 L bench-top fermenter (BIOSTAT B plus, Sartorius, Germany) fitted with accessories and controls for pH, temperature, DO and substrate addition. A schematic of the PSBR setup used in the present study is shown in Fig. 3.2.The bioreactor was fed with synthetic wastewater containing 200 mg/L of $NH_4^+$-N, COD/N ratio of 0.33-0.5 and 250 mg $CaCO_3$/L as alkalinity; the operating conditions were120 rpm agitation, 30˚C temperature and 75 µmol/$m^2$. s illumination. pH was automatically controlled at 7.5 with 1M $NaHCO_3$ solution. After an initial start-up of 4 weeks, 500 mL of the of algae-AOB mixed culture was inoculated into the bioreactor and operated under

sequencing batch mode for further experiments, as illustrated in Fig.3.1 and Table 3.1. The main objectives of this start-up phase was to inhibit the activity of NOB, avoid the toxic effect of methanol, achieve high DO concentration and obtain significant growth of algal as well as MUD in the photo-sequencing batch reactor (PSBR). During the start-up phase, hydraulic retention time (HRT) was maintained at 4 days and the sludge retention time (SRT) of the algae-AOB consortium was determined to be 30 days. Following the start-up phase, nitrogen removal experiments (BNR phase) were carried out using algae-AOB-MUD consortium. During the start-up phase, no methanol was added during the dark period, whereas in the BNR phase methanol was added during the dark period for denitritation.

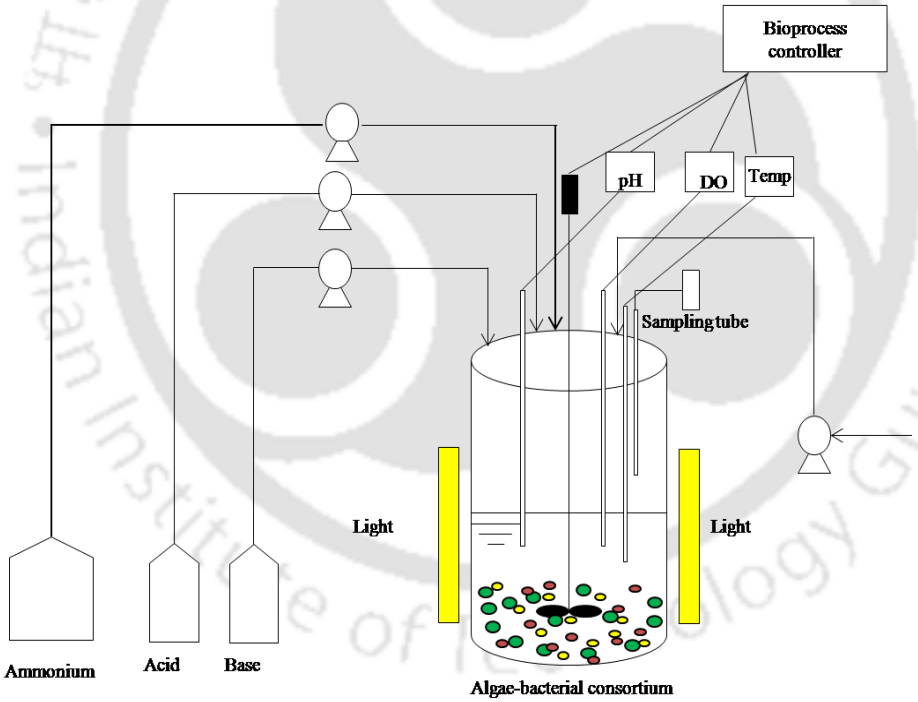


**Fig. 3.2.** Schematic representation of the photo-sequencing batch reactor used in this study.

**Table 3.1:** Operating conditions of the PSBR during start-up and BNR phases

| Phase | Light intensity (µmol/ $m^2$ s) | Wastewater alkalinity (mg $CaCO_3$/L) | HRT (days) | SRT (days) | Operation period (days) | Methanol addition (ml/L) |
|---|---|---|---|---|---|---|
| Start-up phase | 100 | 250 | 4 | 30 | 0-82 | Nil |
| BNR phase | 140 | 450 | 2 | 20 | 82-151 | 0.75 |

### 3.2.4 Bio-kinetic modeling of nitrogen removal

For modeling the kinetics of nitrogen removal in this study four different metabolic models were formulated. In all these models, biomass due to microalgae ($X_A$), AOB ($X_{AOB}$), NOB ($X_{NOB}$) and MUD ($X_H$) were considered along with the concentrations of dissolved substrates, viz bicarbonate ($S_{HCO_3}$), phosphate ($S_{PO_4}$), ammonium ($S_{NH_4}$), nitrite ($S_{NO_2}$), and nitrate ($S_{NO_2}$), which constituted the synthetic ammonium rich wastewater used in this study. Besides, respective terms for dissolved concentration of nitrogen ($S_{N_2}$) and oxygen ($S_{O_2}$) were considered. These models are presented in Table 3.2 along with the input variables and their equivalent parameter for these models is presented in Table 3.3. The basis for choosing all these models is described further. It is well-known that, microalgae can grow and produce $O_2$ in the presence of light with $NH_4^+$ as nitrogen source and by using $HCO_3^-$. The growth rate of the microalgae is modeled as the product of algal biomass concentration ($X_A$),maximum specific growth rate$(\mu_{max,A})$, and switching functions of $NH_4^+$, $HCO_3^-$, $PO_4^{3-}$and light intensity. Equations 3.1 and 3.2 represent the oxygen production and ammonia uptake, respectively by algae for its growth. Equation 3.3, which represents combined process rate of algal growth ($R_1$) on $NH_4^+$ in the presence of $HCO_3^-$ and $PO_4^{3-}$

newly proposed in this study. All the other rate equations (3.5-3.16) were adopted from Kaelin et al. (2009

$$R_1 = \mu_{max,A}\left(\frac{S_{NH_4}}{K_{NH_4,P}+S_{NH_4}}\right)\left(\frac{S_{HCO_3}}{K_{HCO_3}+S_{HCO_3}}\right)\left(\frac{S_{PO_4}}{K_{PO_4}+S_{PO_4}}\right)\left(\frac{I}{K_I+I}\right)X_A \quad (3.5)$$

Similar to the growth rate of algae, decay rate of algae ($R_2$) can be modeled as the product of algal biomass concentration ($X_A$) and its decay rate ($b_A$) as represented by Equation (3.6)

$$R_2 = b_A \cdot X_A \quad (3.6)$$

In this study, autotrophic growth of AOB on $HCO_3^-$ is considered based on dissolved DO produced by algae and $NH_4^+$ oxidation to $NO_2^-$. The rate of AOB growth ($R_3$) is modeled as the product of AOB biomass concentration ($X_{AOB}$), its maximum growth rate $(\mu_{max,AOB})$and switching function for oxygen and ammonium.

$$R_3 = \mu_{max,AOB}\frac{S_{O_2}}{K_{O_2,AOB}+S_{O_2}}\frac{S_{NH_4}}{K_{NH_4,AOB}+S_{NH_4}}X_{AOB} \quad (3.7)$$

Equation 3.8 describes the oxidation of $NH_4^+$ to $NO_2^-$by AOB.

$$NH_4^+ + 1.24\,O_2 + 0.16\,CO_2 + 0.04HCO_3^- \rightarrow 0.04C_5H_7O_2H + 0.96NO_2^- + 0.96H_2O + 1.92H^+ \quad (3.8)$$

where $K_{O_2,AOB}$ is the half saturation constant for oxygen, and $K_{NH_4,AOB}$ is the half saturation constant for ammonium.

Rate of AOB decay ($R_4$) is expressed as the product of AOB biomass concentration ($X_{AOB}$) and decay rate ($b_{AOB}$) (Equation 3.9)

$$R_4 = b_{AOB}.X_{AOB} \quad (3.9)$$

**Table 3.2a.** Process matrices for the four metabolic models evaluated in this study

| Model component | 1 | 2 | 3 | 4 | 5 | 6 | 7 | 8 |
|---|---|---|---|---|---|---|---|---|
| | $X_A$ $\frac{g\ COD}{m^3}$ | $X_{AOB}$ $\frac{g\ COD}{m^3}$ | $S_{HCO_3}$ $\frac{g\ HCO_3^-}{m^3}$ | $S_{PO_4}$ $\frac{g\ PO^-_4 - P}{m^3}$ | $S_{NH_4}$ $\frac{g\ NH^+_4 - N}{m^3}$ | $S_{NO_2}$ $\frac{g\ NO^-_2\text{-}N}{m^3}$ | $S_{O_2}$ $\frac{g\ O_2}{m^3}$ | Process rate |
| **1. Algae growth on $NH_4$ and,$HCO_3$,$PO_4$ and light intensity** | 1 | - | $-\frac{1}{Y_{HCO_3}}$ | $-\frac{1}{Y_{PO_4}}$ | $-\frac{1}{Y_{NH_4}}$ | - | $Y_{O_2}$ | $\mu_{max,A}\left(\frac{S_{NH_4}}{K_{NH_4,A}+S_{NH_4}}\right)\left(\frac{S_{HCO_3}}{K_{HCO_3,A}+S_{HCO_3}}\right)\left(\frac{S_{PO_4}}{K_{PO_4,A}+S_{PO_4}}\right)\left(\frac{I}{K_I+I}\right)X_A$ |
| **2. Algae decay** | -1 | - | - | - | - | - | - | $b_A X_A$ |
| **3. AOB growth** | - | - | - | - | $-i_{N,BM}-\frac{1}{Y_{AOB}}$ | $\frac{1}{Y_{AOB}}$ | $-\frac{3.43-Y_{AOB}}{Y_{AOB}}$ | $\mu_{max,AOB}\frac{S_{O_2}}{K_{O_2,AOB}+S_{O_2}}\frac{S_{NH_4}}{K_{NH_4,AOB}+S_{NH_4}}X_{AOB}$ |
| **4. Bacteria decay of AOB** | - | `- | - | - | $-i_{Xbac}$ | - | - | $b_{AOB}X_{AOB}$ |
| **5. Transfer $O_2$** | - | - | - | - | - | - | 1 | $K_L a_{o2}(S_{o2}^{*}-S_{o2})$ |

**Table 3.2b.** Process matrices for the four metabolic models evaluated in this study

| Model component | 1 | 2 | 3 | 4 | 5 | 6 | 7 | 8 | 9 | 10 |
|---|---|---|---|---|---|---|---|---|---|---|
| **Process** | $X_A$ $\frac{\text{g COD}}{\text{m}^3}$ | $X_{AOB}$ $\frac{\text{g COD}}{\text{m}^3}$ | $X_H$ $\frac{\text{g COD}}{\text{m}^3}$ | $S_{HCO_3}$ $\frac{\text{g } HCO_3^-}{\text{m}^3}$ | $S_{PO_4}$ $\frac{\text{g } PO^-_4 - P}{\text{m}^3}$ | $S_{NH_4}$ $\frac{g\ NH^+_4 - N}{\text{m}^3}$ | $S_{NO_2}$ $\frac{\text{g } NO^-_2\text{-N}}{\text{m}^3}$ | $S_{O_2}$ $\frac{\text{g } O_2}{m^3}$ | $S_{N_2}$ $\frac{\text{g } N_2}{m^3}$ | |
| **1.Algae growth on $NH_4$ and,$HCO_3$,$PO_4$ and light intensity** | 1 | - | - | $-\frac{1}{Y_{HCO_3}}$ | $-\frac{1}{Y_{PO_4}}$ | $-\frac{1}{Y_{NH_4}}$ | - | $Y_{O_2}$ | - | $\mu_{max,A}\left(\frac{S_{NH_4}}{K_{NH_4,A}+S_{NH_4}}\right)\left(\frac{S_{HCO_3}}{K_{HCO_3,A}+S_{HCO_3}}\right)\left(\frac{S_{PO_4}}{K_{PO_4,A}+S_{PO_4}}\right)\left(\frac{I}{K_I+I}\right)X_A$ |
| **2. Algae decay** | -1 | - | - | - | - | - | - | - | - | $b_A X_A$ |
| **3.AOB growth** | - | - | - | - | - | $-i_{N,BM}-\frac{1}{Y_{AOB}}$ | $\frac{1}{Y_{AOB}}$ | $-\frac{3.43-Y_{AOB}}{Y_{AOB}}$ | - | $\mu_{max,AOB}\frac{S_{O_2}}{K_{O_2,AOB}+S_{O_2}}\frac{S_{NH_4}}{K_{NH_4,AOB}+S_{NH_4}}X_{AOB}$ |
| **4. Bacteria decay of AOB** | - | ` $-1$ | - | - | - | $-i_{X,AOB}$ | - | - | - | $b_{AOB}X_{AOB}$ |
| **5.Anoxic growth on nitrite** | - | - | - | - | - | $-i_{N,BM}$ | $-\frac{1-Y_{H,NOx}}{1.71\cdot Y_{H,NOx}}$ | - | $\frac{1-Y_{H,NOx}}{1.71\cdot Y_{H,NOx}}$ | $\mu_{max,H}\eta_H\frac{K_{I,O_2}}{K_{I,O_2}+S_{O_2}}\frac{S_{NH_4}}{K_{NH_4,H}+S_{NH_4}}\frac{X_{STO}/X_H}{K_{STO}+(X_{STO}/X_H)}\frac{S_{NO_2}}{K_{NO_2,H}+S_{NO_2}}X_H$ |
| **6. Bacteria decay of heterotrophs** | - | - | $-1$ | - | - | - | - | - | - | - |
| **7.Transfer $O_2$** | - | - | - | - | - | - | - | 1 | - | $K_L a_{o2}(S_{o2^*}-S_{o2})$ |

**Table 3.3** Parameters of all the four models evaluated in this study along with their values used

| Parameter | Definition | Values | Source |
|---|---|---|---|
| $Y_{NH_4}$ | Algal growth yield on $NH_4$, g DW $g^{-1} NH_4{}^+N$ | 15.84 | Estimated |
| $Y_{HCO_3}$ | Algal growth yield on $NH_4$, g DW $g^{-1} HCO_3{}^-$ | 0.5494 | Estimated |
| $Y_{PO_4}$ | Algal growth yield on $NH_4$, g DW $g^{-1} PO_4{}^{3-}P$ | 110.93 | Estimated |
| $Y_{O_2}$ | Oxygen production yield by algae on $NH_4$, g $O_2$ $g^{-1}$ COD | 0.996 | Estimated |
| $\mu_{max,A}$ | Maximum specific growth rate of algae, $d^{-1}$ | 0.96 | Sasi et al., 2011 |
| $K_{NH_4,A}$ | Saturation constant for $S_{NH_4}$ for algae, g N $m^{-3}$ | 0.3 | Wolf et al., 2017 |
| $K_{HCO_3,A}$ | Half saturation constant for algae growth on $HCO_3$, g $HCO_3 m^{-3}$ | 3 | Decostere et al., 2013 |
| $K_{PO_4,A}$ | Half saturation constant for algae growth on $PO_4$, g $Pm^{-3}$ | 0.08 | Tyrrell et al., 1999 |
| $K_{I,A}$ | Half saturation constant for algae growth on I, µmol $m^{-2} s^{-1}$ | 0.1 | Zambrano et al, 2016 |
| $b_A$ | Algae decay, $d^{-1}$ | 0.1 | Reichert et al., 2001 |
| $\mu_{max,AOB}$ | Maximum specific growth rate of AOB, $d^{-1}$ | 0.9 | Kaelin et al., 2009 |
| $K_{O_2,AOB}$ | Saturation constant for $S_{O_2}$ for AOB, g $O_2 m^{-3}$ | 0.79 | Manser et al., 2005 |
| $K_{NH_4,AOB}$ | Saturation constant for $S_{NH_4}$ for AOB, g $Nm^{-3}$ | 2.4 | Wiesmann et al., 1994 |
| $i_{N,BM}$ | N content of bacterial biomass ($X_H$, $X_{AOB}$, $X_{NOB}$) g N $(gCOD_{X_{BM}})^{-1}$ | 0.07 | Henze et al., 2000 |
| $Y_{AOB}$ | Aerobic yield of $X_{AOB}$ g $COD_{X_{AOB}}$ $(g\ COD_{S_{NH_4}})^{-1}$ | 0.2 | Sin et al., 2008 |
| $b_{AOB}$ | Respiration rate constant for AOB, $d^{-1}$ | 0.061 | Iacopozzi et al. 2007 |
| $\mu_{max,NOB}$ | Maximum specific growth rate of NOB, $d^{-1}$ | 0.65 | Kaelin et al., 2009 |
| $K_{O_2,NOB}$ | Saturation constant for $S_{O_2}$ for NOB, g $O_2 m^{-3}$ | 0.47 | Manser et al., 2005 |
| $Y_{NOB}$ | Aerobic yield of $X_{NOB}$, g $COD_{X_{NOB}}$ $(g\ COD_{S_{NO_2}})^{-1}$ | 0.05 | Sin et al., 2008 |
| $K_{NO_2,NOB}$ | Saturation constant for $S_{NO_2}$ for NOB, g $NO_2{}^-$ N $m^{-3}$ | 0.28 | Manser et al., 2005 |
| $K_{I,NH_4}$ | Ammonia inhibition of nitrite oxidation, g $NH_4{}^+$ N $m^{-3}$ | 5 | Iacopozzi et al., 2007 |
| $b_{NOB}$ | Respiration rate constant for AOB, $d^{-1}$ | 0.061 | Iacopozzi et al., 2007 |
| $\mu_{max,H}$ | Maximum specific growth rate of heterotrophs, $d^{-1}$ | 2 | Henze et al., 2000 |
| $\eta_H$ | Anoxic reduction factor for heterotrophs | 0.6 | Henze et al., 2000 |
| $Y_{H,NO_x}$ | Anoxic yield of $X_H$, g $COD_{X_H}$ $(g\ COD_{X_{STO}})^{-1}$ | 0.54 | Henze et al., 2000 |

| | | | |
|---|---|---|---|
| $\mathbf{K_{I,O_2}}$ | Oxygen inhibition for heterotrophs, g $O_2 m^{-3}$ | 0.2 | Kaelin et al., 2009 |
| $\mathbf{K_{NH_4,H}}$ | Saturation constant for $S_{NH_4}$ for heterotrophs, g N $m^{-3}$ | 0.01 | Henze et al., 2000 |
| $\mathbf{K_{STO}}$ | Saturation constant for $X_{STO}$, g $COD_{X_{STO}}$ $\left(g\ COD_{X_H}\right)^{-1}$ | 1 | Henze et al., 2000 |
| $\mathbf{b_H}$ | Aerobic endogenous respiration rate for heterotrophs, $\mathbf{d^{-1}}$ | 0.1 | Iacopozzi et al., 2007 |
| $\mathbf{K_L a_{o2}}$ | Mass transfer coefficient of $O_2$. $d^{-1}$ | 4 | Solimeno et al., 2015 |
| $\mathbf{S_{o2^*}}$ | Saturation concentration for $O_2$ in water, g $O_2 m^{-3}$ | 8.58 | Estimated |

This study assumes autotrophic growth of NOB based on dissolved nitrite produced by AOB, thus oxidizing the nitrite formed into nitrate. The growth rate of NOB ($R_5$) is modeled as the product of NOB biomass concentration ($X_{NOB}$), maximum specific growth rate ($\mu_{max,NOB}$) and switching function for oxygen, ammonium and ammonia inhibition as represented in Equation (3.10).

$$R_5 = \mu_{max,NOB} \frac{S_{O_2}}{K_{O_2,NOB}+S_{O_2}} \frac{S_{NO_2}}{K_{NO_2,AOB}+S_{NO_2}} \frac{K_{I,NH_4}}{K_{I,NH_4}+S_{NH_4}} X_{NOB} \quad (3.10)$$

Equation 3.11 describes the oxidation of $NH_4^+$ to $NO_2^-$ by AOB.

$$NO_2^- + 0.5\ O_2 \rightarrow NO_3^- \quad (3.11)$$

where, $K_{O_2,NOB}$ is the half saturation constant for $S_{O_2}$, $K_{NO_2,AOB}$is the half saturation constant for $S_{NO_2}$ and $K_{I,NH_4}$ is the inhibition constant of nitrite reduction due to ammonia.

The rate of NOB decay ($R_6$) is expressed as the product of the NOB biomass concentration ($X_{NOB}$) and its specific decay rate ($b_{NOB}$) as shown in Equation (3.12)

$$R_6 = b_{NOB} \cdot X_{NOB} \qquad (3.12)$$

Denitritation in this study is attributed to MUD population, which is heterotrophic and this conversion reaction uses dissolved nitrite and methanol to produce nitrogen gas. The rate of MUD growth ($R_7$) on nitrite is modeled as the product of its maximum specific growth rate ($\mu_{max,H}$),

anoxic reduction factor ($\eta_H$) and switching function for oxygen inhibition, ammonium, organic stored by heterotrophs, nitrite and heterotrophic biomass concentration, and the same is expressed as follows (Equation 3.13).

$$R_7 = \mu_{max,H}\eta_H \frac{K_{I,O_2}}{K_{I,O_2}+S_{O_2}} \frac{S_{NH_4}}{K_{NH_4,H}+S_{NH_4}} \frac{X_{STO}/X_H}{K_{STO}+(X_{STO}/X_H)} \frac{S_{NO_2}}{K_{NO_2,H}+S_{NO_2}} X_H \quad (3.13)$$

where, $K_{I,O_2}$ is a constant for inhibition due to oxygen, $K_{NH_4,H}$ is half saturation constant for $S_{NH_4}$, $K_{STO}$ is the half saturation constant for $X_{STO}$ and $K_{NO_2,H}$ is the half saturation constant for $S_{NO_2}$.

Equation 3.14 describes the utilization of $NO_2^-$ formed with along with $CH_3OH$ to produce $N_2$ gas by MUD.

$$8NO_2^- + 3CH_3OH + 11H^+ \leftrightarrow 4N_2 + 5CO_2 + 10H_2O \quad (3.14)$$

Decay rate of heterotrophs is expressed as the product of its biomass concentration ($X_H$) and its specific decay rate ($b_H$) as per Equation (3.15)

$$R_8 = b_H \cdot X_H \quad (3.15)$$

The transfer of $O_2$ between the liquid and head space ($R_9$) is expressed as the oxygen volumetric mass transfer coefficient ($K_L a_{o2}$) according to Equation (3.16)

$$R_9 = K_L a_{o2}(S_{o2^*} - S_{o_2}) \quad (3.16)$$

Where $S_{o2^*}$ is the saturation concentration of oxygen in water.

### 3.2.5 Effect of different ammonium, pH and DO concentration on BNR

In order to study the effect of different ammonium, pH and DO concentration on nitrogen removal by algae-AOB-MUD consortium, experiments were carried out with the PSBR by varying the

levels of these factors one at a time (Table 3.4). For maintaining the DO level in the experiments, the total air and $N_2$ flow were set at 1.0± 0.2 L/min and 2.0± 0.2 L/min, respectively. Other

**Table 3.4:** Experimental scheme followed for evaluating the effect of ammonium, DO and pH on nitrogen removal in the study

| Test series | pH | $NH_4^+$-N (mg/L) | DO (mg/L) | Ammonium removal rate (mg N/L-hr) | Nitrite reduction rate (mg N/L-hr) |
|---|---|---|---|---|---|
| **1** | 8 | 200 | 0.45 | 21.46±1.2 | 27.46±1.34 |
| | 8 | 200 | 1.0 | 28.24±0.56 | 23.13±2.1 |
| | 8 | 200 | 1.5 | 28.53±1.23 | 22.25±1.2 |
| | 8 | 200 | 2.0 | 29.20±0.77 | 22.13±0.88 |
| | 8 | 200 | 2.55 | 29.73±0.23 | 20.44±1.2 |
| | 8 | 200 | Control | 8.16±0.22 | 28.24±2.34 |
| **2** | 7 | 200 | 0.45 | 20.78±1.1 | 25.45±1.45 |
| | 7 | 200 | 1.0 | 27.43±1.32 | 21.89±2.22 |
| | 7 | 200 | 1.5 | 27.5±1.45 | 20.34±1.89 |
| | 7 | 200 | 2.0 | 27.56±1.32 | 19.76±0.78 |
| | 7 | 200 | 2.55 | 27.63±0.89 | 19.01±0.97 |
| | 7 | 200 | Control | 8.2±0.12 | 26.45±0.56 |
| **3** | 8 | 50 | 0.45 | 6.88±1.67 | 12.56±0.34 |
| | 8 | 50 | 1.0 | 9.91±1.78 | 12.03±0.23 |
| | 8 | 50 | 1.5 | 10.00±2.3 | 10.34±0.12 |
| | 8 | 50 | 2.0 | 10.09±1.66 | 9.67±0.1 |
| | 8 | 50 | 2.55 | 10.19±0.56 | 9.56±0.67 |
| | 8 | 50 | Control | 8.23±0.34 | 20.13±2.56 |

conditions such as agitation, temperature, light intensity and light/dark period duration were maintained the same as mentioned previously. Also, methanol was added during the dark phase for denitritation by MUD. For comparing the results of nitrogen removal in this study, a separate set of experiments without DO control in the PSBR were carried out. Another set of two experiments were carried out to check the effect of different DO concentration and methanol addition at the beginning of light and dark period i.e step wise decrease during the light period and step wise increase during the dark period on $NH_4^+$oxidation by algae-AOB and $NO_2^-$ reduction by MUD in the PSBR.

### 3.2.6 Analytical methods

Analysis of ammonium ($NH_4^+$-N), nitrate ($NO_3^-$-N), nitrite ($NO_2^-$-N), were carried out according to the standard methods (APHA et al., 2012). Chlorophyll a, b and carotenoids were determined according to Cuaresma et al. (2011) and for which the following modified Arnon's Equations (3.17-3.19) were used.

$$Chl_b=(16.72\times A_{665}-9.16\times A_{652})\times \text{dilutionfactor } [mgL^{-1}] \quad (3.17)$$

$$Chl_a=(34.9\times A_{652}-15.28\times A_{665})\times \text{dilutionfactor } [mgL^{-1}] \quad (3.18)$$

$$Car_{tot}=\frac{\text{dilutionfactor}\times 1000\times A_{470}-1.63\times Chl_a-104.96\times Chl_b}{221}\ [mgL^{-1}] \quad (3.19)$$

where $A_{665}$, $A_{652}$, and $A_{470}$ denote the absorbance of the culture at 665, 652 and 470 nm, respectively.

Sludge volume index (SVI) and sedimentation rate, volatile suspended solids (VSS) and total suspended solids (TSS) were calculated based on the equations (3.20), (3.21) and (3.22), respectively and the floc size of biomass was determined by using an optical microscope (Model

YS 100, Nikon, USA). For SVI analysis in this study, sample of 1L volume was taken during the settling period (1 hr) of the SBR operation and returned back to the bioreactor immediately after the test. All the experiments were carried out in triplicates and results were reported as mean ± standard deviation. It can be observed from the results that the standard deviation value is within ± 5% range, which shows good statistical validity of the experimental data.

$$\text{SVI} = \frac{\text{Settled sludge volume } (\frac{\text{mL}}{\text{L}}) \times 1000}{\text{Suspended solids } (\frac{\text{mg}}{\text{L}})} \qquad (3.20)$$

$$\text{mg total suspended solids/L} = \frac{(\text{A-B}) \times 1000}{\text{Sample volume, mL}} \qquad (3.21)$$

where: A=weight of filter + dried residue, mg, and B=weight of filter, mg

$$mg\ volatile\ suspended\ solids/L = \frac{(A-B) \times 1000}{Sample\ volume,mL} \qquad (3.22)$$

where A = weight of residue + dish before ignition, mg, and B = weight of residue + filter or dish after ignition, mg.

Methanol concentration was measured by gas chromatography (GC) with flame ionization detection (FID). For determination of ammonia monooxgenase (AMO), nitrate reductase (NR), nitrite oxidoreductase (NOR), and nitrite reductase (NIR) activities, 10 ml of algae-bacterial culture were sonicated at 20 kHz and 4 °C for 5 min and centrifuged at 12000g and 4 °C for 10 min and the crude extracts in supernatant were used for the enzyme activity measurement (Zheng et al., 2011). Assays for AMO and NOR activity were carried out in serum bottles (10 ml) containing 100 µL crude extracts and 1.9 mL of 0.01 M phosphate buffer containing 2mM $(NH_4)_2SO_4$, pH 7.4 or 0.01 M phosphate buffer containing 1mM $NaNO_2$, pH 7.4. The serum bottles were shaken in a water bath at 30 ˚C for 30 min and then centrifuged instantly, followed by

measuring the increase of nitrite due to AMO activity or the decrease of nitrite due to NOR activity assay in the supernatant. The NR and NIR activities were estimated by using methyl viologen as the electron donor. A volume of 300 µL crude extracts was added to start the reaction in the serum bottle containing 0.01 M phosphate buffer (pH 7.4), 1mM $NaNO_3$ or 1 mM $NaNO_2$, 1mM methyl viologen and 5 mM sodium hyposulfite ($Na_2S_2O_4$) in a final volume of 2 mL. The incubation was carried out at 30 C for 30 min, followed by measuring the increase of nitrite in NR activity assay or the decrease of nitrite in NIR activity assay. All the experimental analyses were done in triplicates and the results were presented in figures and tables along with the average values.

## 3.3 Results and discussion

### 3.3.1 Identification of algae

By 23S rRNA sequence analysis and fitting the results to GenBank databases through BLAST, the algal isolate was identified as *Chlorella sorokiniana* which showed 99 % similarity with one known strain (Fig. 3.3). The sequence results obtained was submitted to GenBank with accession number MH379981.The genus chlorella is a member of the family chlorophyceae.

### 3.3.2 Nitritation and denitritation in start-up phase and BNR phase


**Fig.3.3** Phylogram showing similarity between *Chlorella sorokiniana* and related species based on 23srRNA gene sequence of the algae isolated in this study

The algae-AOB consortium during the start-up phase showed excellent biomass growth by utilizing the ammonium rich wastewater. The start-up phase with the PSBR was followed by the

BNR phase and during both these phases several parameters, including TSS, VSS, DO, SVI, $NH_4^+$, $NO_2^-$, $NO_3^-$, chlorophyll a, chlorophyll b and carotenoids, were monitored. DO concentration profile in the PSBR (Fig. 3.4a) reveals that the average DO concentration during the start-up phase was 6.5 mg $O_2$ /L, which decreased to 0.84 mg $O_2$/L at the beginning of the BNR phase. The average concentrations of TSS, VSS, sedimentation rate and SVI during the start-up phase were 1006 ±100 mg/L, 639 mg/L, 0.4 m $h^{-1}$ and 24 ml/g which increased to 1930 mg/L, 1240 mg/L, 0.7 m $h^{-1}$ and 41 ml/g, respectively, at the end of the start-up phase (Fig. 3.4b). An increase in the TSS, VSS, sedimentation rate and SVI at the end of the start-up phase is due to the addition of MUD in the bioreactor. The average concentrations of chlorophyll a, chlorophyll b and carotenoid during the start-up phase were 10.86±0.5, 4.92±1.0 and 0.45 mg/L which were found to be high (34.5, 6.7 and 0.93 mg/L, respectively) during the BNR phase (Fig. 3.4c). Whereas the values of chlorophyll a and b indicate high algal biomass growth, low value of carotenoid obtained

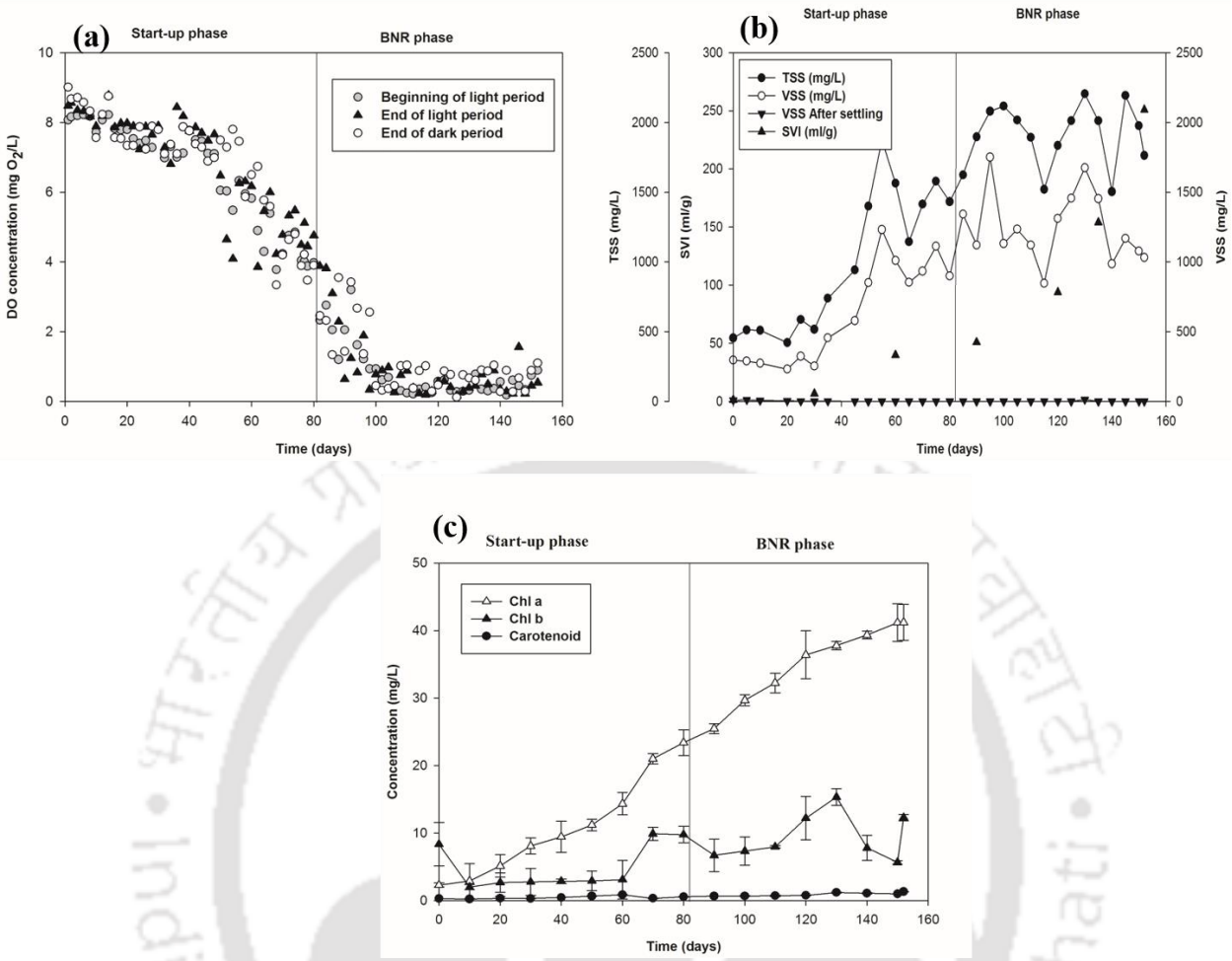


**Fig.3.4** Time profile of (a) dissolved oxygen, (b) VSS, TSS, SVI and (c) chlorophyll a and b, carotenoids concentrations in the photo-sequencing batch reactor.

in the study indicates the absence of oxidative photosynthesis, which usually takes place under stress conditions, such as high light intensity, high salt content, high temperature, etc. (Karya et al. 2013). Value of SVI of the algal-AOB consortium during the BNR phase was estimated to be 51 ml/g. The ammonium removal rate during light period of the start-up phase was determined to be 7.69 of $NH_4^+$-N $L^{-1}h^{-1}$. For a better understanding of nitrogen removal in the PSBR, samples were taken every two hours during the entire BNR phase. Fig. 3.5 shows the profile of various nitrogen species, pH, DO, methanol and alkalinity during the experiments. It can be seen that during the

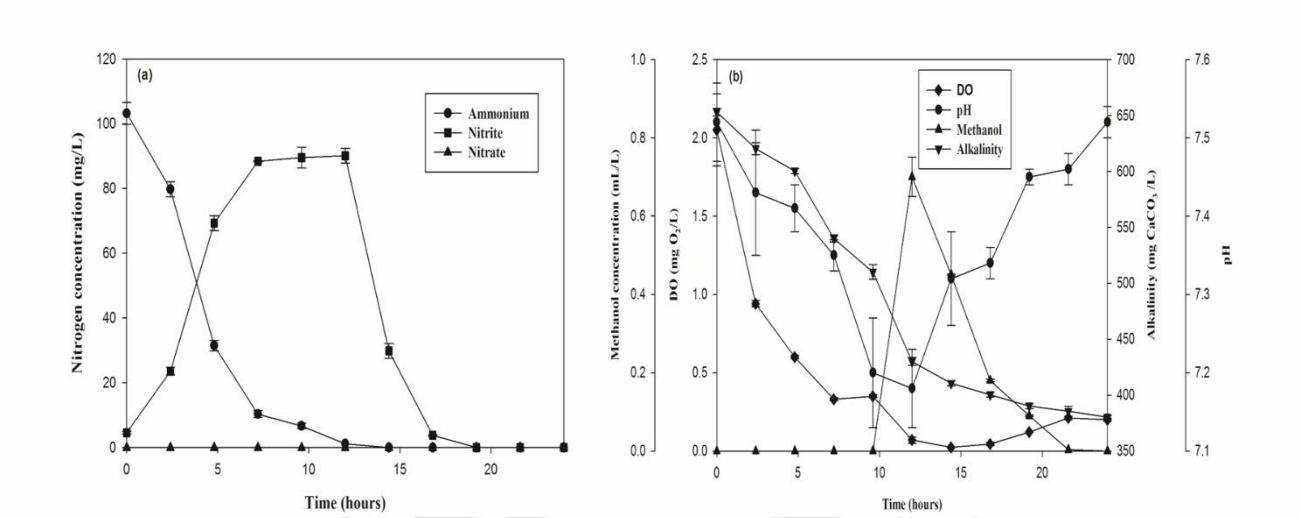


**Fig.3.5** Concentration of nitrogen (a) and DO, pH, methanol and alkalinity (b) in the photo-sequencing batch reactor during the BNR phase.

light period $NH_4^+$-N, pH, alkalinity, and DO decreased whereas $NO_2^-$-N increased due to AOB activity in the PSBR; during the dark period, decrease in both methanol and $NO_2^-$-N were observed due to MUD activity. The decrease in pH during the light period is due to the release of $H^+$ ions caused by oxidation of ammonia by AOB. Whereas increase in pH during the dark period is due to the release of $OH^-$ ions caused by reduction of nitrite by MUD. These results were further supported by the fact that methanol concentration remained constant during the light period whereas $NH_4^+$-N and alkalinity concentrations remained constant during the dark period. It is reported that even in the presence of $NO_2^-$, algae utilize ammonium for its growth (Wang et al., 2015). The average concentration of DO during the BNR phase was 2.23 mg/L $O_2$ during light period and it decreased to 0.03 mg/L during the dark period indicating that MUD activity was not inhibited due to a high DO concentration during the dark period. The concentrations of TSS, VSS, sedimentation rate and SVI during this phase were 1572 mg/L, 1112 mg/L, 0.7m $h^{-1}$and 50 ml/g, which increased to 1793 mg/L, 1032 mg/L, 1.7 m $h^{-1}$ and 256 ml/g, respectively. A similar trend was observed for chlorophyll a, chlorophyll b and carotenoid concentrations which increased from

24.5, 26.4 and 1.23 mg/L to 42, 12 and 15 mg/L, respectively. The maximum $NH_4^+$ removal rate (ARR) and $NO_2^-$reduction rate(NRR) during the light and dark periods of this phase were determined to be 8.09 of $NH_4^+$-N $L^{-1}h^{-1}$and 28.12 of $NO_2^-$-N $L^{-1}h^{-1}$, respectively. Nitrogen metabolism during the start-up phase and BNR phase with the PSBR was calculated based on influent ammonium loading (Wang et al., 2015) and the results were presented in **Table 3.5,** which confirmed that during the start-up phase, ammonium was removed via nitrite formation.

**Table 3.5** Metabolism of $NH_4^+$-N during the start-up and BNR phase

| **Phase** | **Effluent $NH_4^+$-N (%)** | **Effluent $NO_2^-$-N (mg/L)** | **Effluent $NO_3^-$-N (%)** | **Biomass uptake** | **Denitritation** |
|---|---|---|---|---|---|
| Start-up phase | 2.48 | 79.78 | 1.32 | 16.42 | 1.11 |
| BNR phase | BDL | BDL | 0.32 | 18.2 | 82.12 |

The activity of NOB and denitrifier were negligible during the start-up phase due to the following conditions: high $NH_4^+$concentration, low DO concentration and lack of organic carbon source (Ma et al., 2015; Wang et al., 2015). Furthermore, during the start-up phase, biomass (algae, AOB and MUD) contributed to 16.42% nitrogen removal in the PSBR. Upon methanol addition at the beginning of dark period (BNR phase), the ratio of ammonium removed by denitritation was

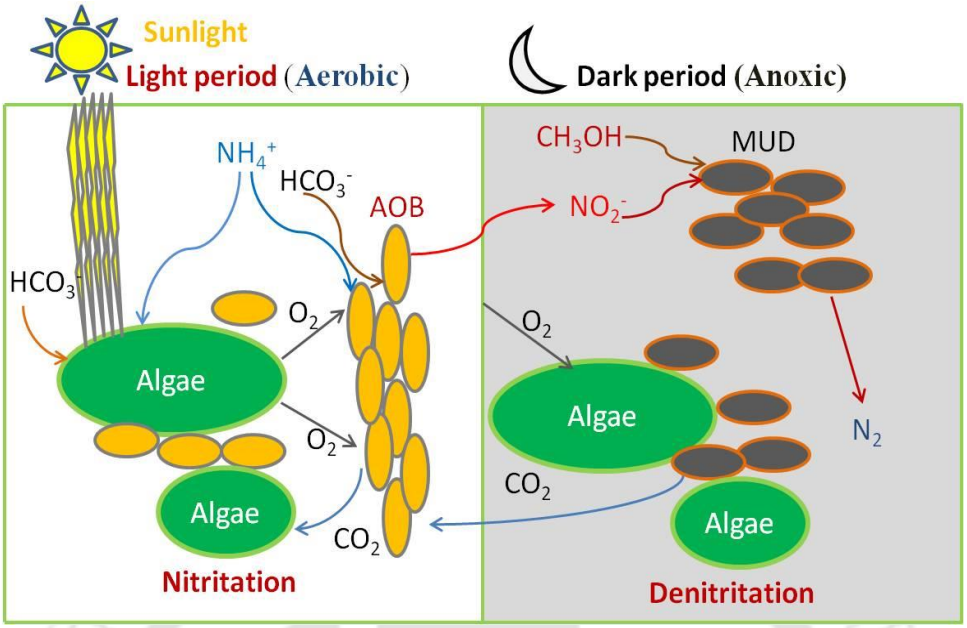


**Fig. 3.6.** Schematic showing the mechanism involved in shortcut nitrogen removal using the algae-bacterial consortium.

significantly high with negligible effect on the algal growth. Thus, over 99% of ammonium was removed by denitritation in the BNR phase without nitrate formation in comparison with only 90% nitrogen removal efficiency observed by Wang et al. (2015).

A major factor for the observed shortcut nitrogen removal in this study is the inhibition of NOB, which is more sensitive than AOB to free ammonia and free nitrous acid (Ma et al., 2015). As the high-strength ammonium wastewater used in this study contained an initial ammonium concentration more than 50 mg/L, (equivalent to 2.4 mg/L of free ammonia) and $NO_2^-$ was accumulated during the start-up phase, which is higher than 1.5 mg/L of free ammonia and 0.013 mg/L of free nitrous acid concentrations, NOB activity was inhibited under these conditions (Ma el al., 2015; Vadivelu et al., 2006; Villaverde et al., 1997). Such alternating inhibitory conditions due to free ammonia and free nitrous acid have been shown to promote the activity of AOB over NOB for nitrogen removal. The low DO concentration (less than 0.5 mg/L) in the start-up phase

also favored inhibition of NOB and as a result of which nitrite was accumulated without nitrate formation (Picaioreanu et al., 1997; Schrammet al., 1999, 2000). The combination of high ammonium and nitrite along with low DO concentration are thus attributed to nitritation by AOB during the light period; the nitrite produced was subsequently reduced by MUD during the dark period in the presence of methanol, thereby achieving shortcut nitrogen removal by algae-AOB-MUD consortium in the PSBR. A schematic showing the mechanism involved in shortcut BNR using the algae-bacterial consortium is depicted in Fig. 3.6.

### 3.3.3 Effect of different pH, initial ammonium and DO concentration on nitrogen removal

Fig.3.7 shows that change in DO, pH and $NH_4^+$concentration resulted in an immediate change in $NH_4^+$ oxidation and $NO_2^-$ reduction. In all the three set of experiments, $NH_4^+$ oxidation increased with an increase in DO concentration from 0.45 to 2.55 mg/L of $O_2$. An increase in both $NH_4^+$ concentration (from 50 mg $NH_4^+$-N/L to 200 mg $NH_4^+$-N/L) and pH (from 7 to 8) resulted in an enhanced $NH_4^+$ oxidation in this study. Conditions that favored the specific ammonium oxidation rate (AOR) and nitrite reduction rate (NRR) are shown in Fig. 3.7(a) and 7(b). The activity of nitrite. oxidizing bacteria (NOB) was negligible as the $NO_3^-$ concentration was less than 1 mg $NO_3^-$-N $L^{-1}$ during the start-up phase as well as during the BNR phase. The very low concentration of nitrate is due to both negligible NOB activity and unutilized nitrite in the medium. The results of $NH_4^+$oxidation and $NO_2^-$ reduction obtained under different conditions of pH, DO and initial $NH_4^+$ concentration were further confirmed by a step wise increase or decrease in DO and methanol addition at the beginning of light and dark period. From Fig. 3.9, under aerobic condition. (0.45 to 2.55 DO mg/L), an increase or decrease in the DO concentration significantly affected both $NH_4^+$ oxidation and $NO_2^-$ reduction (Figure 3.9(a) and (b)).

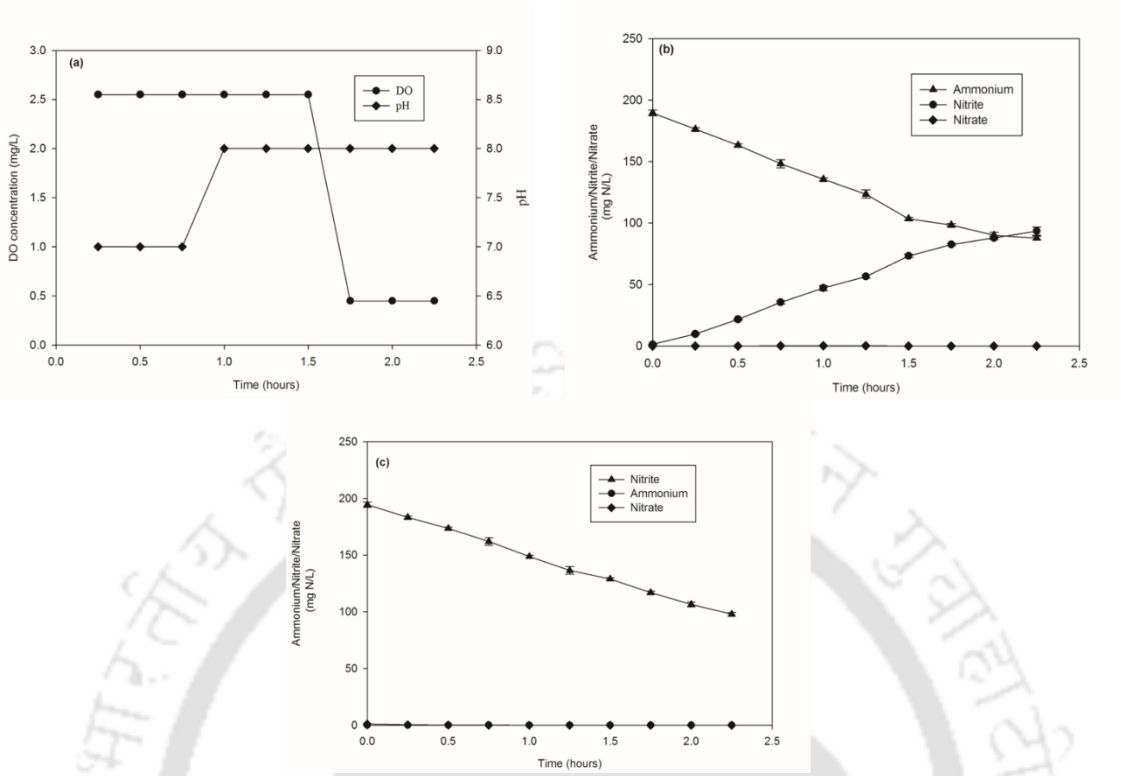


**Fig.3.7.** Profile of (a) DO and pH (b) concentrations of $NH_4^+$, $NO_2^-$ and $NO_3^-$during the experiments to study the effect of pH, DO and initial ammonium concentration on nitrogen removal, and (c) Nitrite reduction with methanol as the organic carbon source.

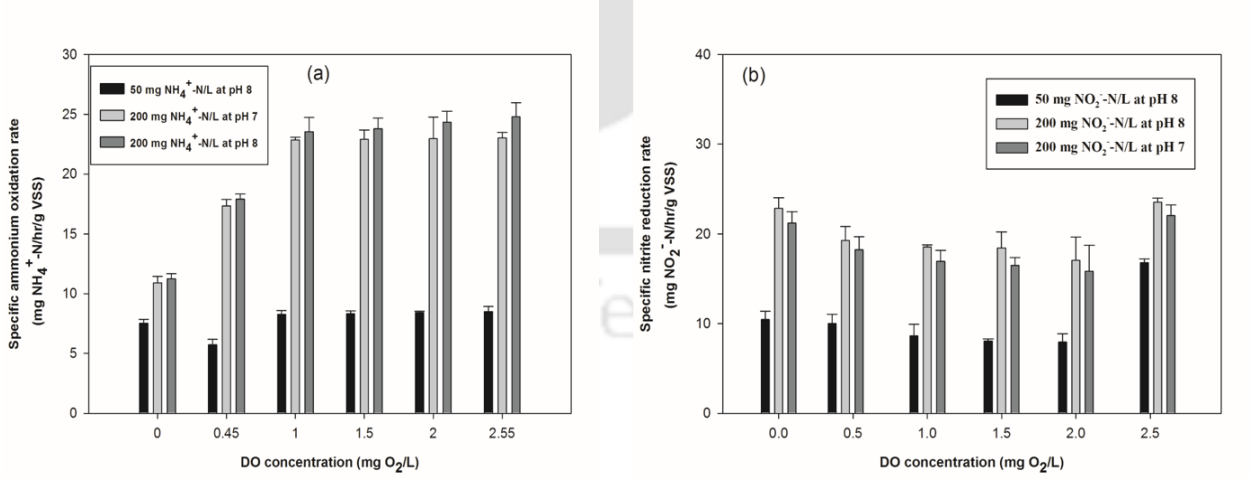


**Fig. 3.8.** Combined effect of varying DO, pH and $NH_4^+$ concentration on (a) specific ammonium oxidation rate and (b) specific nitrite reduction.

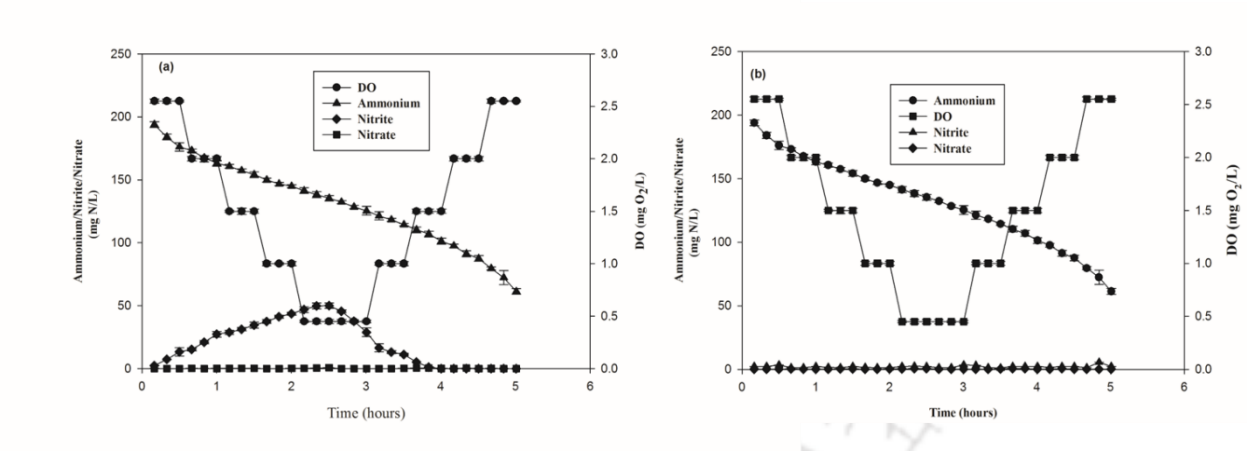


**Fig.3.9.** Effect of step wise decrease and step wise increase in DO on ammonium oxidation and nitrite reduction adding methanol addition at (a) beginning of the dark period and (b) methanol addition at beginning of light period

This is mainly because an increase in DO concentration from 0.45 to 2.55 caused an increase in AOR with a minimum at 4.02 mg $NH_4^+$-N g $VSS^{-1}$ $h^{-1}$, but the $NO_2^-$ reduction showed a reverse trend, i.e. it decreased when DO concentration was increased (Fig. 3.8 (a) and (b)). Oxygen involved in this process is directly related to oxidation of ammonium by AOB. Based on the stoichiometric calculation, oxygen utilized was estimated to be 80 mg/L. Ammonium oxidation during the start-up phase and BNR phase was further found to be directly associated with the activities of various key enzymes present in the algae-bacterial consortium (Table 3.6). The average activities of these enzymes, viz. AMO, NOR, NR and NIR during the start-up phase were 0.064, 0.001, 0.00014 and 0.021 µmol nitrite/min·mg protein, respectively, and the activities of the same enzymes during the BNR phase were 0.066, 0.00013, 0.00012 and 0.078 µmol nitrite/min·mg protein, respectively.

**Table 3.6:** Enzyme activities of ammonia monooxygenase (AMO) (µmol nitrite /min.mg protein), nitrite oxidoreductase (NOR) (µmol nitrate /min.mg protein), nitrate reductase (NR) (µmol nitrite /min.mg protein) and nitrite reductase (NIR) during (a) start-up phase and (b) BNR phase

| **Enzyme activity** | **AMO (µmol nitrite /min·mg protein)** | **NOR (µmol nitrate /min·mg protein)** | **NR (µmol nitrite /min·mg protein)** | **NIR µmol nitrite /min·mg protein** |
|---|---|---|---|---|
| Start-up phase | 0.064±0.002 | 0.0001 | 0.00034 | 0.00014 |
| BNR phase | 0.066±0.0058 | 0.0001 | 0.00012 | 0.078±0.0023 |

Based on $NH_4^+$ metabolism in the PSBR experiments, nitritation and denitritation were found to occur during both light and dark periods when methanol was added at the beginning of each of these two periods (Fig. 3.9). The results of simultaneous nitritation and denitritation along with low DO concentration in the PSBR demonstrate the existence of both aerobic and anoxic zones in the biomass present in the PSBR. It is reported that floc formation due to algae-bacterial consortium facilitates DO gradient inside the floc structure, which is beneficial for maintaining an aerobic activity of AOB exterior to the floc, whereas inner portion of the floc remains anoxic thereby favoring MUD activity for denitrification. Hence, the specific nitrite reduction rate observed in this study remained mostly unaffected in presence or absence of DO. This is despite the fact that DO concentration in the PSBR was less than 2.55 mg/L during light and dark periods, which is in agreement with the results reported by other researchers in the literature (Karya et al., 2013; Manser et al., 2016; Wang et al., 2015).

Methanol as an organic carbon source proved effective as an electron donor for denitritation in this study. Based on the $NH_4^+$ loading rate and $NO_2^-$production in the PSBR during the BNR phase, the methanol requirement was estimated to be 0.75 ml/L. d. Besides MUD, *Chlorella sp* have been

shown to utilize methanol as an organic carbon source (1% (v/v)) with a maximum biomass concentration of 4.2 g dry wt/L. Moreover, *Chlorella sp* is known to exhibit heterotrophic metabolism during the dark conditions, which enables it to compete with MUD for available methanol during the BNR phase (Choi et al., 2011; Perez-Garcia et al., 2011).

### 3.3.4. Validation of the experimental results with metabolic models

Experimental vs predicted results of oxygen consumption, ammonium oxidation, nitrite reduction and nitrite oxidation due to the different metabolic models are shown in figure 3.10. It could be seen that the experimental results did not match well with the values predicted by Models 2 and 3 as these models considered NOB activity, which was however not present in the algae-bacterial consortium. On the other hand, the models 1 and 4 accurately predicted the experimental data on ammonium oxidation, nitrite reduction and algal photosynthetic oxygen production during the start-up phase and BNR phase. However, this model did not consider the effect of methanol on algae growth or AOB in this study.

This is the first study to demonstrate a clear correlation among algal photosynthesis, ammonium oxidation and nitrite reduction in an algae-bacterial consortium. In a previous study by Arashio et al. (2017) and Zambrano et al. (2016) a simple model for algae bacterial consortium was used to describe dissolved oxygen profile and nitrate oxidation by NOB. However, the values ranged between 26.9 and 96 mg $NH_4^+$-N $L^{-1}$ with nitrate as an intermediate. In this study, growth due to algae or MUD on nitrate was not observed owing to the inhibition of NOB. Moreover, a direct correlation between $NH_4^+$ oxidation and $NO_2^-$reduction is observed which is attributed to $NH_4^+$ oxidation by AOB during the light period and $NO_2^-$ reduction by MUD during the dark period without the formation of nitrate as an intermediate.

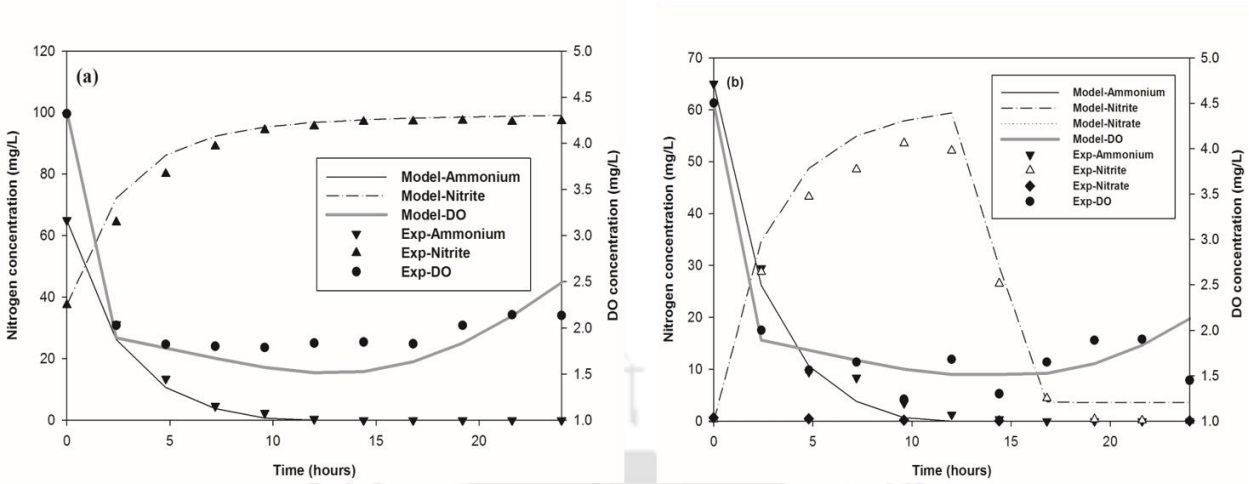


**Fig. 3.10**. Experimental and predicted values for DO consumption, ammonium oxidation, nitrite reduction and nitrate oxidation: (a) Model 1: algae-AOB pathway and (b) model 4: algae-AOB-MUD pathway.

The results obtained in this study are also in agreement with a previous study which showed that ammonium oxidation increased with an increase in DO concentration, whereas nitrite reduction was high at low DO concentration (Wang et al., 2015). Thus, the high concentrations of ammonium and DO in the absence of methanol resulted in a high ammonium oxidation and very low nitrite reduction during the light period, which subsequently lowered the DO concentration during the dark period. In the presence of methanol, the low DO concentration and high nitrite concentration resulted in a high nitrite reduction efficiency. These results reveal a strong association among the algae-AOB-MUD for achieving shortcut nitrogen removal via $NH_4^+$ oxidation and $NO_2^-$ reduction.

By fitting the experimental data to the four metabolic models, the nitrogen removal in this study was found to involve algae-AOB and MUD for nitritation and denitritation, respectively. The oxygen produced during algal photosynthesis was previously demonstrated to be used for $NH_4^+$ oxidation during the light period followed by $NO_2^-$ reduction during the dark period without nitrate formation as an intermediate step (Wang et al., 2015). In a previous study by Manser et al. (2016)

and Wang et al. (2013), high ammonium concentration and low DO concentration along with free nitrous acid and free ammonia were found to be necessary for NOB inhibition (Vadivelu et al., 2006). At a high DO concentration, no $NO_3^-$ formation was observed even when high amount of $NO_2^-$ was accumulated due to ammonium oxidation.

In this study, the model based on algae-AOB pathway does not describe the effect of increased $NO_2^-$ accumulation observed during the start-up phase. However, such an increase in $NO_2^-$ accumulation during the transition from light to dark period has previously been reported due to algae-AOB activity as a result of $NH_4^+$oxidation (Karya et al., 2013). Because, maximum $NO_2^-$ reduction in this study was observed during the dark period and $NO_3^-$ production rate was negligible (less than 1 mg/L of $NO_3^-$ -N), the ammonium oxidation mechanism involved is attributed to algae-AOB pathway only. A major challenge for this pathway is the oxygen produced by algal photosynthesis in the presence of light for ammonium oxidation and the dark period

required for $NO_2^-$ reduction (Wang et al., 2015). The increased activities of NIR and NR enzymes during the start-up phase (Table 3.6) further indicate that algae as well contributed to the utilization of $NO_2^-$ and $NO_3^-$ under ammonium limiting conditions (Glass et al., 2009; Solomonson, 1975). It could also be reasoned on the growth of denitrifier on cell lysate produced organic carbon for de-nitrification during the dark period, which however needs to be further confirmed. Hence, it could be surmised that the mechanism involved in $NO_2^-$ reduction by algae in the presence of light is likely different from that responsible for ammonium uptake, as strongly demonstrated by the NIR activity during the start-up phase (Table 3.6).

Zheng et al. (2011) reported that BNR is affected due to the activity of AMO, NOR, NIR and NR. In this study, the BNR phase is recognized as the key to shortcut nitrogen removal by algae-bacterial consortium (Wang et al., 2015). $NO_2^-$ produced by AOB was converted to dinitrogen gas

by MUD with a maximum conversion efficiency of 99 %. This value is so far the highest as compared with the values reported in the literature using other shortcut nitrogen removal method employing such algae-bacterial systems (Karya et al., 2013; Manser et al., 2016; Wang et al., 2015).

This work shows that a high $NH_4^+$and $NO_2^-$ concentration along with a low DO concentration suppress NOB activity and avoids $NO_3^-$ production thus leading to shortcut nitrogen removal at a quick rate. Ammonium concentration used in the present study (100 – 200 mg/L) was well beyond the ammonium concentration of 5 – 20 mg/L, noticed in real wastewater like aquaculture wastewater (Andreotti et al., 2020; Lang et al., 2020). Further, almost 100% ammonium removal was observed with an initial ammonium concentration of 100 mg/L which endorses the feasibility of the current strategy in treating industrial wastewater. It is recognized that the gene structure and gene regulation of microalgae, AOB and denitrifier in response to $NH_4^+$, $NO_2^-$and DO differ even among closely related species. The control and regulation of oxygen production and $NH_4^+$ uptake by algae, $NH_4^+$ oxidation by AOB, $NO_2^-$ reduction by MUD may also change in different algal-bacterial strains and isolates (Cua and Stein,

2011; Ramanan et al., 2016). Therefore, the cultivation condition of the algae-AOB-MUD consortium under high concentration of $NH_4^+$, $NO_2^-$, and methanol and at low DO concentration seem to be highly essential for achieving the desired results of shortcut nitrogen removal demonstrated in this study.

### 3.4. Significant findings

The hybrid photosynthesis-nitritation-denitritation process using algae-AOB-MUD consortium is highly suited for treating $NH_4^+$ rich wastewater at a quick rate. Alternating high concentrations of

$NH_4^+$ and $NO_2^-$ along with a low level of DO concentration favored AOB over NOB activity in the algae-AOB-MUD consortium. Addition of methanol at the beginning of dark period resulted in almost complete removal of $NH_4^+$ via nitritation/denitritation. The association among algal photosynthesis, $NH_4^+$ oxidation and $NO_2^-$ reduction by the algae-bacterial consortium in the PSBR was successfully modeled based on metabolic models that incorporated algae-AOB and algae-AOB-MUD pathways.

# Chapter 4

## Effect of light intensity on nitrification by microalgae-nitrifying bacteria consortia in a photo-sequencing batch reactor

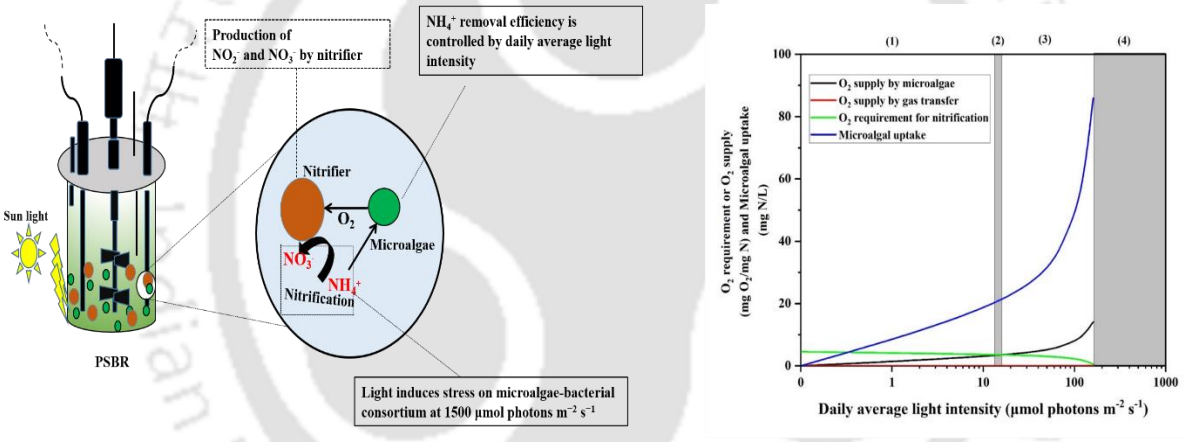

**ABSTRACT**

$NH_4^+$ removal by consortium of microalgae, AOB and NOB was examined in a photosequencing batch reactor under various light intensities (150, 500, 1500 and 2000 μmol photons $m^{-2}$ $s^{-1}$). Nitrification performance showed that the light stress tolerance of the consortium was up to 1500 μmol photons $m^{-2}$ $s^{-1}$ during the 12 h study. $NH_4^+$ removal efficiencies due to nitrification and microalgae uptake at 150, 500, 1500 and 2000 μmol photons $m^{-2}$ $s^{-1}$ light intensities are 100, 100, 6.2 and -2.2%, respectively. The nitrogen mass balance revealed that the microalgal-AOB-NOB consortium utilized 19.89% of supplied ammonium for the growth and maintenance of algae, whereas 79.29% was eliminated through bacterial nitrification process at 150 μmol photons $m^{-2}$ $s^{-1}$. Ammonium uptake and bacterial nitrification were affected at light intensity ≥ 1500 μmol photons $m^{-2}$ $s^{-1}$, thus revealing that ammonium removal mechanism is strongly governed by the daily average light intensity. Based on the empirical equations to predict the $O_2$ available to microalgal-AOB-NOB consortium by considering the effect of light intensity for the PSBR, were developed as follows: (i) below 40 μmol photons $m^{-2}$ $s^{-1}$: insufficient $O_2$ for nitrification; (ii) above 40 μmol photons $m^{-2}$ $s^{-1}$ : sufficient oxygen for nitrification with less than saturated dissolved oxygen; (iii) 40-160 μmol photons $m^{-2}$ $s^{-1}$: sufficient oxygen for nitrification with significant dissolved oxygen; (iv) above 160 μmol photons $m^{-2}$ $s^{-1}$: failure of nitrification, due to inhibition of microalgal-bacterial consortia.

## 4.1 Introduction

Anaerobic digestion is a widely practiced method for treating wastewater and solid waste, which tends to generate effluent with high concentrations of ammonium and phosphorous (Gong et al., 2019; Huang et al., 2019; Xie et al., 2019; Yan et al., 2019). High ammonium concentration in the anaerobic digestate poses serious environmental problems as well as it inhibits microalgae growth during its treatment (Gong et al., 2019; Xie et al., 2018). $NH_4^+$ removal from such wastewater can be achieved by microalgae-bacterial consortium. During this process $NH_4^+$ is first oxidized to nitrate via nitrification by oxygen from algal photosynthesis and nitrate or nitrite is subsequently reduced to $N_2$ by bacteria through the denitrification process under dark condition. In this method, algal photosynthesis is critical for nitrification and also for minimizing the need of an external carbon source for denitrification (Van der Steen et al., 2015).

Other advantages of using microalgae-AOB-NOB consortium for treating ammonium rich wastewater include good settleability of biomass (Wang et al., 2015), increased tolerance towards light inhibition without affecting the performance (Akizuki et al., 2020) and production of valuable biohydrogen, pigments, bio-fertilizers, bioplastics, etc. by the microalgae.

Among the different process parameters that influence $NH_4^+$ removal by microalgae-nitrifying bacterial consortium, oxygen balance and light intensity play important roles (Akizuki et al., 2020). A study by Wang et al. (2015) established that proper oxygen balance is important for improving the treatment process (oxygen required for nitrification, oxygen produced by microalgae and oxygen transfer by gas transfer). However, most of the studies on microalgae-AOB-NOB bacterial consortium have focused on using a maximum of up to 150 μmol photons $m^{-2}$ $s^{-1}$ in photobioreactor (Karya et al., 2013; Vargas et al., 2016; Wang et al., 2015), and there is very limited information on the effect of high light intensities.

In microalgae-nitrifying bacterial consortia, ammonium removal occurs through two different mechanisms: microalgal uptake and oxidation by nitrifier. However, if microalgae biomass concentration is low, $O_2$ supply through algal photosynthesis limits the nitrification efficiency (Akizuki et al., 2020; Azov and Goldman, 1982; González et al., 2008). Conversely, if microalgae biomass concentration is high, $O_2$ produced by microalgae may still affect nitrification due to accumulation of free ammonia and Reactive oxygen species. Hence, light intensity is key to control the $NH_4^+$ removal mechanism in microalgae-bacterial consortia (González et al., 2008). For instance, Akizuki et al. (2020) operated a photobioreactor with light intensity of 135 μmol photons $m^{-2}$ $s^{-1}$ and $NH_4^+$ concentration of 100 mg/L, and 36.1% $NH_4^+$ was removed by AOB and the remaining by microalgal uptake (63.9%). In a similar work by van der Steen et al. (2015), an algal-bacterial photobioreactor was operated at a light intensity of 66 μmol photons $m^{-2}$ $s^{-1}$ and $NH_4^+$ concentration of 66 mg $NH_4^+$-N/L, which revealed that nitrification contributed to 77% of $NH_4^+$ removal. Hence, the mechanism involved in controlling the $NH_4^+$ removal by light intensity in microalgae-bacterial consortia is not clear.

This study aimed to find the effect of various light intensities on $NH_4^+$ removal by microalgae-nitrifying consortia. In addition, other controlling parameters on the relative contribution of microalgal uptake, nitrification and $O_2$ gas transfer for $NH_4^+$ removal were examined.

## 4.2 Materials and methods

### 4.2.1 Enrichment of microalgae-bacterial consortium

Microalgae-bacterial consortium used in this study was obtained from a 3L parent PSBR treating ammonium rich wastewater. The PSBR was initially inoculated with *Chlorella sorokiniana* and activated sludge from IIT Guwahati wastewater treatment plant. The PSBR was operated under sequential batch mode with the following conditions: filling: 15 min, reaction: 9 h, settling 2.5 h

and decanting:15 min. Prior to the experiments, the ammonium concentration was gradually increased, which aided in acclimatizing the microalgae-nitrifying consortium to assimilate $NH_4^+$ in the system. Synthetic wastewater used in this study contained 5.63 g/L of $NH_4HCO_3$, 0.064 g/L of $KH_2PO_4$, 0.064 g/L of $K_2HPO_4$ and 2ml of trace element solution.

### 4.2.2 Effect of light intensity on ammonium removal

A 5L bioreactor (Sartorius, Biostat A, Germany) with a working volume of 2L was used in this study to examine the effect of light intensity in the range 150-2000 µmol photons $m^{-2}$ $s^{-1}$. Microalgae-nitrifying consortium were inoculated into PSBR to achieve 1.9 g $L^{-1}$ of volatile suspended solid (VSS). Throughout the experiments, the pH was maintained at 7.5 ± 0.05 by using 1 M $NaHCO_3$; initial DO in the experiments was set to 6 ± 0.03 mg $L^{-1}$ for all the experiments. The PSBR was operated continuously for 12 h without any external aeration, and throughout the experiments temperature and agitation were maintained at 30±1 °C and 120 rpm, respectively.

### 4.2.3 Analytical methods

Prior to the experiment, VSS concentration of the microalgae-AOB-NOB bacterial consortium was determined according to American Public Health Association (APHA, 2012). DO was monitored online using a polarographic probe (0-100%). During the experiments, samples were collected from PSBR at a regular interval of 0.25 h and filtered via 0.45 µm membrane filters for analysis. The $NO_2^-$-N and $NO_3^-$-N contents of the samples were determined by calorimetric method, whereas $NH_4^+$-N content was evaluated by phenate method (APHA, 2012).

### 4.2.4 Calculations

Nitrification efficiency using the PSBR at various light intensities in this study was determined as per the following equation: (4.1)

$$\text{Nitrification efficiency (\%)} = \frac{\text{Maximum accumulated } NO_X^-}{\text{Influent } NH_4^+} \times 100 \quad (4.1)$$

where maximum accumulated $NO_x^-$ and influent $NH_4^+$ refer to the maximum amount of $NO_2^-$ and $NO_3^-$ under various light intensities (0, 150, 500, 1500 and 2000 µmol photons $m^{-2}$ $s^{-1}$) at a specific $NH_4^+$ concentration.

Ammonium removal efficiency was calculated from the following equation: (4.2)

$$\text{Ammonium removal efficiency}(\%) = \frac{NH_{4\,Initial}^+ - NH_{4\,Final}^+}{NH_{4\,Initial}^+} \times 100 \quad (4.2)$$

where $NH_4^+{}_{Initial}$ and $NH_4^+{}_{Final}$ refer to initial and final ammonium concentrations, respectively. Ammonium balance at the end of experiment for each tests was calculated based on calculated nitrogen concentrations and stoichiometry of the nitrification reaction as represented by equation 4.3 (Karya et al., 2013).

$$NH_4^+ + 1.32O_2 + 0.8H_2O + 1.98HCO_3^- \rightarrow 0.021C_5H_7O_{110}NO_2 + 0.98NO_3^- + 2.02H_2O + 1.88H_2CO_3 \quad (4.3)$$

The amount of ammonium uptake by microalgae was calculated according to Karya et al. (2013) as represented in equation 4.4, in which ammonium volatilization was calculated according to Wang et al. (2015).

$$\begin{aligned}&\text{Amount of ammonium uptake by microalgae} = \text{Amount of}\\ &\text{initial } NH_4^+\text{-Amount of final } NO_X^-\text{ -Amount of ammonium uptake by nitrifier-}\\ &NH_3\text{volatilization}\end{aligned} \quad (4.4)$$

The individual contribution of microalgae and nitrifier towards ammonium removal was calculated according to Akizuki et al. (2020) as represented by equation 4.5 and 4.6, respectively.

$$\text{Contribution of microalgae (\%)}=100\text{-contribution of nitrifier} \quad (4.5)$$

$$\text{Contribution of nitrifier}(\%)=\frac{\text{Ammonium removal by nitrification}}{\text{Total ammonium removal}}\times 100 \quad (4.6)$$

Based on the experimental results obtained, linear regression method was employed to estimate the relative contribution of ammonium removal in PSBR for predicting parameters such as pH, temperature, light intensity, $NH_4^+$ concentration and daily average light intensity (DALI). This investigation is based on the experimental values reported in the literature and from this work considering microalgae-bacterial consortia (de Godos et al., 2009; Karya et al., 2013; Pizzera et al., 2013; van der Steen et al., 2015; Wang et al., 2015; Vargas et al., 2016; Muys et al.; 2018)

### 4.2.6 Development of empirical model equations

Linear regression analysis of the experimental results obtained in this study, revealed that DALI and $O_2$ gas transfer are the main parameters controlling $NH_4^+$ removal (Fig. 4.5)

Oxygen supplied by microalgae, oxygen supplied by gas transfer and total $O_2$ consumption for nitrification at different DALI were estimated using the correlation between DALI and the ammonium removal percentage due to nitrification ($y = -0.5436x + 106.33$, $R^2 = 0.9341$). Stoichiometric oxygen requirement for nitrifying bacteria in nitrate pathway was found to be 4.57 mg-$O_2$ mg-$N^{-1}$ (Table 4.1) (Muys et al., 2018). Values of oxygen production by microalgae, oxygen supplied by gas transfer and total oxygen requirement for nitrification at different DALI are presented in Table 4.2. and the same was shown in figure 4.6 in the form of plot.

Formulated empirical equations used in the model are as follows:

$$O_2 \text{ required for nitrification } (\text{mg } O_2 \text{ mg } N^{-1}) = 4.552 + \text{DALI} \times -0.0235 \quad (4.7)$$

$$O_2 \text{ produced by microalgae } (\text{mg } O_2 \text{ mg } N^{-1}) = 0.03 + \text{DALI} \times 0.0883 \quad (4.8)$$

$$O_2 \text{ supplied by gas transfer } (\text{mg } O_2 \text{ mg } N^{-1}) = -0.0028 + \text{DALI} \times 0.0007 \quad (4.9)$$

$$NH_4^+ \text{ uptake by microalgae} (\text{mg N } L^{-1}) = -0.02 + \text{DALI} \times 0.5095 \quad (4.10)$$

## 4.3 Results and discussion

### 4.3.1 PSBR performance

Nitrogen concentration in the PSBR at various light intensities is shown in Figure 4.1, which clearly reveals that $NO_3^-$ was formed due to $NH_4^+$ oxidation. However, change in nitrogen removal is observed with respect to the different light intensities. For instance, at the light intensities 150 and 500 µmol photons $m^{-2}$ $s^{-1}$, nitrification sustained until the end of light period, with the $NO_3^-$concentrations reaching 77.18 and 74.02 mg-N $L^{-1}$, respectively.

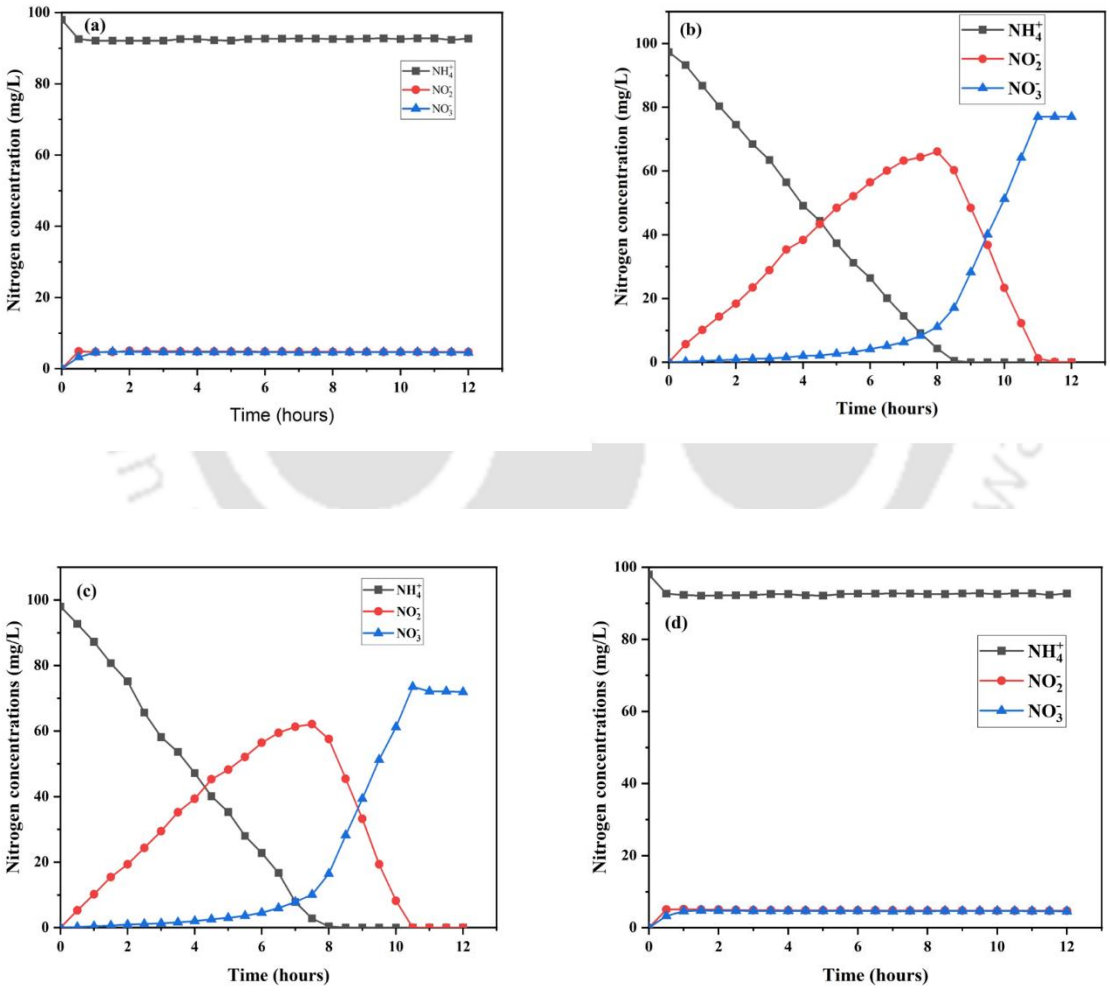

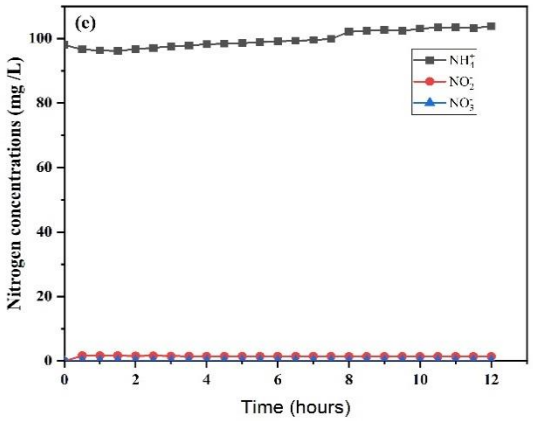


**Fig.4.1.** Change in nitrogen concentration with respect to different light intensities (a) 0; (b) 150; (c) 500 and (d) 1500 and (e) 2000 µmol photons $m^{-2}$ s.

Saturation in ammonium concentration is observed after 4h of the experiment at 1500 µmol photons $m^{-2}$ $s^{-1}$, which is attributed to inhibition of nitrification by light. At the maximum light intensity (2000 µmol photons $m^{-2}$ $s^{-1}$) nitrification stopped after 1 h, and as a result of this peak in $NH_4^+$ concentration was observed in this experiment. Vergara et al. (2016) observed that photoinhibition of AOB and NOB bacteria is microalgae-bacterial consortium due to denaturation of ammonia monooxygenase enzyme (photooxidative damage) at a high light intensity. In addition to the inhibitory effect on ammonia oxidization, the results in this study reveal that nitrifying bacterium in microalgae-bacterial consortium is inhibited at a light intensity ≥ 1500 µmol photons $m^{-2}$ $s^{-1}$, which is in close agreement with previous studies (Akizuki et al., 2020; Vergara et al., 2016). It is well-known that enzymes present in nitrifying bacteria tend to get inactivated (Akizuki et al., 2020), and the biomass contents from decayed nitrifying bacteria are released into the medium at higher light intensities (Akizuki et al., 2020).

Previous studies have shown that microalgae-nitrifying bacterial consortia can tolerate high light intensity up to 3000 µmol photons $m^{-2}$ $s^{-1}$ (Vergara et al., 2016). However, in this study poor

tolerance towards, high light intensity is observed in microalgae-nitrifying bacteria consortium. Significant decrease in $NO_3^-$production is observed at above 1500 µmol photons $m^{-2}$ $s^{-1}$ in this work, which is due to variation in composition and size of microalgae-bacterial flocs under different light conditions. Figure 4.2 depicts the nitrification efficiencies at different light intensities. At 12 h nitrification efficiency almost remained at 79.29% with increasing light intensity up to 500 µmol photons $m^{-2}$ $s^{-1}$, and the value is comparable with that reported in the literature (Akizuki et al., 2020; Vergara et al., 2016).

Vergara et al. (2016) reported that high light intensities of 500 and 1250 µmol photons $m^{-2}$ $s^{-1}$ in microalgal-nitrifying bacterial culture reduced the $NH_4^+$ removal rate by 20% and 60, respectively. Akizuki et al. (2020) studied the effect of high light intensity on microalgae-bacterial culture and reported a reduction in the ammonium removal efficiencies with increase in light intensity in a PSBR. In the current study, an average microalgal-bacteria flocs size of 900 µm was observed, which might be the reason for low light induced stress at 500 µmol photons $m^{-2}$ $s^{-1}$.However, at higher light intensity (≥1500 and 2000 µmol photons $m^{-2}$ $s^{-1}$), the $NH_4^+$ removal efficiencies were almost the same (6.2% and -2.2%). Akizuki et al. (2020) reported that a high intensity of 1600 µmol photons $m^{-2}$ $s^{-1}$ enhanced nitrification activity of microalgae-AOB consortium due to the presence of AOB in the form of partial nitrifying granules. Vergara et al. (2016) reported a decrease in activity of nitrifying bacteria by up to 60% due to photoinhibition and the activity further declined at 1250 and 1600 µmol photons $m^{-2}$ $s^{-1}$. In this study, at light intensity of 1500 µmol photons $m^{-2}$ $s^{-1}$ the stress induced was very high, but at 2000 µmol photons $m^{-2}$ $s^{-1}$ high amount of ammonium oxidation was observed. Therefore, maintaining an optimum light intensity is essential for microalgae-nitrifier consortia for enhancing ammonium removal from wastewater.

**Table 4.1. Estimated value of oxygen production by microalgae, gas transfer and consumption by AOB and NOB bacteria at various light intensities and at an ammonium concentration of 100 mg $NH_4^+$-N/L.**

| DALI (µmol photons $m^{-2}$ $s^{-1}$) | Relative contribution to $NH_4^+$ removal (%) [a] | | | $NH_4^+$ uptake rate by microalgae (mg-N $L^{-1}$ $d^{-1}$) [b] | $O_2$ supply rate by microalgae (mg-$O_2$ $L^{-1}$ $d^{-1}$) [c] | $O_2$ supply by gas transfer (mg- $O_2$ $L^{-1}$ $d^{-1}$)[d] | $O_2$ consumption rate by nitrification (mg-N $L^{-1}$ $d^{-1}$) [e] |
|---|---|---|---|---|---|---|---|
| | Microalgae Uptake | Nitrifier Uptake | Nitrification | | | | |
| 0 | 0 | 0 | 100 | 0 | 0 | 0 | 457 |
| 40 | 21.99 | 0.81 | 77.2 | 21.55 | 369.43 | 2.49 | 352 |
| 80 | 41.89 | 0.81 | 57.3 | 41.05 | 686.99 | 5.6 | 261.86 |
| 120 | 53.86 | 0.81 | 45.33 | 52.78 | 883.30 | 8.77 | 207.15 |
| 160 | 85.97 | 0.81 | 13.22 | 84.25 | 1409.90 | 11.88 | 60.41 |

a: values were calculated from nitrogen mass balance and based on nitrogen content of biomass according to Eq. (3) (Karya et al., 2013); b: it is considered that all supplied $NH_4^+$ was removed by nitrifier uptake, microalgae uptake and nitrification; c: values were calculated according to a stoichiometric equation used for microalgae growth (Karya et al., 2013); d:values were obtained from the slope of linear regression between daily $NH_4^+$ (x) uptake and $O_2$ supplied by gas transfer (y) ($y = - 0.5802x - 2.8117$, $r= 0.9796$); e; values were calculated according to stoichiometric equations used for nitrification (Akizuki et al., 2020)

**Table 4.2. Estimated values of oxygen production by microalgae, supplied by gas transfer and oxygen needed for nitrification at different light intensities**

| Daily average light intensity (μmol photons $m^{-2}$ $s^{-1}$) | $O_2$ production by microalgae (mg-$O_2$ mg-$N^{-1}$) | $O_2$ supplied by gas transfer (mg-$O_2$ mg-$N^{-1}$) | $O_2$ needed for nitrification (mg-$O_2$ mg-$N^{-1}$) | Microalgae uptake (mg-N $L^{-1}$) |
|---|---|---|---|---|
| 0 | 0 | 0 | 4.57 | 0 |
| 40 | 3.69 | 0.0249 | 3.52 | 21.99 |
| 80 | 6.86 | 0.0560 | 2.61 | 41.89 |
| 120 | 8.83 | 0.0877 | 2.07 | 53.86 |
| 160 | 14.09 | 0.1188 | 0.60 | 85.97 |

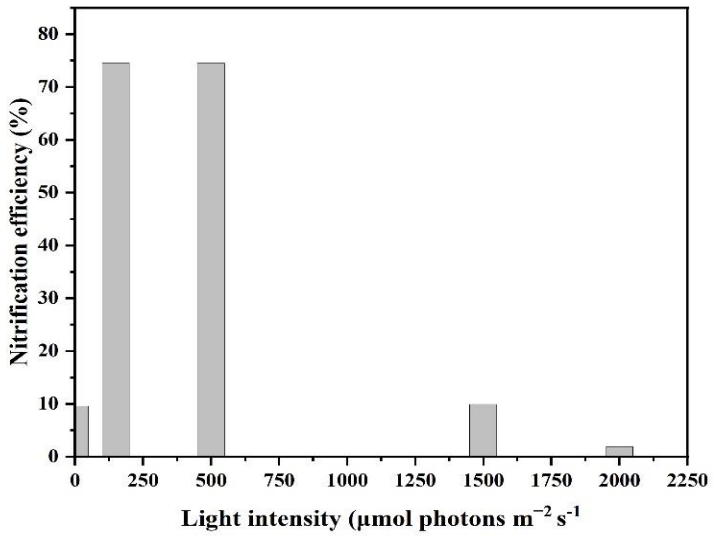


**Fig. 4.2.** Correlation plot between different light intensity and nitrification efficiency

From Figure 4.3, similar values of $NH_4^+$ removal rates (8.92 and 12.18 mg-N $L^{-1}$ $h^{-1}$) were obtained for 150 and 500 µmol photons $m^{-2}$ $s^{-1}$, respectively. At 1500 µmol photons $m^{-2}$ $s^{-1}$, drastic reduction in $NH_4^+$ removal rate was observed (0.461 mg N $L^{-1}$ $h^{-1}$), and the $NO_3^-$ production rate reduced with an increase in light intensity: the values were 6.41, 6.08, 0.38 and 0.0193 mg N $L^{-1}$ $h^{-1}$ at 150, 500, 1500 and 2000 µmol photons $m^{-2}$ $s^{-1}$, respectively. At 2000 µmol photons $m^{-2}$ $s^{-1}$, the $NO_3^-$ production rate was slightly low as $NO_2^-$ production decreases after 1 h of the experiment. Whereas the $NO_3^-$ production rate at 500 µmol photons $m^{-2}$ $s^{-1}$ is slightly lower than that of 150 µmol photons $m^{-2}$ $s^{-1}$, similar trend in ammonium removal rates is observed. These result reveals that the ammonium oxidation is through AOB, which is in addition to ammonium uptake by algae at 500 µmol photons $m^{-2}$ $s^{-1}$ light intensity.

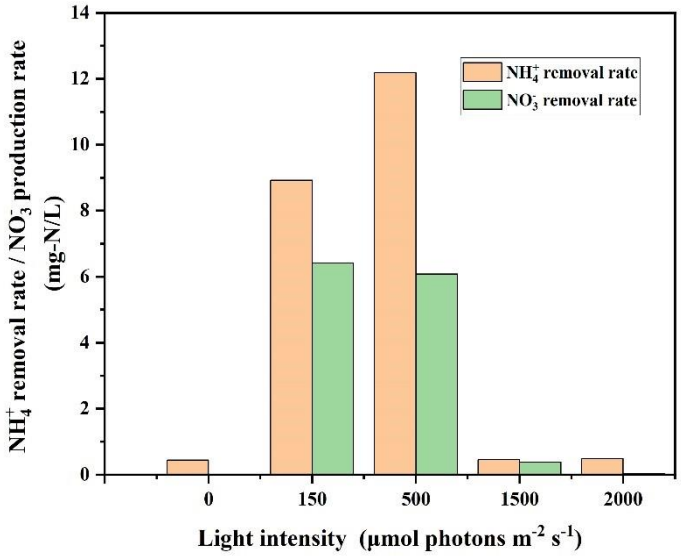


**Fig. 4.3.** $NH_4^+$ and $NO_3^-$ removal rate at different light intensities

Dissolved oxygen (DO) profile (Fig. 4.4.) for different light intensities of 0, 150, 500, 1500 and 2000 µmol photons $m^{-2}$ $s^{-1}$ showed that, during the entire experimental period the minimum DO concentration was 0.3 mg/L, which is sufficient for complete nitrification (Karya et al., 2013; Wang et al., 2015). The DO values for 150 and 500 µmol photons $m^{-2}$ $s^{-1}$, reveal maximum $O_2$ utilization for nitrification by microalgae-nitrifying consortia. Although $NH_4^+$ oxidation is not observed at 2000 µmol photons $m^{-2}$ $s^{-1}$, $O_2$ production was higher than that at 1500 µmol photons $m^{-2}$ $s^{-1}$. These results indicate that nitrifying bacteria undergo photoinhibition at 2000 µmol photons $m^{-2}$ $s^{-1}$, whereas at 0 µmol photons $m^{-2}$ $s^{-1}$ high intensity nitrification is affected due to insufficient oxygen for the reaction.

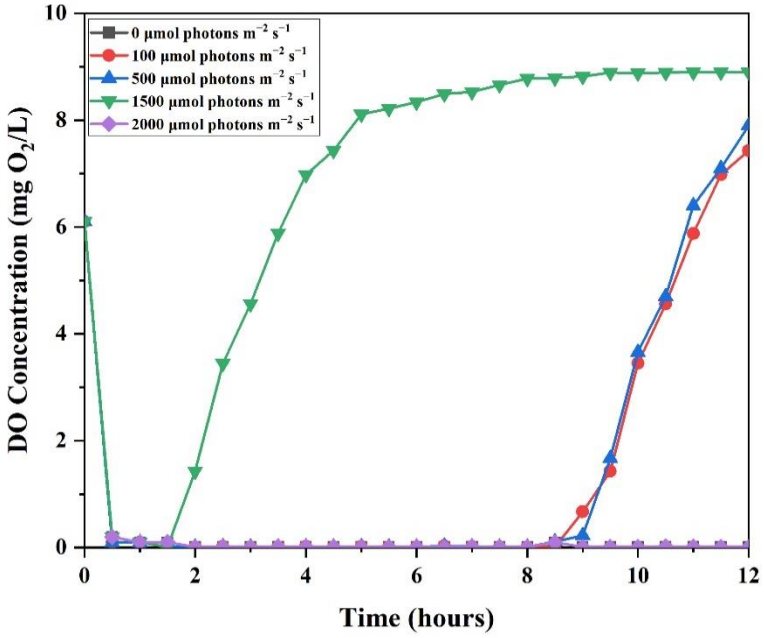


**Fig. 4.4.** DO profiles at different light intensities

### 4.3.2 Parameters and their effect on $NH_4^+$ removal mechanism in microalgae-bacterial consortia

Parameters such as $NH_4^+$ uptake by microalgae, $NH_4^+$ uptake by nitrifier and $O_2$ supply by gas transfer were considered for understanding the ammonium removal mechanism involved by microalgae-bacterial consortium. Parameters involved in the ammonium removal process were evaluated from the literature and compared with this study as presented in Table 4.4. It is evident that the contribution of nitrification towards ammonium removal changes from 0 to 100% based on the experimental conditions. From Table 4.4, nitrification by microalgae-bacterial consortium play a vital role in $NH_4^+$ removal (79%) as compared to that by microalgal uptake (19%). Karya et al. (2013) reported that both microalgal uptake and nitrification (17.4% and 82.6%) played the

main role. Whereas, van der Steen et al. (2015) revealed that $NH_4^+$ removal mechanism was primarily by nitrification (92.5%) in such microalgae-bacterial consortia.

The correlation plots between nitrification due to ammonium removal and the different parameters involved are depicted in Fig. 4.6, which included the results from the literature and this study, excluding the values obtained at high light intensities of 500, 1500 and 2000 μmol photons $m^{-2}$ $s^{-1}$ (Fig. 4.4 and Table 4.3). Based on the slope of the linear regressions obtained from Figure 4. 6, DALI showed the maximum effect on nitrification (Fig. 4.5a), followed by light intensity, $O_2$ produced by microalgae, $O_2$ supplied by gas transfer and $NH_4^+$ uptake by microalgae. Though light intensity affects the nitrification in PBR or PSBR (Karya et al., 2013; Wang et al., 2015), DALI controls the $NH_4^+$ removal mechanism more strongly in microalgae-bacterial consortium. Previous studies have shown that increase in light intensity and the $O_2$ supply rate by gas transfer tend to reduce nitrification in the PSBR or PBR (Karya et al., 2013; Wang et al., 2015). For example, Wang et al. (2015) reported a high ammonium removal efficiency by microalgae-nitrifying consortia in PSBR with a gas transfer (26%) as compared to that in a serum bottle. DALI can influence ammonium removal by microalgal-nitrifying bacteria within the light intensity range 0-160 μmol photons $m^{-2}$ $s^{-1}$ depending on the reactor type (PSBR or PBR), pH (7.5-8.1), temperature

**Table 4.3. Different parameters involved in ammonium removal mechanism by microalgal-nitrifying consortia**

| Reactor operation mode | Reactor Volume | Consortium | Light source and T (ºC) | Light intensity (µmol photons $m^{-2}$ $s^{-1}$) | DALI (µmol photons $m^{-2}$ $s^{-1}$) | Light duration | pH | Initial $NH_4^+$-N (mg N/L) | Total $NH_4^+$ Removal (%) | Relative contribution to $NH_4^+$ removal (%) [a] | | | Reference |
|---|---|---|---|---|---|---|---|---|---|---|---|---|---|
| | | | | | | | | | | Microalgae Uptake | Nitrifier uptake | Nitrification | |
| Sequencing batch reactor | 1L | M1, B1 | Warm white lamp, 30 | 63 | 49 | 9.5 | 7.5 | 26.6<br>28.1<br>26.7 | 100<br>99.9<br>99.9 | 13.3<br>16.7<br>17.4 | 1.8 | 86.7<br>83.3<br>82.6 | Karya et al. (2013) |
| Continuous | 7.5L | M2, B2 | Fluorescent lamp, N.A | 180 | 180 | 24 | 7.8-8.1 | 60<br>150<br>290<br>650 | 80<br>87<br>97<br>96 | 100<br>93<br>77<br>92 | n.d | 0<br>7<br>23<br>8 | De Godos et al. (2009) |
| Sequencing batch reactor | 1.75L | M3,B3 | HQI lamp, 23.1 | 66 | 66 | 24 | 7.5 | 66 | 84.8 | 7.5 | 1.2 | 92.5 | Van der steen et al. (2015) |
| Continuous | 1.5 | n.d | n.d, 27.2 | 67.5 | 67.5 | 24 | 7.8 | 1400 | 98 | 40 | n.d | 60 | Vargas et al. (2016) |
| Sequencing batch reactor | 2L | M4, B4 | Warm white lamp, 30 | 0<br>150<br>500<br>1500<br>2000 | 0<br>75<br>250<br>750<br>1000 | 12<br>12<br>12<br>12<br>12 | 7.5<br>7.5<br>7.5<br>7.5<br>7.5 | 100<br>100<br>100<br>100<br>100 | 7.2<br>100<br>100<br>6.2<br>-2.2 | 0.7<br>19.89<br>23.66<br>0<br>0 | 0<br>0.81<br>0.81<br>0<br>0 | 99.3<br>79.29<br>75.54<br>100<br>100 | This study |

M1: *Scenedesmus quadricauda*; M2: *Chlorella sorokiniana*; M3: mixed species of microalgae; B1: mixed bacterial culture; B2: nitrifying bacterial culture; B3: nitrifying activated sludge; M4: *Chlorella sorokiniana;* B4:nitrifying bacterial culture; a: based on the nitrogen mass balance (Karya et al., 2013; Pizzera et al., 2019; Van der steen et al., 2015); b: based on the measured values and oxygen mass balance (Karya et al., 2013; Muys et al., 2018); c: based on the $k_La$ calculation; d: estimated based on the $O_2$ produced by microalgae and $O_2$ supplied by gas transfer

(23.1-30), light intensity (0 to 2000 µmol photons $m^{-2}$ $s^{-1}$) and initial $NH_4^+$ concentration (26.6-1400 mg N/L) condition.

**Table 4.4. Nitrogen balance and $NH_4^+$ removal efficiency value based on this study**

| DALI (µmol photons $m^{-2}$ $s^{-1}$) | $NH_4^+$ (mg N/L) | $NO_2^-$ (mg N/L) | $NO_3^-$ (mg N/L) | Relative contribution to $NH_4^+$ removal (mg N/L) [a] | | | $NH_4^+$ removal efficiency (%) [b] |
|---|---|---|---|---|---|---|---|
| | | | | Microalgae Uptake | Nitrifier Uptake | Nitrification | |
| 0 | 92.7 | 4.7 | 4.56 | 0.686 | 0 | 7.056 | 7.2 |
| 150 | 0 | 0 | 77.16 | 19.49 | 0.793 | 79.71 | 100 |
| 500 | 0 | 0 | 71.93 | 23.18 | 0.793 | 76.02 | 100 |
| 1500 | 91.4 | 4.56 | 0.12 | 0 | 0 | 6.07 | 6.2 |
| 2000 | 103.8 | 1.44 | 0.13 | 0 | 0. | 0 | -2.2 |

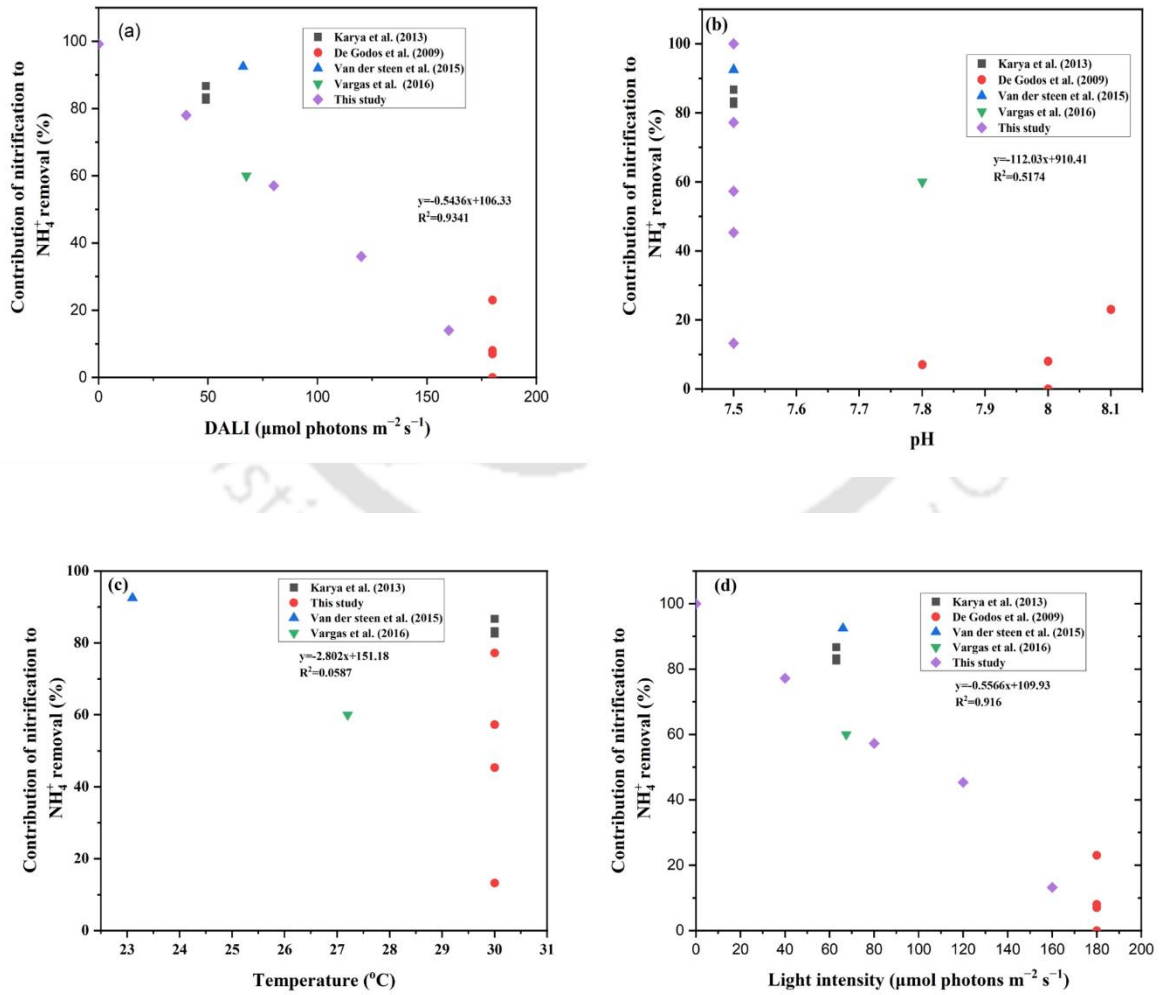

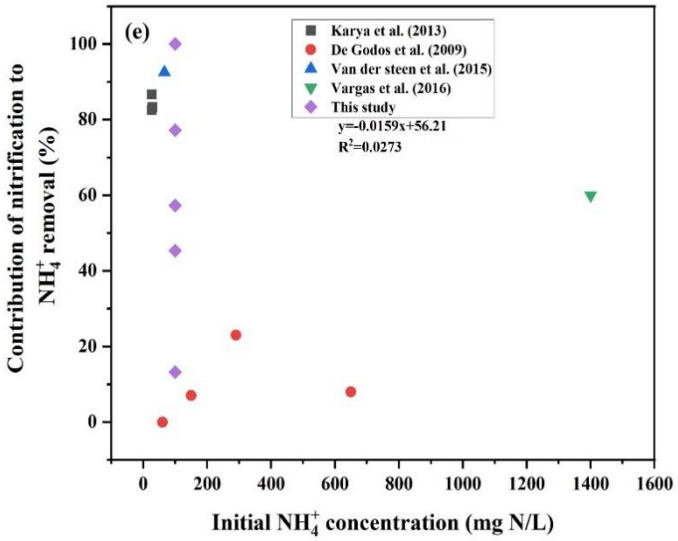


**Fig. 4.5.** Relationship between ammonium removal and possible parameters controlling the ammonium removal: (a) DALI, (b) pH, (c) temperature, (d) light intensity, and (e) initial ammonium concentration

The correlation between the different parameters and ammonium removal can also vary for photobioreactor or photosequencing batch reactor. The corresponding slope values from these plots further these revealed that pH is strongly correlated to the ammonium removal mechanism (Fig. 4.5b). However, some difference in pH values with respect to ammonium removal by different microalgal-bacterial consortia have been reported (7.5; Karya et al., 2013; 7.8-8.1; De Godos et al., 2009; 7.5, van der Steen et al., 2015; 7.8; Vargas et al., 2016). Therefore, the positive correlation observed between pH and ammonium removal may have an indirect significance in such closed photobioreactor systems.

### 4.3.3 Nitrogen mass balance

The results of nitrogen mass balance and $NH_4^+$ removal efficiency at the end of the 12 h experiment are presented in Table 4.4. Complete $NH_4^+$ removal efficiency was achieved at 150 and 500 µmol

photons $m^{-2}$ $s^{-1}$, respectively. The $NH_4^+$ removal efficiency was drastically reduced to 6.2% at 1500 µmol photons $m^{-2}$ $s^{-1}$ and further reduced to -2.2% (protein release through cell lysis) at 2000 µmol photons $m^{-2}$ $s^{-1}$. The nitrogen mass balance also showed a significant uptake of $NH_4^+$ by microalgae (23.18 mg N $L^{-1}$) at 500 µmol photons $m^{-2}$ $s^{-1}$, but the uptake was very low at 1500 and 2000 µmol photons $m^{-2}$ $s^{-1}$. This result shows that high light intensity tends to inhibit the activities of microalgae, AOB and NOB bacteria in the consortium. Reduction of microalgal activity is due to inhibition of photosystem II (PSII) owing to the production of reactive oxygen species (ROS) (Akizuki et al., 2020; Ananyev et al., 2017). In a PSBR or PBR containing microalgae-nitrifier at high light intensity (more than 2000 µmol photons $m^{-2}$ $s^{-1}$) nitrification is affected due to insufficient $O_2$ production by microalgae. At low light intensity, failure in nitrification and low ammonium uptake are also due to insufficient $O_2$ supply from microalgae for the reaction.

### 4.3.4 Optimization of DALI and comparison of nitrification with PBR or PSBR

In a reactor with microalgae-nitrifying bacterial consortium and without mechanical aeration, DO concentration tends to vary due to the following reasons: oxygen produced by microalgae, oxygen supplied by gas transfer and total $O_2$ utilized by microalgae-bacterial consortia. The complete utilization of microalgae produced oxygen decreases the energy cost of nitrification process. Whereas, at a low light intensity incomplete nitrification occurs due to insufficient $O_2$ produced by algae. In addition, an increase in DALI may cause (i) oxygen oversaturation, which reduces microalgal activity (Akizuki et al., 2020) and (ii) inhibition due to free ammonia on microalgae-AOB consortia, which affects nitrification efficiency (Akizuki et al., 2019; Azov and Goldman, 1982). Hence, proper oxygen balance needs to be considered for nitrification.

At DALI below 40 µmol photons $m^{-2}$ $s^{-1}$, oxygen produced by microalgae is insufficient than the oxygen needed for nitrification (Fig. 4.6), which necessitated of external aeration. When the light intensity is above 40 µmol photons $m^{-2}$ $s^{-1}$ , the $O_2$ supply due to algal photosynthesis is more than that required for nitrification (Fig. 4.6). This result shows that the integration of microalgae with AOB and NOB is an effective method for reducing aeration costs along with $NH_4^+$ removal as compared to conventional nitrification process with mechanical aeration.

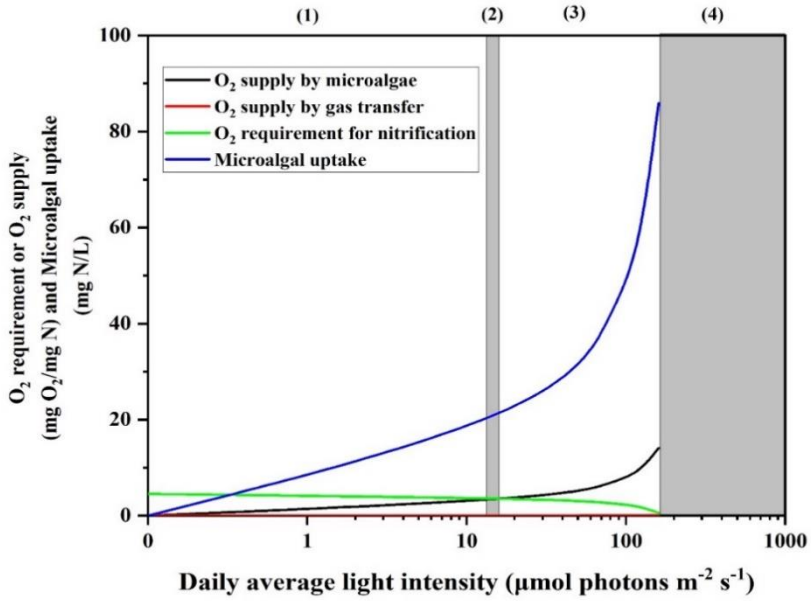


**Fig. 4.6.** Relationship between total $O_2$ required for nitrification, oxygen produced by microalgae and oxygen supplied by gas transfer and microalgal uptake

Even a light intensity above 40 µmol photons $m^{-2}$ $s^{-1}$ reduces the aeration cost by 70%, and complete nitrification can be achieved with light intensity up to 160 µmol photons $m^{-2}$ $s^{-1}$ (Fig. 4.6). Beyond this value, oxygen supply may reduce due to decrease in microalgal activity owing to excessive light intensity thereby affecting the nitrification efficiency. For example, Jemenez et al. (2003) observed a reduction in microalgae biomass concentration at high DO concentration (30 mg/L) in open raceways. Besides, increase in light intensity can increase free ammonia

concentration unless pH is controlled, particularly when treating ammonium rich wastewater. Akizuki et al. (2019) reported the effect of changing pH (4.1-10.2) on microalgae-bacterial consortium for treating synthetic wastewater containing 102 mg-N $L^{-1}$ of ammonium, which resulted in high free ammonia concentrations (0-59.4 mg/L). Maintaining constant pH is thus necessary for reducing the FA concentration in the photobioreactor or PSBR to eliminate inhibitory effect on microalgae-nitrifying consortia. Moreover, high light intensity (1500 and 2000 μmol photons $m^{-2}$ $s^{-1}$) may further inhibit the activity of microalgae-bacterial consortium, as observed in this study. Based on the formulated empirical equation, the performance of microalgae-nitrifying consortia with respect to different light intensity may be studied as follows: (i) nitrification fails to occur owing to the absence of $O_2$ at light intensities < 40 μmol photons $m^{-2}$ $s^{-1}$, (ii) simultaneous nitrification and microalgal photosynthesis occur at light intensities > 40 μmol photons $m^{-2}$ $s^{-1}$, (iii) nitrification happens between 40-160 μmol photons $m^{-2}$ $s^{-1}$, (iv) nitrification fails to occur due to light inhibition of microalgae-bacterial consortia at light intensity >160 μmol photons $m^{-2}$ $s^{-1}$.

It is recognized that light intensity enhances the oxygen production and AOB-NOB bacteria compete for the oxygen to remove maximum nitrogen. Certain advantages of shortcut nitrogen removal by microalgae-bacterial consortia are: reduced inhibition due to FA, low DO concentrations due to $O_2$ consumption. In order to further understand the nitrogen removal by microalgae-bacterial consortia, the effect of pH, temperature, low and high light intensity, can be carried out

### 4.4 Significant findings

The effect of light intensity on $NH_4^+$ removal by microalgae-nitrifying consortia in a PSBR was examined. Ammonium removal efficiencies were similar at 150 and 500 μmol photons $m^{-2}$ $s^{-1}$,

but the removal efficiency reduced significantly to 6.2 and -2.2% at 1500 and 2000 µmol photons $m^{-2}$ $s^{-1}$, respectively. Among the different parameters involved, DALI strongly influenced the overall $NH_4^+$ removal mechanism ($R^2$ =0.9341). An empirical model based on algal photosynthesis showed that DALI below 40 µmol photons $m^{-2}$ $s^{-1}$ leads to process failure owing to insufficient oxygen, above 40 µmol photons $m^{-2}$ $s^{-1}$ is effective for nitrification and microalgal uptake, and 40-160 µmol photons $m^{-2}$ $s^{-1}$ is found to be effective for complete nitrification. This empirical model also showed that light intensity above 160 µmol photons $m^{-2}$ $s^{-1}$ results in process failure due to inhibition of microalgae-bacterial consortium.

# Chapter 5

## Effect of different nitrogen sources on nitrification by microalgae-nitrifying bacterial consortium

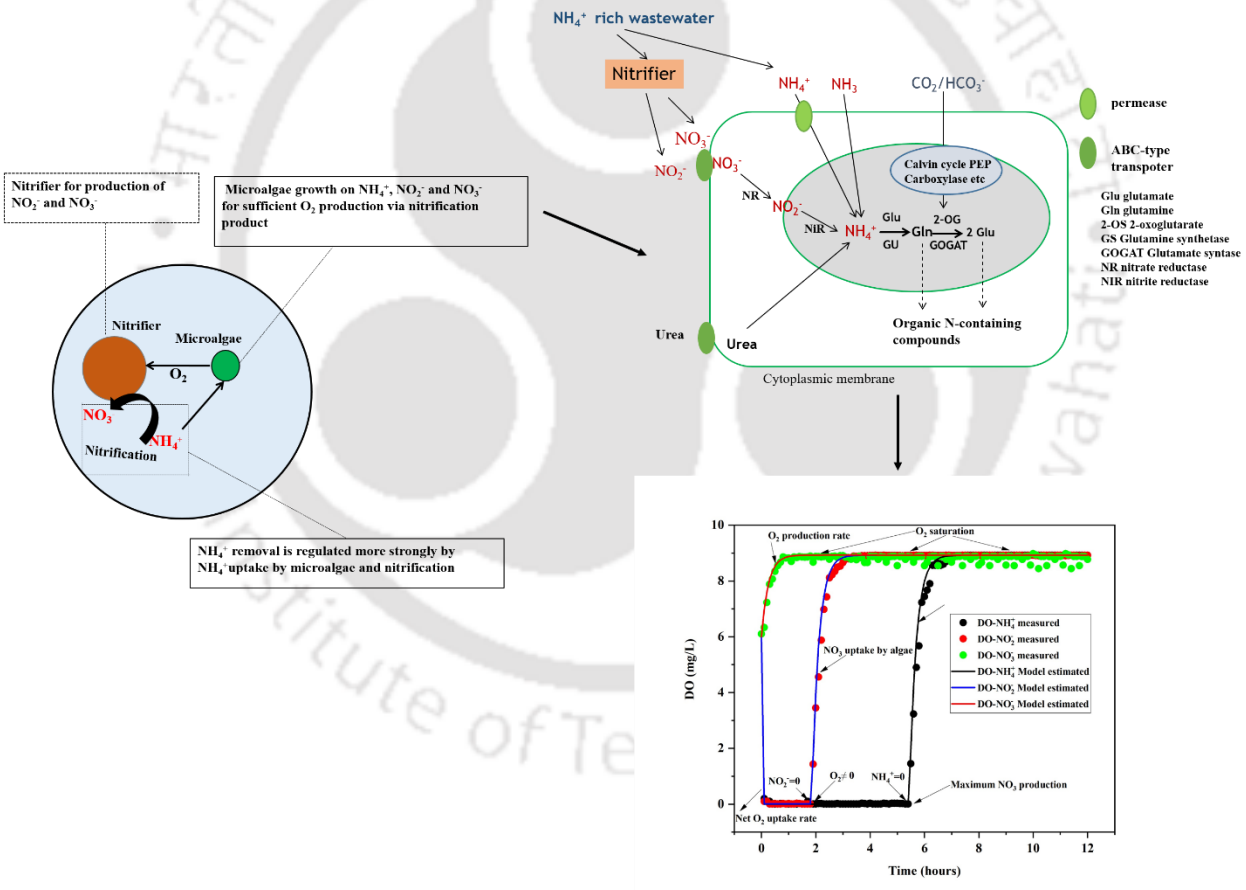

**ABSTRACT**

$NH_4^+$ removal by microalgae-bacterial consortium was examined in a photosequencing batch reactor at 50, 100 and 200 mg $NH_4^+$-N/L concentrations. Results showed that sufficient amount of oxygen was available due to algal photosynthesis for nitrification at 50 and 100 mg/L of ammonium, as compared to 200 mg/L. The ammonium removal efficiency values were 100, 100, 74.47% at 50, 100 and 200 mg $NH_4^+$-N/L concentrations, respectively. Nitrogen mass balance in the system revealed that microalgae and nitrifying bacteria contributed to 20.26% and 76.41% of $NH_4^+$ removal at 50 mg $NH_4^+$-N/L initial concentration. However, ammonium uptake was reduced with increase in nitrogen concentration in the form of $NH_4^+$, $NO_2^-$ and $NO_2^-$. Activated sludge model and algae-bacterial (ASM-AB) model were developed to explain the effect of oxygen on nitrogen removal at different $NH_4^+$concentrations which revealed the following: (i) complete removal of $NH_4^+$ with saturated dissolved oxygen at 50 and 100 mg $NH_4^+$-N/L concentration (ii) $O_2$ limitation occurs with reduction in nitrification at 200 mg $NH_4^+$-N/L concentration.

## 5.1. Introduction

Oxygen production by microalgae is one of the main advantages of using microalgal-bacterial consortium in a photo-bioreactor (PBR) or photosequencing batch reactor (PSBR) (González-Fernández et al., 2011; Karya et al., 2013; Manser et al., 2016; Wang et al., 2015). Nitrification is recognized as a two-step process, in which $NH_4^+$ is first oxidized to $NO_2^-$ by ammonia oxidizing bacteria (AOB) and then to $NO_3^-$ by nitrite oxidizing bacteria (NOB). In general, $NO_2^-$ and $NO_3^-$ act as secondary nitrogen sources for microalgae in the absence of ammonium (Colliver and Stephenson, 2000). However, it is reported that $NO_3^-$ is preferred over ammonium by microalgae in photobioreactor treating domestic wastewater (Honda et al., 2012). On the other hand, the complete assimilation of inorganic nitrogen in microbes consists of sequential reduction of $NO_3^-$ by nitrate reductase and nitrite reductase to produce $NH_4^+$, which is then assimilated into amino acid (glutamine) by glutamine synthase (Cai et al., 2013; Maestrini et al., 1986).

$O_2$ produced by microalgae contributes significantly to ammonium removal by AOB and NOB in PBR or PSBR (Karya et al., 2013; Manser et al., 2016; Wang et al., 2015), but the presence of other nitrogen sources, in particular $NO_2^-$ and $NO_3^-$ affects ammonium removal due to competition for $O_2$ produced by microalgae (González-Fernández et al., 2011). Hence, utilization of ammonium relative to nitrite or nitrate is important for nitrification to occur (Karya et al., 2013; Wang et al., 2015). Moreover, a high N assimilation and nitrification is desired to achieve a maximum ammonium removal efficiency by microalgae-bacterial consortia (Molinuevo-Salces et al., 2010).

Foladori et al. (2018) reported that 34% of influent ammonium was oxidized to $NO_3^-$ via nitrification at 55 mg/L $NH_4^+$-N concentration. Likewise, Zhang et al. (2018) observed that 13–20% of influent ammonium was oxidized to $NO_3^-$ at 200 mg $NH_4^+$-N /L concentration in a

photobioreactor. Swine farm wastewater containing 12.3 mg/L ammonium and 53.8 mg/L nitrate were removed efficiently through nitrification (75.7%) and denitrification (53.8%), respectively (Hernández et al., 2013). Consortium consisting of microalgae and activated sludge collected from primary settler of a domestic wastewater treatment plant is reported to remove 98% ammonium at 152.7 mg $NH_4^+$-N /L by (Yang et al., 2018).

The afore-mentioned studies suggest that $O_2$ production by microalgal photosynthesis using ammonium as the sole nitrogen source may not be sufficient for nitrification by microalgae-bacterial consortium. Therefore, it is proposed to use a mixture of nitrogen sources such as ammonium, nitrite and nitrate for sufficient oxygen production by microalgae and complete ammonium removal by AOB and NOB (Akizuki et al., 2020). As there is no study performed thus far to validate this suggestion, this study investigated the effect of different nitrogen sources under various ammonium loading rates, on oxygen competition between AOB and NOB for nitrification as well as on microalgae growth.

## 5.2 Materials and methods

### 5.2.1 Microalgae-nitrifying bacterial consortium and culture enrichment

The microalgae-nitrifying bacteria consortium utilized in this study was taken from a 5L lab scale PSBR treating ammonium rich wastewater. The PSBR was operated at 30ºC with 24 h photoperiodic cycle, which consisted of 12 h light (12 h aeration) and 12 h dark (15 min feeding, 60 min settling, 10 min decanting, 10 min wasting). The sludge retention time (SRT) in the PSBR was 20 days. Dissolved oxygen (DO) concentration and pH in the reactor were monitored online and pH was controlled automatically at 7.5 ± 0.1 by using 1 M $NaHCO_3$ stock solution. During the culture enrichment, ammonium, nitrite, nitrate concentrations were analyzed every 1 h interval. Mixed liquor suspended solids (MLSS) and mixed liquor volatile suspended solids (MLVSS)

concentrations were measured every week during the culture enrichment. The PSBR was fed with synthetic wastewater containing 5.63 g/L of $NH_4HCO_3$, 0.064 g/L of $KH_2PO_4$, 0.064 g/L of $K_2HPO_4$ and 2 ml of trace element solution during the culture enrichment phase (Wang et al., 2015). The MLSS and MLVSS concentrations were stable at 1.3 and 1.1 g/L, respectively, along with complete removal of ammonium, nitrite and nitrate was observed during the culture enrichment.

### 5.2.2 PSBR experiments

A 5L bioreactor (Sartorius-Biostat A, Germany) was used to study the effect of different nitrogen sources on nitrification. At the beginning of each experiment, the bioreactor was first added with microalgae-nitrifying bacterial biomass from the parent PSBR at the end of nitrogen removal phase. $K_La$ was measured by sparging nitrogen gas for about 15 min to remove oxygen from the system. Temperature (30 ° C) and pH (7.5± 0.05) for this study were selected based on our previous work (Chapter 4).

### 5.2.3 Experiment 1: Nitrification under oxygen saturated condition

In order to study the effect of ammonium, nitrite and nitrate on nitrification by microalgae-nitrifying bacterial consortium. Seven different experiments were carried with different combinations of nitrogen source as presented in Table 5.1. The individual concentrations of ammonium, nitrite and nitrate were maintained at 50 mg N/L along with 500 mg/L of $NaHCO_3$ in the mixed liquor. Samples were taken every 30 min interval for ammonium, nitrite and nitrate analysis. The MLVSS estimation was triplicated at the end of each experiment, whereas sample analyses were carried out in triplicate.

### 5.2.4 Experiment 2: Nitrification under oxygen limited condition

In order to study the effect of different nitrogen sources on nitrification under $O_2$ limited condition the same experimental scheme as represented in Table 5.1 was followed. However, a high concentration of ammonium (200 mg $NH_4^+$-N/L) was used in the PSBR at the beginning of the experiments to induce $O_2$ limited condition on nitrification. All the analysis and estimations were done as mentioned earlier.

**Table 5.1.** Experimental scheme to study the effect on nitrification

| **Experimental run** | **1** | **2** | **3** | **4** | **5** | **6** | **7** |
|---|---|---|---|---|---|---|---|
| Nitrogen source added | $NH_4^+$ | $NO_2^-$ | $NO_3^-$ | $NH_4^+$ $NO_2^-$ | $NH_4^+$ $NO_3^-$ | $NO_2^-$ $NO_3^-$ | $NH_4^+$ $NO_2^-$ $NO_3^-$ |

### 5.2.5 Experiment 3: Nitrification at optimum oxygen condition

In order to study the effect of optimum $O_2$ concentration on nitrification, two different ammonium concentrations (100 ± 0.1mg/L) were used; the latter concentration is optimum as earlier study (Chapter 4). In this experiment, ammonium was supplied to the PSBR at the beginning of experiment.

### 5.2.6 Analytical methods

Liquid samples taken from the reactor were immediately filtered via 0.22 μm membrane using syringe filter for analyzing concentrations of $NH_4^+$, $NO_3^-$ and $NO_2$ by phenate and colorimetric method. All the estimations including MLVSS was carried out by following Standard methods for the examination of water and wastewater (APHA, 2012).

### 5.2.7 Oxygen production rates and nitrogen mass balance

The oxygen production rates were calculated based on uptake of ammonium, nitrite and nitrate by microalgae and the stoichiometry involved as reported by Karya et al. (2013). Oxygen produced and oxidation of ammonium and nitrite was estimated from equations 5.1 and 5.2.

$$16NH_4^+ + 92H_2O + HPO_4^{2-} + 106HCO_3^- \rightarrow C_{106}H_{263}O_{110}N_{16}P + 92OH^- + 106O_2 \quad (5.1)$$

$$16NO_3^- + 140H_2O + HPO_4^{2-} + 106HCO_3^- \rightarrow C_{106}H_{263}O_{110}N_{16}P + 124OH^- + 138O_2 \quad (5.2)$$

Oxygen balance used for the calculation is as follows:

Net photosynthetic $O_2$ production + $O_2$ input by re-aeration = $O_2$ utilized for nitrification (g) (5.3)

Mass transfer coefficient ($K_La$) for oxygen was estimated to find the $O_2$ input by gas transfer which however excluded oxygen consumption by heterotrophic bacteria. $O_2$ utilized for nitrification was estimated from equation 5.4.

$$NH_4^+ + 1.32O_2 + 0.8H_2O + 1.98HCO_3^- \rightarrow 0.021C_5H_7O_{110}NO_2 + 0.98NO_3^- + 2.02H_2O + 1.88H_2CO_3 \quad (5.4)$$

$NH_4^+$ balance during the reaction was estimated based on the equation 5.4 and the measured values. Parameters considered for ammonium mass balance calculations are summarized in Table 5.2. Ammonium uptake by microalgae was calculated by deducting initial nitrate formed from ammonium uptake by nitrifiers with ammonium as the sole nitrogen source. The amount of nitrate uptake by algae was estimated from the maximum measured $NO_3^-$-N concentration during the experiment and the effluent $NO_3^-$- N concentration.

### 5.2.8 Modelling of effect of nitrogen source

Microalgae-bacterial models were developed to explain the effect of different oxygen conditions on nitrogen removal using green microalgal growth (ASM-A) model (Wager et al., 2018) and ammonium oxidizing bacteria growth (ASM-AB) model (Zambrano et al., 2016). The hybrid model developed in this work based on these two earlier reported models on microalgae and nitrifying bacteria, respectively, considered ammonium oxidation, nitrite oxidation and microalgae growth on three different nitrogen sources ($NH_4^+$, $NO_3^-$, $NO_2$-). All these models and the parameters involved are presented in Tables 5.3a and 5.3b.

## 5.3 Results and discussion

### 5.3.1 Effect of nitrogen source under saturated oxygen condition

Reduction in $NH_4^+$ concentration was observed in all the experiments carried out under $O_2$ saturated condition as shown in Fig. 5.1. Also, increase in nitrate concentration was observed in all the experiments, which indicates successful nitrification occurred under $O_2$ saturated condition. Nitrate production rate was combined with corresponding VSS to estimate the removal and uptake rate of ammonium, nitrite and nitrate.

**Table 5.2** Parameters considered for nitrogen mass balance

| **Parameters** | **Method followed** |
|---|---|
| $NH_4^+$-N input (a) | Analysis of influent ammonium concentration (mg $NH_4^+$-N/L) |
| $NH_4^+$-N effluent (b) | Analysis of effluent ammonium concentrations (mg $NH_4^+$-N/L) |
| $NO_3^-$ produced (c) | Analysis of Maximum $NO_3^-$-N produced (mg $NO_3^-$-N/L) |
| $NH_3$ volatilization(d) | Based on quantity of ammonia volatized at a particular pH |
| $NH_4^+$ uptake by Nitrifiers(e) | Based on N content of biomass produced according to Eq.(5.2) |
| $NH_4^+$ uptake by algae (f) | **d = a – b – c – d – e** |

Previous reports have shown that the ammonium uptake was 13.3 and 1.8% for microalgae and nitrifier, whereas 84.9% was removed through nitrification at the rate of 7.7 mg $NH_4^+$/ L h (Karya et al., 2013; Wang et al., 2015). In this study, high ammonium removal rate (9.65 mg $NH_4^+$/ L. h) was obtained due to nitrification. Complete ammonium removal under oxygen saturated condition was observed along with a high removal rate (9.75 mg $NH_4^+$/ L), partially due to algal growth (Fig. 5.1). Under oxygen saturated condition different nitrogen sources were supplied in different combinations (Table 5.1), and experimental run no. 1, 4, 5 and 7, yielded a similar value of ammonium removal rate (9.65 mg $NH_4^+$/ L h). In experimental run no. 3, the total nitrate removal by microalgae was 10.56 mg $NO_3^-$- N/ L at the rate of 0.50 mg $NO_3^-$- N/ g VSS/L/h (Fig. 5.2a and 2b). High uptake of ammonium, nitrite and nitrate in PBR during the reaction phase is due to the contained activity of microalgae and nitrifiers (Karya et al., 2013; Wang et al., 2015). Reduction in nitrogen uptake was observed in experimental run no. 4, 5 and 6, which was due the addition of two different nitrogen sources. Decrease in ammonium uptake by microalgae was 11% and 50% in experimental run no. 4 and 5, with respect to the experimental run no. 1. Reduction in nitrate was 49.2% and 63% in experimental run no. 4 and 6 with respect to experimental run no. 3. The results of slight reduction in ammonium uptake is consistent with the report of previous studies, which can be improved by varying light conditions in the PSBR (Wang et al., 2015).

**Table 5.3a** Metabolic models and their parameters

| S. No | Model component / Process | 1 $X_A$ $\frac{g\ COD}{m^3}$ | 2 $X_{AOB}$ $\frac{g\ COD}{m^3}$ | 3 $X_{NOB}$ $\frac{g\ COD}{m^3}$ | 4 $S_{NH_4}$ $\frac{g\ NH^+ - N}{m^3}$ | 5 $S_{NO_2}$ $\frac{g\ NO_{2^-} - N}{m^3}$ | 6 $S_{O_2}$ $\frac{g\ O_2}{m^3}$ | Process rate R |
|---|---|---|---|---|---|---|---|---|
| 1 | Algae growth on $NH_4$ | 1 | - | - | $-1$ | | $Y_{O_2}$ | $\mu_{max,A}\left(\frac{S_{NH_4}}{K_{NH_4,A}+S_{NH_4}}\right)\left(\frac{I}{K_I+I}\right)X_A$ |
| 2 | Algae growth on $NO_2$ | 1 | - | - | - | -1 | - | $\mu_{max,A}\left(\frac{S_{NO_2}}{K_{NO_2,A}+S_{NO_2}}\right)\left(\frac{I}{K_I+I}\right)X_A$ |
| 3 | Algae growth on $NO_3$ | 1 | - | - | - | - | - | $\mu_{max,A}\left(\frac{S_{NO_3}}{K_{NO_3,A}+S_{NO_3}}\right)\left(\frac{I}{K_I+I}\right)X_A$ |
| 4 | Algae decay | -1 | - | - | - | - | - | $b_A X_A$ |
| 5 | AOB growth | - | 1 | - | $-\frac{-i_{N,BM}}{Y_{AOB}}$ | $\frac{1}{Y_{AOB}}$ | $-\frac{3.43-Y_{AO}}{Y_{AOB}}$ | $\mu_{max,AOB}\frac{S_{O_2}}{K_{O_2,AOB}+S_{O_2}}\frac{S_{NH_4}}{K_{NH_4,AOB}+S_{NH_4}}X_{AOB}$ |
| 6 | AOB decay | - | $-1$ | - | $-i_{X,AOB}$ | - | - | $b_{AOB}X_{AOB}$ |
| 7 | NOB growth | 1 | - | 1 | $-i_{N,BM}$ | $-\frac{1}{Y_{NOB}}$ | $\frac{1}{Y_{NOB}}$ | $\mu_{max,NOB}\frac{S_{O_2}}{K_{O_2,NOB}+S_{O_2}}\frac{S_{NO_2}}{K_{NO_2,AOB}+S_{NO_2}}\frac{K_{I,NH_4}}{K_{I,NH_4}+S_{NH_4}}X_{NOB}$ |
| 8 | NOB decay | - | - | $-1$ | - | - | - | $b_{NOB}X_{NOB}$ |
| 9 | $O_2$Transfer | - | - | - | - | - | 1 | $K_L a_{o2}(S_{o2^*} - S_{o_2})$ |

**Table 5.3b.** State variables and kinetic parameters of the models evaluated in this study and their values used

| Parameter | Definition | Values | Source |
|---|---|---|---|
| $Y_{NH_4}$ | Algal growth yield on $NH_4$, g DW $g^{-1}NH_4{}^+N$ | 15.84 | Estimated |
| $Y_{O_2}$ | Oxygen production yield by algae on $NH_4$, g $O_2 g^{-1}$ COD | 0.996 | Estimated |
| $\mu_{max,A}$ | Maximum specific growth rate of algae, $d^{-1}$ | 0.96 | Sasi et al., (2011) |
| $K_{NH_4,A}$ | Saturation constant of $S_{NH_4}$ for algae, g $Nm^{-3}$ | 0.3 | Wolf et al., (2017) |
| $K_{HCO_3,A}$ | Half saturation constant for algae growth on $HCO_3$, g$HCO_3 m^{-3}$ | 3 | Decostere et al., (2013) |
| $K_{PO_4,A}$ | Half saturation constant for algae growth on $PO_4$, g$Pm^{-3}$ | 0.08 | Tyrrell, T., (1999) |
| $K_{I,A}$ | Half saturation constant for algae growth on I, $\mu molm^{-2}\,s^{-1}$ | 0.1 | Zambrano et al., (2016) |
| $b_A$ | Algae decay, $d^{-1}$ | 0.1 | Reichert et al., (2001) |
| $\mu_{max,AOB}$ | Maximum specific growth rate of AOB,$d^{-1}$ | 0.9 | Kaelin et al. (2009) |
| $K_{O_2,AOB}$ | Saturation constant of $S_{O_2}$ for AOB, g$O_2 m^{-3}$ | 0.79 | Manser et al. (2005) |
| $K_{NH_4,AOB}$ | Saturation constant of $S_{NH_4}$ for AOB, g$Nm^{-3}$ | 2.4 | Wiesmann (1994) |
| $i_{N,BM}$ | N content of bacterial biomass ($X_H$, $X_{AOB}$, $X_{NOB}$)g N $(gCOD_{X_{BM}})^{-1}$ | 0.07 | Henze et al. (2000) |
| $Y_{AOB}$ | Aerobic yield of $X_{AOB}$ g $COD_{X_{AOB}}(gCOD_{S_{NH_4}})^{-1}$ | 0.2 | Sin et al. (2008) |
| $b_{AOB}$ | Respiration rate constant for AOB, $d^{-1}$ | 0.061 | Iacopozzi et al. (2007) |
| $\mu_{max,NOB}$ | Maximum specific growth rate of NOB,$d^{-1}$ | 0.65 | Kaelin et al. (2009) |
| $K_{O_2,NOB}$ | Saturation constant for $S_{O_2}$ for NOB, $gO_2 m^{-3}$ | 0.47 | Manser et al. (2005) |
| $Y_{NOB}$ | Aerobic yield of $X_{NOB}$, g $COD_{X_{NOB}}(gCOD_{S_{NO_2}})^{-1}$ | 0.05 | Sin et al. (2008) |
| $K_{NO_2,,NOB}$ | Saturation constant of $S_{NO_2}$ for NOB, g $NO_2^-$ N $m^{-3}$ | 0.28 | Manser et al. (2005) |
| $K_{I,NH_4}$ | Ammonia inhibition of nitrite oxidation, g $NH_4^+$ N $m^{-3}$ | 5 | Iacopozzi et al. (2007) |
| $b_{NOB}$ | Respiration rate constant for AOB,$d^{-1}$ | 0.061 | Iacopozzi et al. (2007) |
| $K_L a_{o2}$ | Mass transfer coefficient of $O_2$. $d^{-1}$ | 4 | Solimeno et al., (2015) |
| $S_{o2^*}$ | Saturation concentration for $O_2$ in water,g$O_2 m^{-3}$ | 8.58 | Estimated |

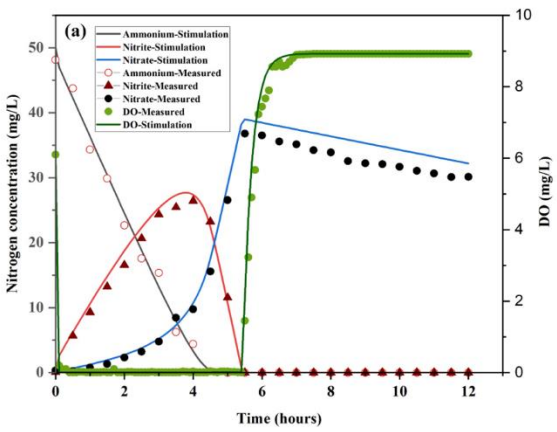


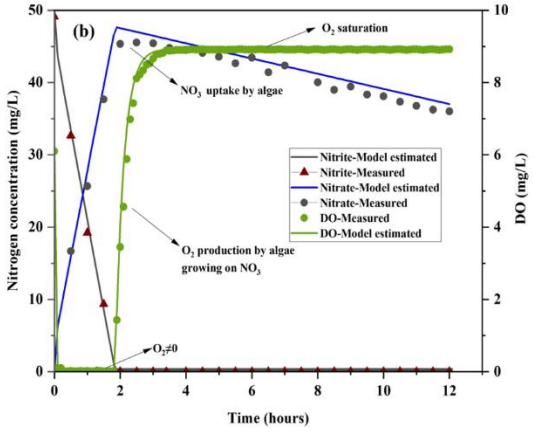


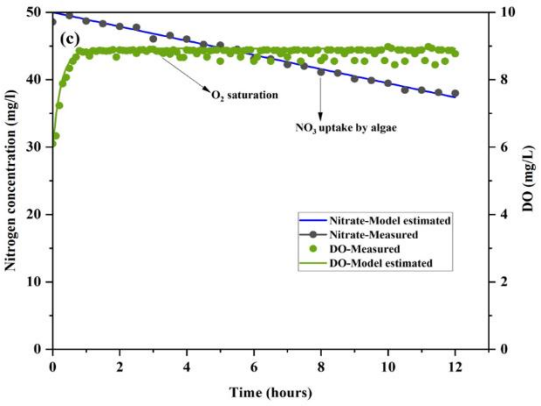


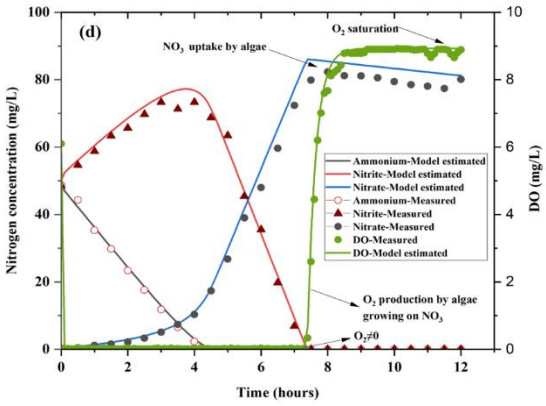


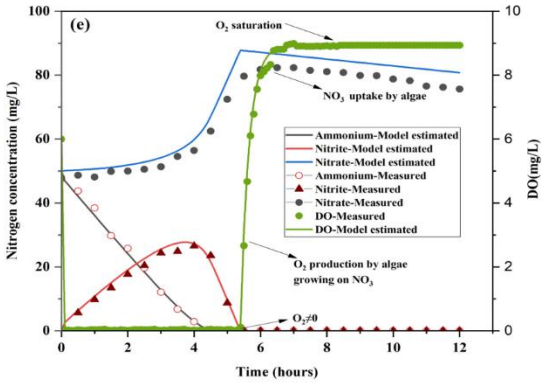


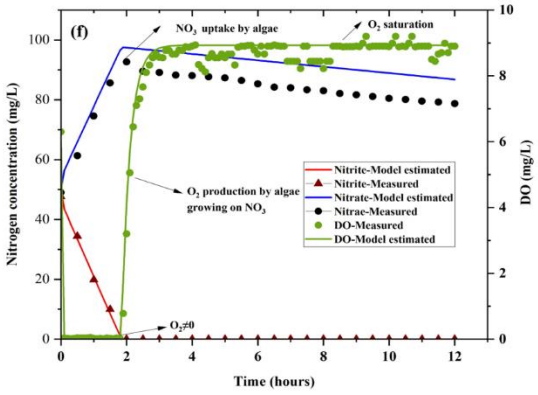

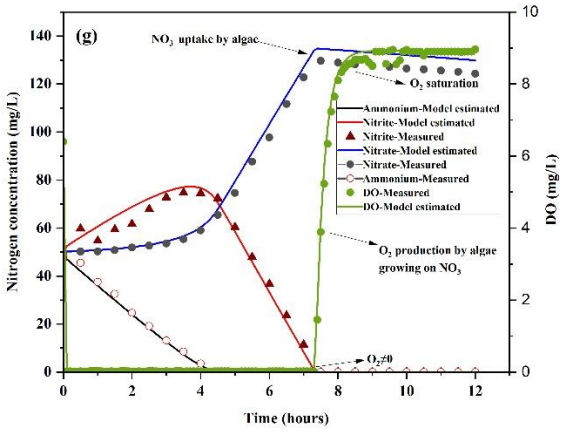


**Fig. 5.1**. Concentration of $NH_4^+$, $NO_3^-$, $NO_2^-$ and DO in the seven experimental runs along with the ASM-AB model estimated values under oxygen saturated condition in the PSBR (a, b, c, d, e, f and g).

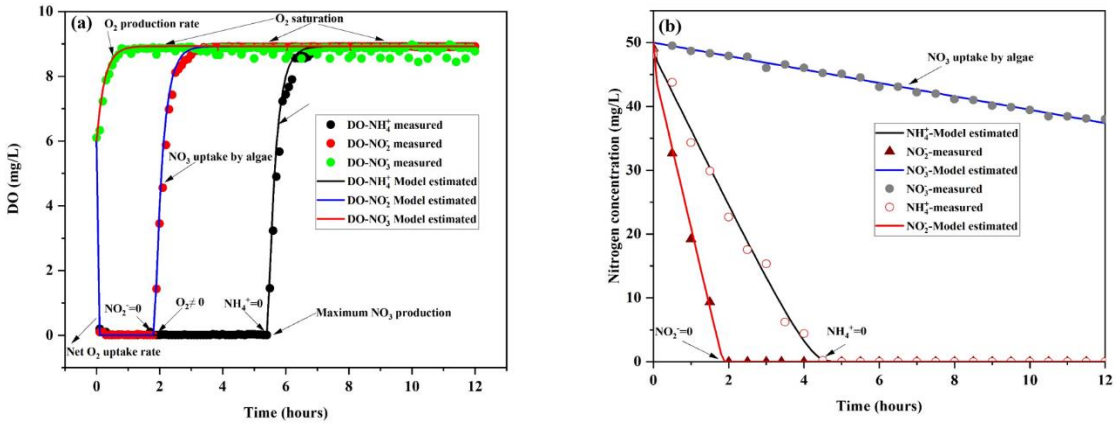


**Fig. 5.2.** DO concentration (a) and nitrogen concentration (b) in the experimental run no. 1, 2 and 3 carried out under $O_2$ saturated condition.

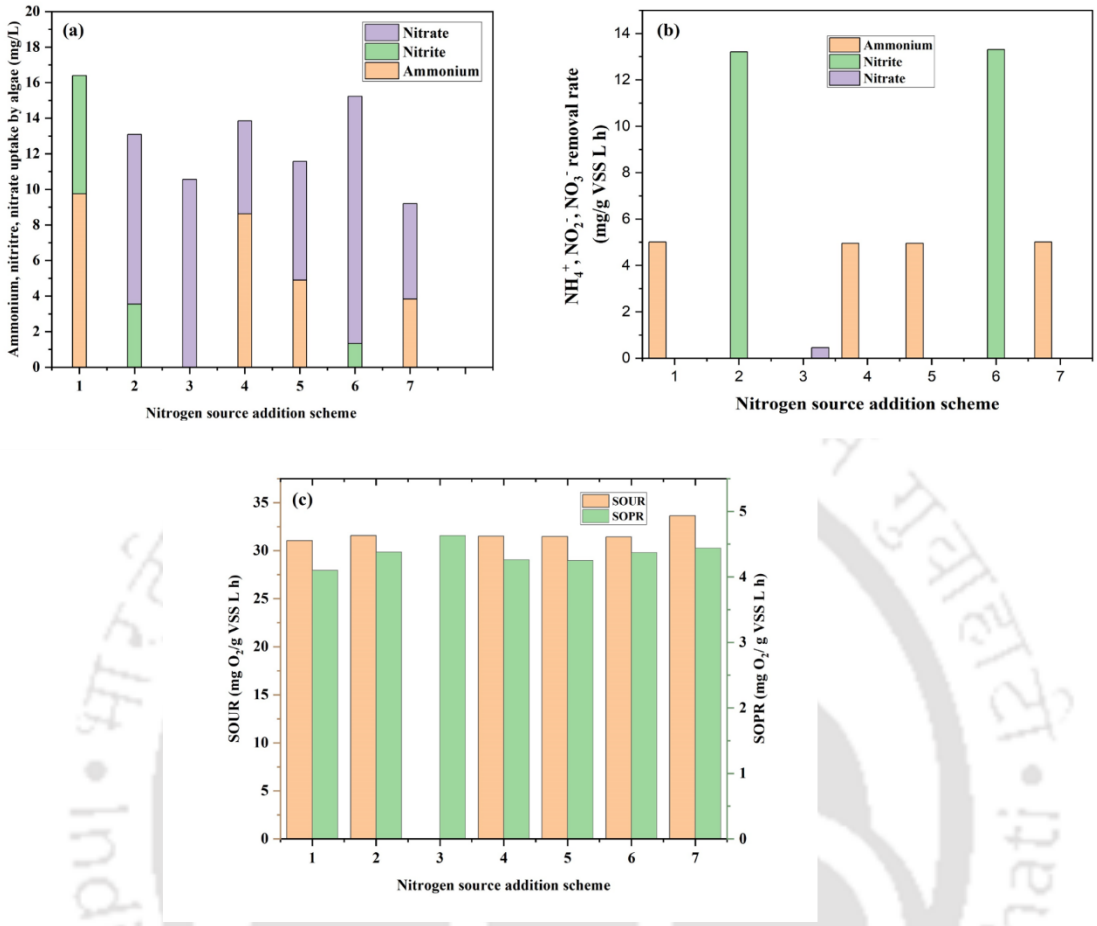


**Fig. 5.3. (a):** Uptake rates of $NH_4^+$, $NO_2^-$ and $NO_3^-$ (b) removal rates of $NH_4^+$, $NO_2^-$ and $NO_3^-$, (c) specific oxygen uptake rate (SOUR) and specific oxygen production rate (SOPR) by microalgae-bacterial consortium in the seven experimental runs carried out under oxygen saturated condition.

Specific oxygen uptake rate (SOUR) due to nitrification and specific oxygen production rate (SOPR) by algal photosynthesis in the experimental runs carried out under oxygen saturated condition are shown in Fig. 5.2c. Variation in SOUR and SOPR is observed in all the experiments. Maximum values of SOUR (33.63 g $O_2$ / g VSS L h) and SOPR (4.63 m*g* $O_2$ / g VSS L h*)* were observed in the experiments with three different nitrogen sources and only nitrate, respectively. Maximum SOPR (4.9 mg $O_2$ / g VSS L h) and SOUR (80 mg $O_2$ /g VSS L h) values has been

reported in the literature using microalgae-bacterial granules in a PSBR, and are attributed to which was due to microalgal activity along with degradation of organic compound by heterotrophic bacteria (Meng et al., 2019; Lee et al., 2016; Van Den Hende et al., 2014).

### 5.3.2 Effect of nitrogen source under oxygen limited condition

Individual and combined effects of ammonium, nitrite and nitrate at 200 mg/L each on nitrification rates under oxygen limiting conditions were studied. In experimental run no. 1, 4 and 5, the ammonium was reduced 50, 48 and 44.83 mg $NH_4^+$-N /L, respectively (Fig. 5.3). $NO_3^-$ produced was very low in all the experiments. Moreover, ammonium removal rate values were nearly the same (6.61 mg $NH_4^+$/ g VSS L h) at 200 mg/L of ammonium in the experimental run no. 1, 4, 5 and 7. Previous studies were revealed that ammonium removal under oxygen limited conditions (80%) was primarily due to nitritation/denitritation using microalgae-bacterial consortium in PSBR at the rate of 5.6 mg / L h (Wang et al., 2015). In the experiments carried out under $O_2$ limited condition, the algae-bacterial consortium could not efficiently utilize ammonium for its metabolic activity (Fig. 5.3). Whereas the previous results of experiments carried out under $O_2$ saturated condition revealed enhancement in ammonium removal by the consortium for nitrification instead of nitritation (Fig. 5.1). From the results shown in Fig. 5.3, $O_2$ produced by microalgae was significant for nitrification at a high ammonium concentration (Karya et al., 2013) (Fig. 5.3). Hence, it could be concluded that at high ammonium concentration the oxygen consumption rate by nitrifier is higher than the oxygen production rate by microalgae.

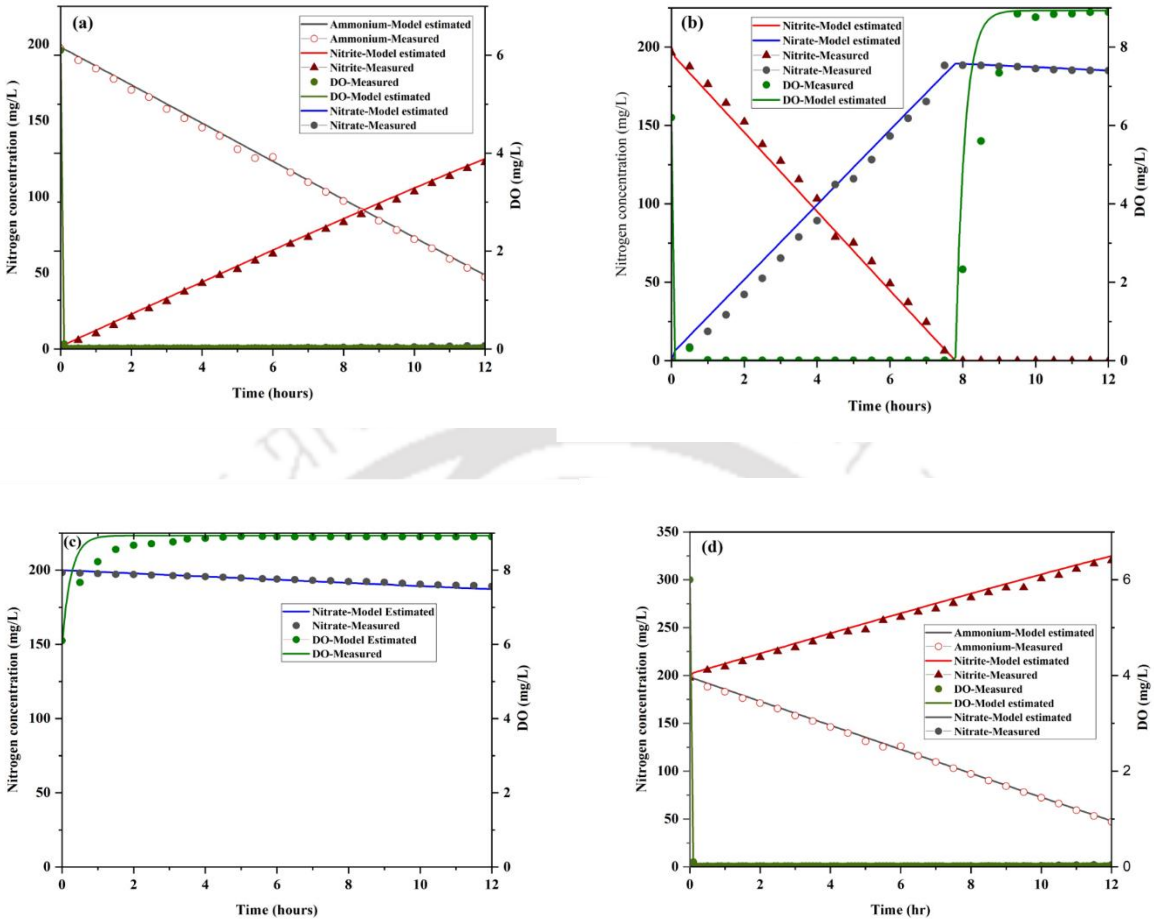

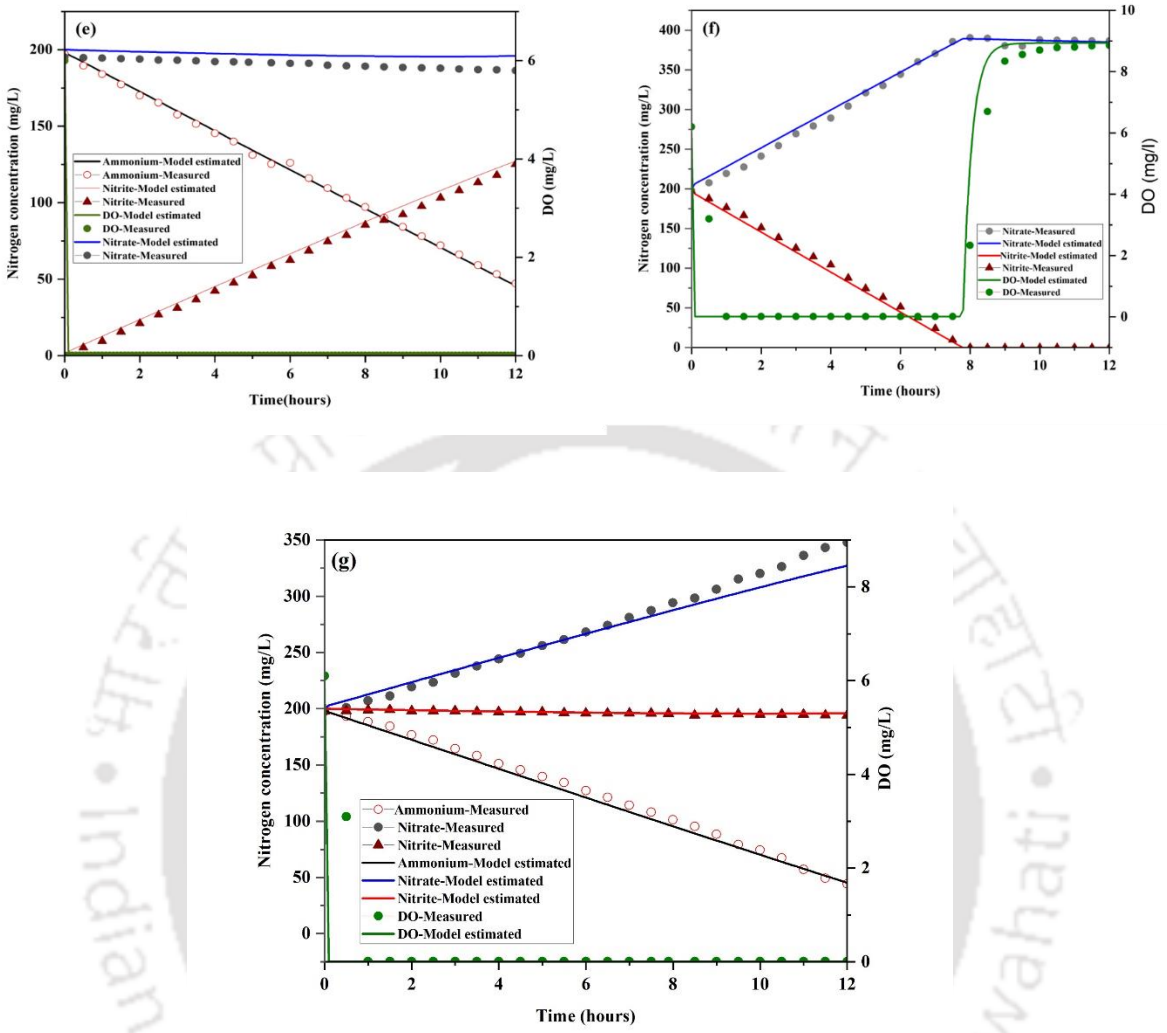


**Fig. 5.4** Concentrations of $NH_4^+$, $NO_2^-$, $NO_3^-$ and DO in the seven experimental run along with model ASM-AB estimated values under oxygen limiting condition (a, b, c, d, e, f and g)

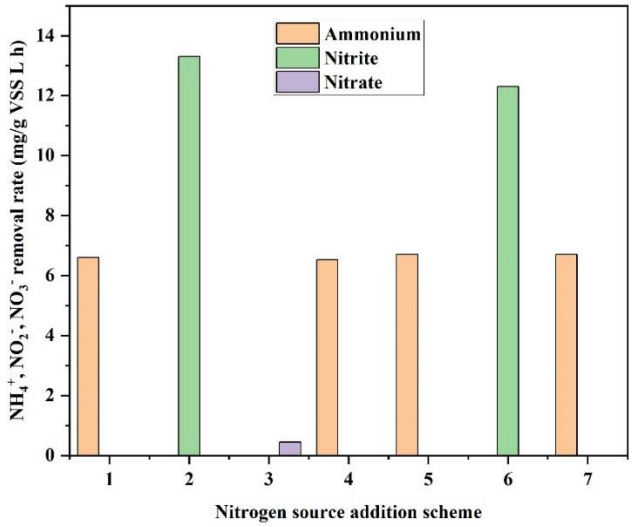


**Fig. 5.5** Removal rates of $NH_4^+$, $NO_2^-$ and $NO_3^-$ by AOB and NOB under oxygen-limiting condition.

In experimental runs no. 1, 2 and 3 with only ammonium, nitrate and nitrite, respectively, their removal rates were 6.61 mg $NH_4^+$- N/ g VSS L h, 13.31 mg $NO_2^-$- N/ g VSS L h and 0.446 mg $NO_3^-$-N/ g VSS L h, respectively (Fig. 5.4). In experimental runs no. 4, 5 and 6 with two different nitrogen sources the similar values of ammonium removal rate (6.53, 6.66 and 6.71 mg $NH_4^+$- N/ g VSS L h ) were observed. These results reveal that under $O_2$ limited condition, oxidation of ammonium to nitrate is ceased, especially due to high $NH_4^+$ concentration in the feed (Karya et al., 2013).

### 5.3.3 Effect of nitrogen source under optimal oxygen condition and mass balance analysis

Ammonium, nitrite and nitrate concentration in the experimental run no. carried out under optimum $O_2$ condition and ammonium concentration are show in Fig. 5.5. In these experiments, ammonium conversion to nitrate occurred without any zero residual ammonium or nitrite; moreover, the nitrate formed was consumed due to algal uptake. A maximum ammonium removal

rate of 11.95 mg $NH_4^+$/ L h is observed due to nitrification (Experimental run no. 1). Removal rate values (k) of ammonium, nitrite and nitrate were estimated from the slope of concentration of nitrogen source vs time in the seven experiments. From the calculated k values presented in Table 5.5, maximum rate values are obtained in experimental run no. 2, 3 and 7 for $NH_4^+$, $NO_2^-$ and $NO_3^-$ A sample plot obtained from experimental run 1is shown in Fig. 5.5 (a), whereas Fig. 5.5b shows DO concentration profile during this experiments.

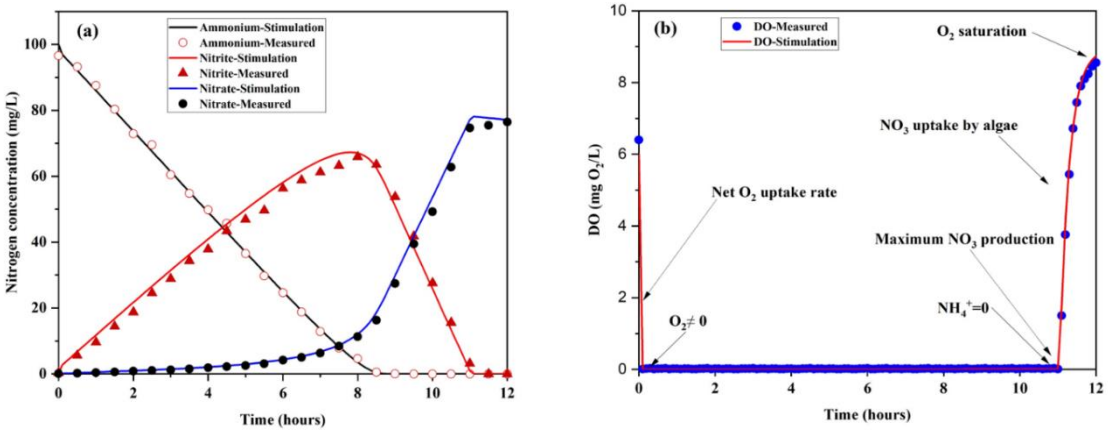


**Fig. 5.6** Concentration of (a) ammonium, nitrite and nitrate, and (b) DO concentration along with estimated values based on ASM-AB model in experimental run no. 1.

The ammonium removal varies for different, ammonium concentrations and reactors (PBR and PSBR) operated in SBR mode. Wang et al. (2015) reported that the ammonium removal rate with PSBR was 5.6 mg N $L^{-1}$ $h^{-1}$ for treating anaerobic digestate containing ammonium concentration of 297 mg $NH_4^+$-N $L^{-1}$. A removal rate of 2.24 mg $NH_4^+$-N/ L h at an ammonium concentration of 23 mg $NH_4^+$-N/L was observed by Rada-Ariza et al. (2019). Compared with these reports, the ammonium removal rate observed in this study for nitrification using PSBR was 11.95 mg $NH_4^+$/ L h.

The DO concentration reduced quickly and reached a constant value between 0.01 and 0.03 mg/L during the fill phase (Fig 5.5b), the combined values of $O_2$ production by microalgae and gas transfer were equal to that of $O_2$ utilized for nitrification by AOB and NOB.

**Table 5.4** Nitrogen removal rate in the experiments carried out under optimum oxygen saturated condition

| Experimental Run | Ammonium removal rate (k) | | Average k* | |
|---|---|---|---|---|
| | mg N/L h | mg N/g VSS L h | mg N/L h | mg N/g VSS L h |
| 1 | -10.169 | -5.35 | -10.08 | -5.3 |
| 2 | -24.03 | -12.64 | -23.55 | -12.58 |
| 3 | -1.025 | -0.539 | -1.012 | -1.011 |
| 4 | -10.50 | -5.52 | -10.45 | -10.43 |
| 5 | -10.50 | -5.52 | -10.45 | -10.43 |
| 6 | -23.95 | -12.60 | -23.44 | -23.38 |
| 7 | -10.66 | -5.61 | -10.56 | -10.52 |

*Average of three replicate in each experimental run

Following complete utilization of $NH_4^+$ and $NO_2^-$, DO reached saturation value during the time period 8.2-11.2 h. Subsequent to this time period, DO concentration increased owing to the growth of microalgae by consuming nitrate.

Nitrogen mass balance was carried out to evaluate the ammonium removal mechanism involves, and for which the concentrations of ammonium, nitrite and nitrate were determined during the experiments. From Table 5.6, ammonium removal by microalgae, nitrifying bacteria (AOB and NOB) and volatilization were 17-30%, 7% and 1%, respectively. These values are higher than the values reported for a microalgae-AOB-NOB consortium in PBR; the ammonium uptake by microalgae was 13-17% (Wang et al., 2013). Ammonium supplied to the PSBR in this study was taken by microalgae as well as by NB, which is in agreement with the literature (Karya et al., 2013; Wang et al., 2015; Manser et al., 2016). However, maximum ammonium removal was obtaine due to AOB and NOB for nitrification. These results reveal that $NH_4^+$, $NO_2^-$ and $NO_3^-$ as the nitrogen

source were removed efficiently at a low ammonium concentration by microalgae-AOB –NOB consortium. It is also reported that low sludge production and minimum algae growth with sufficient $O_2$ production are other advantages of such microalgae-bacterial consortia for ammonium removal from wastewater by nitrification (Karya et al., 2013).

### 5.3.4 Kinetics of nitrification by microalgae-AOB-NOB consortium

Karya et al. (2015) reported that high ammonium concentration is an important factor leading to $O_2$ production which leads to formation of intermediate products (nitrite or nitrate) during nitrification. In this work, combined effect of ammonium, nitrite and nitrate source on oxygen production and removal rate of ammonium, nitrite and nitrate by microalgae-bacterial consortium was studied.

As shown previously in Fig 5.1, the activity of microalgae on utilizing nitrite and nitrate strongly depended on initial ammonium concentrations. The ammonium removal rate (k) increased with an increase in ammonium concentration 50 to 200 mg/L indicating that the microalgae-bacterial consortium has a higher affinity towards ammonium as compared to other nitrogen sources at high ammonium concentrations (Nakamura et al., 2017; Delgadillo-Mirquez et al., 2016). Hence, uptake of nitrite and nitrate by microalgae is limited at high ammonium concentrations (Nakamura et al., 2017; Delgadillo-Mirquez et al., 2016). The ammonium uptake (3.83 - 9.75 $NH_4^+$-N/L, Table 5.5) achieved in this work are considerably higher than the values reported by Karya et al. (2013) and Wang et al. (2015), which are 4.84 $NH_4^+$-N/L and 2.43 mg $N/d^{-1}$, respectively. In this work, the k values were estimated by fitting the experimental removal rate values of ammonium, nitrite and nitrate with the ASM-AB model, which were found to be higher than the experimental k values, but are comparable to the experimental k values reported by Karya et al. (2013).

**Table 5.5** Nitrogen mass balance for oxygen saturated conditions

| Experimental run No. | $NH_4^+$-N initial (mg/L) (a) | $NO_3^-$-N formed (mg/L) (b) | $NH_3$-N volatilization (mg/L) (c) | $NH_4^+$-N uptake by algae (mg/L)(d) | $NH_4^+$-N uptake by AOB and NOB (mg/L) (e) | Percentage $NH_4^+$-N removal due to | | | |
|---|---|---|---|---|---|---|---|---|---|
| | | | | | | Nitrification | Uptake by AOB and NOB | Uptake by algae | $NH_3$ volatilization |
| 1 | 48.12 | 36.77 | 0.8 | 9.75 | 0.8 | 76.41 | 1.66 | 20.26 | 1.66 |
| 4 | 48.78 | 38.55 | 0.8 | 8.63 | 0.8 | 79.02 | 1.64 | 17.69 | 1.64 |
| 5 | 47.66 | 41.16 | 0.8 | 4.9 | 0.8 | 86.36 | 1.67 | 10.28 | 1.67 |
| 7 | 48.66 | 43.23 | 0.8 | 3.83 | 0.8 | 88.8 | 1.64 | 7.87 | 1.64 |

The differences in the experimental and model predicted k values in this study may be due to the consortium used, which needs to be verified further.

As previously shown in Fig. 5.1, in the experiments carried out under $O_2$ saturated condition, the values of $O_2$ production rate are lower than the $O_2$ consumption rate values at all initial ammonium concentrations. Similar observations were reported by González-Fernández et al. (2011) and Foladori et al. (2018). Conversely, $O_2$ produced by microalgae is quickly utilized by nitrifiers (AOB and NOB) in the photobioreactors, as confirmed by the low DO concentration (0.02) in the medium. The experimentally determined measured ammonium removal rates values in this work are also much higher as compared to previous studies in this literature. The photobioreactor utilized in this work is suited for treating wastewater with low ammonium concentrations, whereas the high ammonium concentrations are efficiently removed in open ponds. Karya et al. (2010) found that nitrification by microalgae-bacterial consortium result in high $O_2$ production rate (0.46 kg/$m^3$ d) at optimum condition of light intensity and biomass concentration..

### 5.3.5 Comparison of nitrification efficiency in PSBR, PBR and open ponds

The role of microalgae in PBR or PSBR (González-Fernández et al., 2011; Foladori et al., 2018) is to supply required $O_2$ to AOB and NOB for nitrification. $O_2$ production rate (0.368 kg/$m^3$/day) is significantly high in PBR (0.116–0.133 kg/$m^3$/day) and in PSBR (0.193 kg/$m^3$/day). However, these values are significantly low compared with those in photo-bioreactors operated under optimum condition of temperature, light intensity and biomass concentration (3.20-8.3 kg/$m^3$/day) (de Godos et al., 2010; Wang et al.,2015). However, the $O_2$ produced in PBR or PSBR is sufficient to oxidize ammonium to nitrate by AOB and NOB in the microalgae-AOB-NOB consortium. González-Fernández et al. (2011) obtained a residual ammonium concentration in the range 24-31 mg $NH_4^+$-N/L for treating anaerobic digestate in open ponds, operated at 15d HRT. These values

are higher than the values obtained in this work as the PSBR was operated under sequencing batch mode, whereas the open pond was operated in a simple batch mode. Another possible reason for the high nitrification rates observed in the present study is due to optimum light intensity and pH values in the PSBR. Though the ammonium removal rate of 9.65 mg/L h obtained in this study is lower than the value reported using an activated sludge processes (14-21 mg/L h) (Karya et al., 2013), the value is significantly higher than the previously reported values for PBR treating synthetic wastewater (7.7 mg N/L h) (Karya et al., 2013). In a PSBR, high biomass density decreases the light utilization by microalgae, AOB inhibition occurs at high light intensity and substrate utilization is also affected due to large flocs size. However, a positive effect of high biomass density is through self-shading by biomass which allows AOB to grow even at high light intensities (Manser et al., 2016; Wang et al., 2015). Hence, photo-oxygenation and ammonium removal rates could possibly be further enhanced by proper design of such PBR or PSBR.

### 5.4 Significant findings

The effect of different nitrogen sources on $NH_4^+$ removal by microalgae-bacterial consortium was examined in PSBR. Enhanced ammonium removal through nitrification and microalgae uptake were observed at 50 and 100 mg $NH_4^+$-N/L concentration, respectively. Comparison of the results obtained in this work with the literature revealed that $NH_4^+$ uptake by microalgae and $O_2$ availability strongly influenced the overall $NH_4^+$ removal by the consortium. ASM-AB model based on utilization of $NH_4^+$, $NO_2^-$ and $NO_3^-$ as a substrate for microalgae was developed to understand the effect of ammonium concentration and $O_2$ condition on nitrification by microalgae-bacterial consortium. The model revealed that (a) $NH_4^+$ concentrations in the range 50-200 mg $NH_4^+$-N/L affects nitrification due to insufficient $O_2$ supply, (b) 50 mg $NH_4^+$-N/L concentration is effective for microalgal photosynthesis and therefore nitrification due to oxygen saturated

condition and (c) 100 mg $NH_4^+$-N/L concentration is also suitable for complete nitrification due to optimum oxygen produced by microalgae.

# Chapter 6

## Shortcut nitrogen removal and bioelectricity production by microalgae-bacterial consortia using an integrated membrane photosynthetic microbial fuel cell

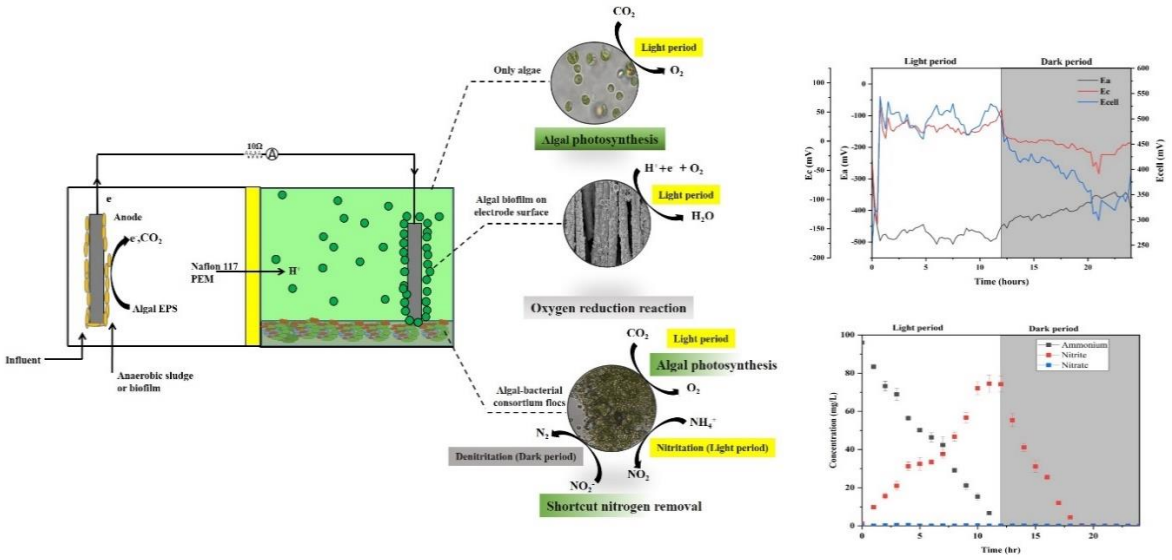

**ABSTRACT**

Membrane photosynthetic microbial fuel cells (MPMFCs) utilize $O_2$, $NO_3^-$ and $NO_2^-$ as cathodic electron acceptor, enabling simultaneous treatment of nitrogen, $CO_2$ and organic carbon in the cathode compartment. In this work, development of a novel cathodic process with *in situ* nitritation via microalgal photosynthesis during the light period is reported for achieving shortcut nitrogen removal (SNR) from ammonium-rich wastewater. Moreover, an indigenously prepared low-cost ceramic membrane was used to separate and recycle the microalgae–bacterial biomass to the cathode compartment during the continuous operation. The influence of $NH_4^+$ concentration and ratio of chemical oxygen demand (COD) to total nitrogen (TN) on the MPMFC performance was examined. Denitritation under dark and anoxic conditions occurred subsequent to nitritation under light and aerobic conditions by ammonia oxidizing bacteria (AOB) and denitrifying bacteria. Final concentrations of $NH_4^+$ and $NO_2^-$ in the effluent of 0.10 mg $NH_4^+$-$L^{-1}$ and 0.02 mg $NO_2^-$-$L^{-1}$, respectively, were obtained using MPMFC which resulted in a nitrogen removal efficiency of 99±0.5%. The maximum electricity production achieved using MPMFC was 56±0.1 mA. This study demonstrated that combining microalgal photosynthesis, nitritation and denitritation in the cathode compartment of MPMFC is advantageous for avoiding the cost due to external aeration and organic carbon source necessary for ammonium removal as well as utilization of $NO_2^-$ or $NO_3^-$ as an electron acceptor.

**Keywords**: Shortcut nitrogen removal; Microalgae-bacterial consortia; Ceramic membrane; Photosynthetic microbial fuel cell; Microalgal photosynthesis

## 6.1 Introduction

Microalgae-bacterial consortia for ammonium-rich wastewater treatment includes any of the following combinations: microalgae-nitrifying bacteria, microalgae-ammonia oxidizing-denitrifying bacterial consortia and microalgae-nitrifying-anammox bacteria (Karya et al., 2013; Manser et al., 2016; Wang et al., 2015). Shortcut nitrogen removal (SNR) using microalgae-ammonia oxidizing-denitrifying bacterial consortia is advantageous for simultaneous nitrification-denitrification, oxygen limited autotrophic nitrification-denitrification, completely autotrophic nitrogen removal over nitrite, anaerobic ammonium oxidation `and aerobic deammonification process in the absence of external aeration with less organic carbon consumption (Karya et al., 2013; Manser et al., 2016; Wang et al., 2015).

SNR involves two stages: (1) nitritation i.e. the aerobic oxidation of $NH_4^+$ to $NO_2^-$ by ammonia oxidizing bacteria (AOB) through oxygen from microalgal photosynthesis during the light period, and (2) denitritation, i.e. dissimilatory reduction of $NO_2^-$ to $N_2$ gas by denitrifying bacteria (DNB) during the dark period characterized by a low dissolved oxygen concentration (Manser et al., 2016; Wang et al., 2015). The latter step needs an electron donor, usually an organic carbon source, for supporting the bacteria by providing activation energy for the denitritation reaction (Virdis et al., 2010). The main cost related to this process is the requirement of an external carbon source for complete denitritation. Efficiency of SNR by microalgae-AOB-DNB consortia is limited due the following reasons: inhibition of nitrite oxidizing bacteria (NOB) over AOB, lack of anoxic condition for denitrification and the requirement of an external carbon source (Karya et al., 2013; Manser et al., 2016; Wang et al., 2015). Therefore, recent studies have focused on inhibition of NOB by selecting high $NH_4^+$ concentration (high nitrous acid/ high free ammonia) with low

dissolved oxygen (DO) concentrations in photosequencing batch reactor (PSBR) (Wang et al., 2015) and utilizing $NO_2^-$ or $NO_3^-$ for cathodic reaction in a microbial fuel cell (Virdis et al., 2010)

Electron acceptors, such as, $O_2$, $NO_2^-$ and $NO_3^-$ produced via microalgal photosynthesis and nitritation or nitrification, are suitable for cathodic reaction, thereby overcoming the requirement of mechanical aeration (Zhu et al., 2017; Yang et al., 2017; Kondaveeti et al., 2014). In addition to the production of electron acceptors, treatment of ammonium rich wastewater can be achieved (Manser et al., 2016; Rashid et al., 2013; Strik et al., 2008; Kondaveeti et al., 2014; Wang et al., 2010). However, the profiles of $O_2$, $NO_2^-$ and $NO_3^-$ by microalgae-AOB-DNB consortia in MFC have not been reported thus far, which is essential for achieving a maximum efficiency of the system. Relationship among the microalgae, AOB and DNB for SNR and cathodic reaction are represented in equations 6.1−6.7. Oxygen production via ammonia uptake by microalgal biomass and nitritation by AOB during the light period are represented in equations 6.1 and 6.2 (Manser et al., 2016).

$$16NH_4^+ + 92H_2O + HPO_4^{2-} + 106HCO_3^- \rightarrow C_{106}H_{263}O_{110}N_{16}P + 92OH^- + 106O_2 \quad (6.1)$$

$$NH_4^+ + 1.24O_2 + 0.16CO_2 + 0.04HCO_3^- \rightarrow 0.04C_5H_7O_2N + 0.96NO_2^- + 0.96\,H_2O + 1.92H^+ \quad (6.2)$$

Equation 6.3 estimates the cathodic reaction via oxygen as the electron acceptor during the light period (Logan et al., 2016).

$$O_2 + 4H^+ + 4e^- \rightarrow 2H_2O\ (E^0 = 1.229\ V) \quad (6.3)$$

Equation 6.4 describes $NO_2^-$ reduction to $N_2$ by DNB during the dark period.

$$2NO_2^- + 6H^+ + 6e^- \rightarrow N_2 + 2H_2O + 2OH^- \quad (6.4)$$

Finally, equations 6.5-6.7 represent nitrite reduction to $N_2$ along with their standard potential values during the dark period (Clauwaert, et al., 2007).

$$NO_2^- + 2H^+ + e^- \rightarrow NO + H_2O \ ((E^0 = +0.350\ V)\ \ (6.5)$$

$$NO + H^+ + e^- \rightarrow 1/2N_2O + 1/2H_2O\ (E^0 = +1.175\ V)\ \ (6.6)$$

$$1/2N_2O + H^+ + e^- \rightarrow 1/2N_2 + 1/2H_2O\ (E^0 = +1.355\ V)\ \ (6.7)$$

The $O_2$ required for both nitritation/nitrification and cathodic reaction can be coupled if microalgae and AOB are directly utilized in the cathodic compartment (Virdis et al., 2010). Virdis et al. (2010) reported that nitrifier (AOB and NOB) and DNB species are capable of using nitrate as electron acceptor in the cathode compartment for simultaneous nitrification and denitrification (Virdis et al., 2010). More recently, shortcut nitrification with a low NOB activity (low nitrate production) was coupled with autotrophic denitrification in a microbial fuel cell (MFC) (Li et al., 2016). Photosynthetic microbial fuel cells (PMFC) are MFC systems that combine the microalgal photosynthesis in the cathodic compartment for the production of oxygen, which is utilized as an electron acceptor for oxidation reaction (Del campo et al., 2013; Powell et al., 2009; Gajda et al., 2015; Ma et al., 2017; Cao et al., 2009; Lan et al., 2013; Wu et al., 2014).

Li et al. (2016) reported the removal of nitrogen using an integrated shortcut nitrification at aerobic cathode compartment and autotrophic denitrification at anoxic cathode compartment of MFC (SNAD-MFC). In this system, synthetic wastewater containing ammonium was sequentially supplied to the cathode compartment for shortcut nitrification at low DO concentrations, and nitrite was reduced to $N_2$ gas via autotrophic denitrification. Although the SNAD-MFC can effectively combine shortcut nitrification and autotrophic denitrification, but it doesn't exclude the use of

costly external aeration and achieve complete shortcut nitrification due to the presence of NOB (Li et al., 2016).

This study was aimed at overcoming the problem with external aeration and incomplete nitrification by combining nitritation with microalgal photosynthesis in the cathodic compartment for enhancing SNR in the same compartment. The effect of different ammonium concentration, COD/N ratio on PMFC performance as well as the activity of microalgae on different nitrogen sources (ammonium, nitrite and nitrate) were examined to understand the electron transport mechanism in the algae assisted cathodes. Oxygen production and consumption for SNR were estimated and compared with the literature for application potential of the PMFC.

## 6.2 Materials and methods

### 6.2.1 Membrane photosynthetic microbial fuel cell (MPMFC) design and performance

An indigenously fabricated a MPMFC consisting of two chambers with a working volume of 500 $cm^3$ each was used in this study. Carbon cloth coated with 0.5 $mg/cm^2$ of Pt (Saienergy Fuel Cell India Pvt. Ltd., Chennai, India) was used as the cathode whereas for the anode only carbon cloth was employed. The area of both the electrodes was 5×5 $cm^2$. An ion exchange membrane (IEM) (Nafion 117, Saienergy Fuel Cell India Pvt, Ltd., Chennai, India) was used to separate the MPMFC compartments. An indigenously prepared a low-cost tubular ceramic membrane (pore size of 0.339 μm) was utilized for biomass separation from a photosequencing batch reactor (PSBR) as well as for recycling the biomass in the cathodic compartment of the MPMFC (Fig. 6.1). Ag/AgCl reference electrodes (Ikon Instruments, Delhi, India) with a potential of +0.230 V were used in both the anode and cathode compartment to record the half-cell potential values and total voltage of the MPMFC. A variable resistor of 10 Ohms was used for estimating the current produced in MPMFC by using Ohm's law (Virdis et al., 2010).

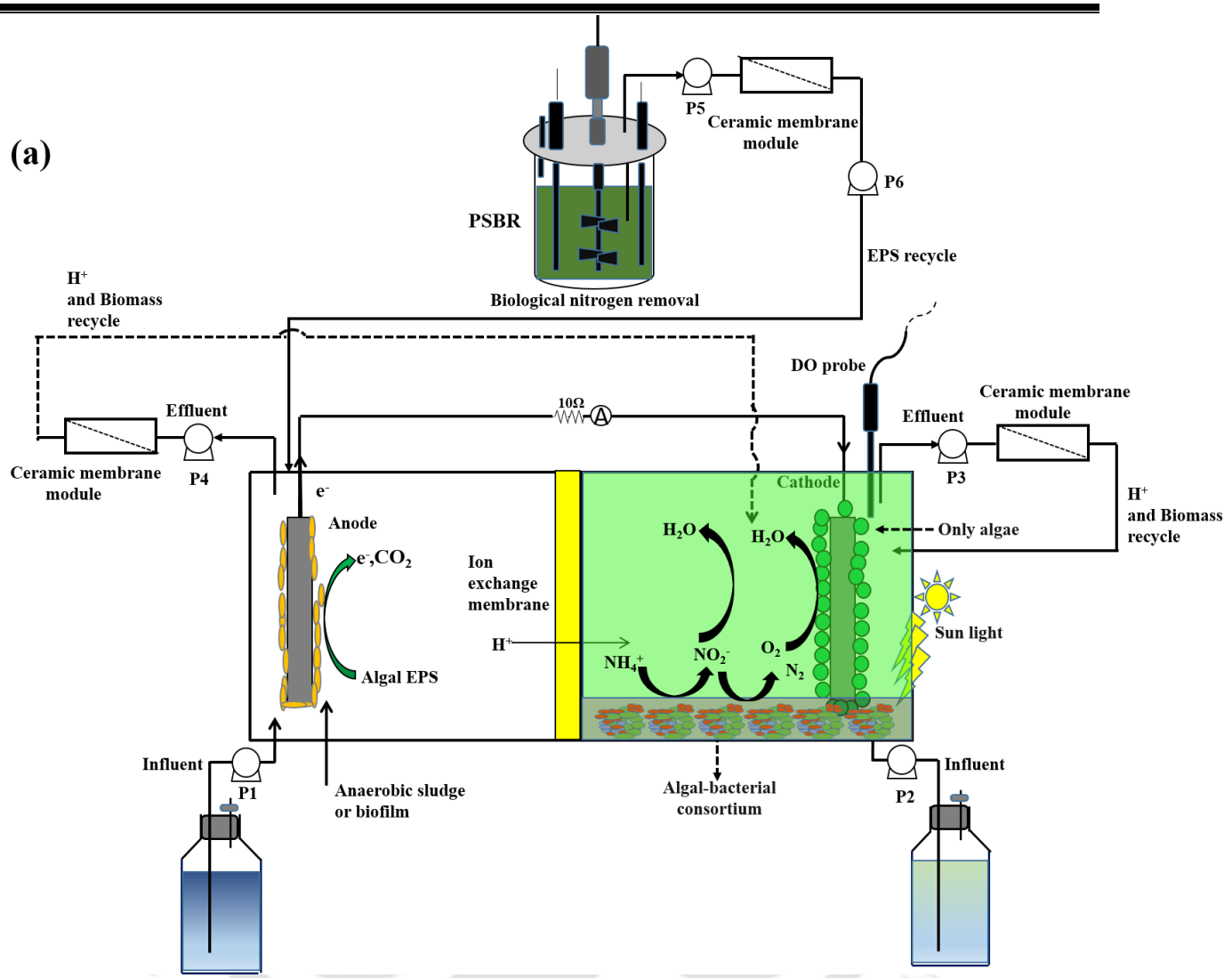

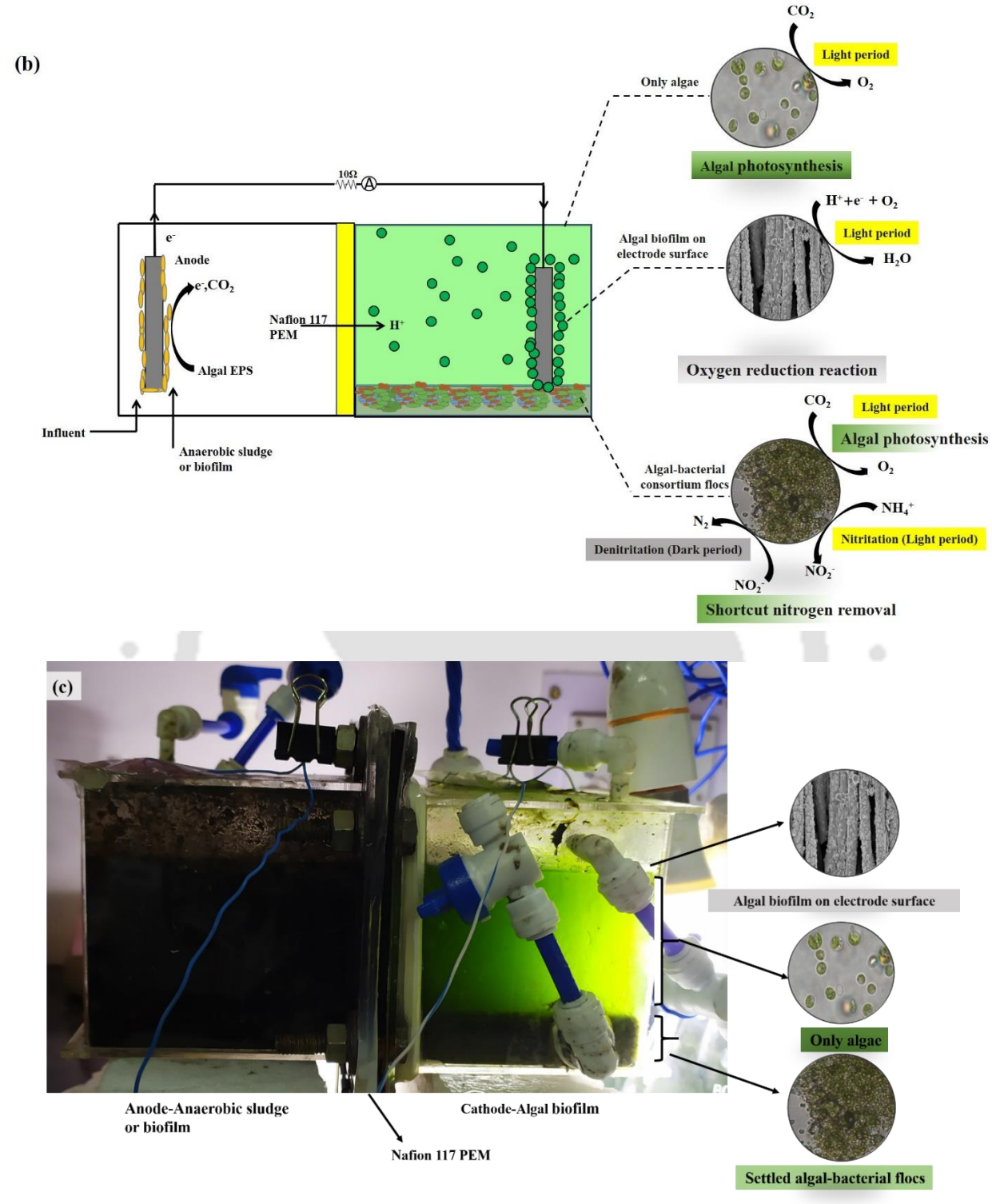


**Fig. 6.1** Schematic (a and b) and (c) picture showing the MPAMFC. Total carbohydrate in the form of algal EPS along with MSM was supplied to the anode via peristaltic pump (P1). Effluent from the PSBR was fed to the anode by pump 5 (P5) for EPS recycle. Recirculation of the effluent

in the cathodic compartment was ensured by pump 3 (P3). Inlet to the cathodic chamber was by pump 2 (P2). DO in the cathode compartment was measured by a DO meter placed inside the cathode compartment

Cathode and anode compartments were inoculated with a consortium of microalgae-AOB and DNB from a PSBR treating ammonium rich wastewater. The anode compartment was supplied with mineral salt medium (MSM) containing 0.3 g $L^{-1}$ NaCl, 0.2 g $L^{-1}$ $NH_4Cl$, 0.11 g $L^{-1}$ $CaCl_2 \cdot 2H_2O$, 0.1 g $L^{-1}$ $MgCl_2 \cdot 6H_20$, 0.1 g $L^{-1}$ $KH_2PO_4$, 0.945 g $L^{-1}$ $FeCl_2$, 0.013 g $L^{-1}$ $CuCl_2$, 0.07 g $L^{-1}$ $ZnCl_2$, 0.065 g $L^{-1}$ $CoCl_2$, 0.021 g $L^{-1}$ $Na_2MoO_4$, 0.63 g $L^{-1}$ $MnCl_2$, 0.13 g $L^{-1}$ $NiCl_2$ and 0.5 g $L^{-1}$ yeast extract as mentioned by Sinharoy et al. (2015). For enrichment of microalgae-AOB-DNB consortia, synthetic ammonium rich wastewater was used. The MPMFC was operated for a period of about 1 month to support biofilm formation. Inlet pH of the feed to the anode and cathode compartment were 7 and 7.5 with conductivity values of 0.218 mS and 0.796 mS, respectively, and hydraulic retention time (HRT) was 24 h (Fig. 6.1). The MPMFC was illuminated using three cool white LED bulbs (Philips Cool White-9W) with an average light intensity of 140 µmol/$m^2$ s.

### 6.2.2 Analytical methods

Samples taken from the cathode and anode chambers were instantly filtered via 0.45 µm membrane filters. Carbohydrate content in the sample was estimated using a total organic carbon analyzer (TOC analyzer; OI Analytical, USA), equipped with a non-dispersive infrared (NDIR) detector. Conductivity was measured using Eutech CON 2700 meter (Eutech instruments, Singapore). Ammonium, nitrite and nitrate concentrations were determined following American Public Health Association (APHA) method [25]. Dissolved oxygen was monitored with a portable DO meter (Hach DHR India Pvt. Ltd. Bangalore, India) (Fig. 6.1).

Microalgal-bacterial biomass was collected from a photosequencing batch reactor, which was used for nitrogen removal. 50 mL of the biomass was centrifuged at 4300×g for 10 min for the separation of soluble EPS from the biomass. Protein and carbohydrate present in the microalgal EPS were estimated using Lowry and Anthrone methods respectively (Junping et al., 2019).

### 6.2.3 Batch tests

#### 6.2.3.1 Nitritation and denitritation at the cathode compartment

Oxidation of $NH_4^+$ to $NO_2^-$ by AOB and $NO_2^-$ reduction to $N_2$ gas by DNB were verified by analysis of the liquid samples. Anode and cathode in the MPMFC were fed separately as follows: the cathode chamber was initially supplied with synthetic wastewater, whereas the anode compartment was supplied with MSM medium along with 400 mg $L^{-1}$ of carbohydrate in the form of EPS. The cathode was supplied with 100 mg $NH_4^+$-N $L^{-1}$ and glucose was supplied stoichiometrically for achieving denitritation.

#### 6.2.3.2 Effect of nitrite and carbohydrate on denitrification at the cathode during dark period

In order to study the influence of total carbohydrate and nitrite on denitritation during the dark period, the chambers were disconnected followed by washing of the cathodic chamber. After washing, the cathode was purged with $N_2$ at 10 mL $min^{-1}$ followed by addition of 400 mg $L^{-1}$ total carbohydrate (glucose) and 10 mg $L^{-1}$ nitrite. Samples were withdrawn every 1 hour for the analysis of total carbohydrate, $NH_4^+$, $NO_2^-$, $NO_3^-$ and the voltage produced was measurement every 15 minutes. The coulombic efficiency of the electrode was estimated by integrating the current during the batch operation.

### 6.2.4 Effect of ammonium, nitrite and nitrate at the cathode during the light period

Similar to the previous experiment, in addition to 400 mg $L^{-1}$of total carbohydrate (EPS) in the anode chamber either 10 mg $L^{-1}$ $NH_4^+$-N or 4 mg $L^{-1}$ $NO_2^-$-N or 4 mg $L^{-1}$ $NO_3^-$-N was added to the cathode after initial washing with MSM. Liquid samples were withdrawn every 10 min for the analyses of ammonium, nitrite and nitrate, whereas voltage measurements was measured every 10 min.

### 6.2.5 Open circuit experiment

In order to study the shortcut nitrogen removal in open circuit, the cathode and anode compartments were disconnected and supplied with different substrates (ammonium, nitrite and nitrate) at a constant flow rate of 0.5 L $d^{-1}$ for 12 h. Both the anode and cathode were supplied with the wastewater; the anode compartment was additionally supplied with 400 mg $L^{-1}$ carbohydrate (EPS). Before beginning the test, feeding of the cathode compartment was stopped with open circuit and 1 h prior to the test 100 mg $NH_4^+$-N $L^{-1}$ was supplied. Half-cell potential values in open circuit were measured every 10 minute and samples were taken every 1 h for analyses.

### 6.2.6 Continuous feeding test

#### 6.2.6.1 Effect of ammonium concentration

MSM medium containing 50-200 mg $L^{-1}$ $NH_4^+$-N and stoichiometrically equivalent amount of glucose was supplied to the cathodic compartment for attaining denitritation. Effluent from the cathode was treated by tubular ceramic membrane for biomass separation and recycled using pump 3 (Fig. 6.1). Ammonium conversion to nitrite by utilizing $O_2$ produced from microalgal photosynthesis was monitored by measuring anodic and cathodic half-cell potential values. During the continuous operation, the MPMFC performance was assessed for every 12 h duration and

samples from both the compartments were analyzed at every 1 h interval. Half-cell potentials and voltage were measured and their results were presented as average values.

### 6.2.6.2 Effect of COD/N ratio

In order to determine the effect of different COD/N ratio (1, 2, 3 and 4) on the MPMFC performance, MSM medium containing 100 mg $L^{-1}$ algal EPS (total carbohydrate) and different concentrations of ammonium (100, 50, 33.3 and 25 mg $NH_4^+$-N $L^{-1}$), were added under continuous mode to the cathode compartment. Prior to the experiment, $NH_4^+$, $NO_2^-$ and $NO_3^-$concentrations at the cathode compartment were checked at regular intervals. After, achieving steady state, samples were taken every 1 h interval for 12 h period for analyses, and voltages were measured every 15 minutes. All the experiments were performed in duplicate and the analyses carried out in triplicate.

### 6.2.7 Polarization, power and cyclic voltammetry curve (CV)

Polarization, power and CV curves were determined using a potentiostat (Interface 1010 E, Gamry instruments, USA). Whereas the anode compartment was continuously fed with a total carbohydrate concentration of 400 mg $L^{-1}$ in the form of algal EPS during the measurement, the cathodic compartment was supplied with either 10 mg $NH_4^+$-N $L^{-1}$or 4 mg $NO_3^-$-N $L^{-1}$or 4 mg $NO_2^-$-N $L^{-1}$ at the beginning of the test (both light and dark period). The MPMFC was initially conducted in open circuit for 1h, and then the voltage was changed at a scan rate of 0.1 mV/s. The experiments were monitored from open to closed circuit and conversely. Cyclic voltammetry measurement at the cathode was conducted for three different nitrogen sources during the light and dark periods: 10 mg $NH_4^+$-N $L^{-1}$, 4 mg $NO_3^-$-N $L^{-1}$, 4 mg $NO_2^-$-N $L^{-1}$ against Ag/AgCl electrode at a scan rate of 10 mV $s^{-1}$.

### 6.2.8 Scanning electron microscopy (SEM)

In order to evaluate microalgal biofilm growth on MPMFC cathode, samples of the cathode were analyzed by FESEM at an acceleration voltage of 3 kV. Morphology analysis of the electrode was carried out using FESEM (Model Sigma 300, Zeiss, Germany) fitted with an omega detector. For FESEM analysis, an area of 0.10 $cm^2$ sample of the cathode electrode was cut, dried and fixed in the sample support and then coated with a fine layer of gold prior to the morphology analysis

## 6.3 Results and discussion:

### 6.3.1 Shortcut nitrogen removal by microalgae-AOB-DNB consortia in MPMFC

The objectives of using shortcut nitrification by microalgae-AOB-DNB consortia is to decrease aeration cost by utilizing oxygen in microalgal photosynthesis and to cut down the nitratation step by inhibiting the NOB. In order to study the ammonium removal by nitritation and to produce bioelectricity in MPMFC, light intensity in this study was maintained at 140 µmol/$m^2$ s. The half-cell potentials of cathode produced was steady (short-circuit) and exponential (open circuit) at the initial $NH_4^+$ concentration of 100 mg $NH_4^+$-N/L. At the resistance of 10 Ω, the half-cell potentials of cathode was around 55 mV at short circuit and 96.1 mV at open circuit (Fig. 6.2 and 6.3a). Time for nitritation was reduced at open circuit due to higher availability of dissolved oxygen than in short circuit, which facilitated the AOB activity for an enhanced ammonium oxidation (Virdis et al., 2010). Likewise, the number of coulombs transferred due to the short-cut nitritation was 2160 C at 100 mg $NH_4^+$-N/L, which is 32.15 times higher than the value reported by Li et al. (2016) short-cut nitrification in a MFC supported by external aeration. These results confirmed the advantages of oxygen production by microalgal photosynthesis coupled to short-cut nitritation in MFC which yielded maximum ammonium removal along with electricity generation.

For complete $NH_4^+$ oxidation by AOB for an initial concentration of 100 mg $NH_4^+$–N/L, 12 h light period is found to be optimum (Fig. 6.2b). The $NH_4^+$ removal rates were 8 mg $NH_4^+$-N/L h (short circuit), and 8.72 mg $NH_4^+$-N/L h (open circuit), which are higher than the value: 0.69–1.04 mg $NH_4^+$-N/L h reported in the literature (Li et al., 2016). The ratio of $NO_2^-$ and $NO_3^-$ was above 3.0 at a low DO concentration (< 3.5 mg/L). The better results obtained in this study compared with the previous report is attributed to the high biomass activity and optimum oxygen supply by algal photosynthesis for an efficient nitritation, which is indicated by the negligible nitrate concentration (0.22 mg $NO_3^-$/L). During short circuit and open circuit in the MPMFC cathode compartment,

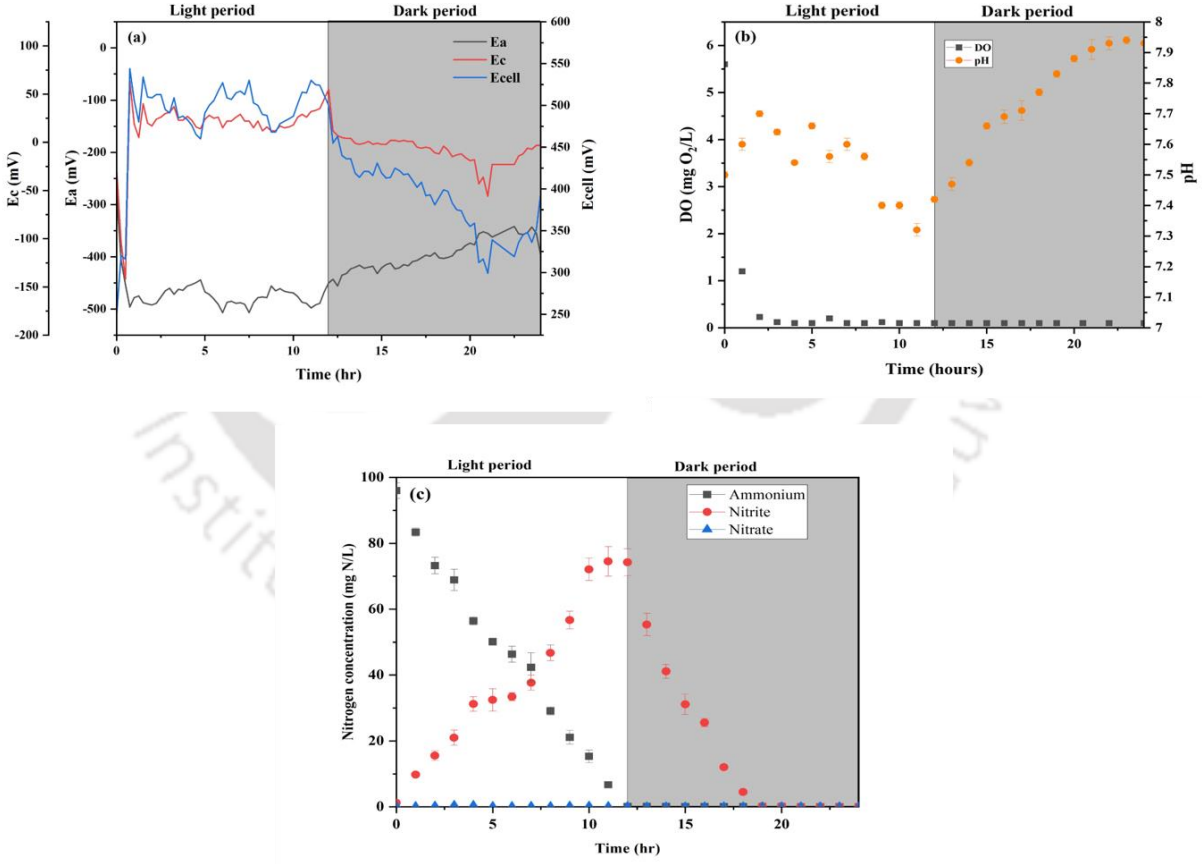

**Fig. 6.2** Results of batch tests at the cathode compartment of the MPMFC in short circuit: (a) cathodic potential, (b) Variation in pH and DO concentration and (c) Changes in ammonium, nitrite and nitrate concentration during the experiments.

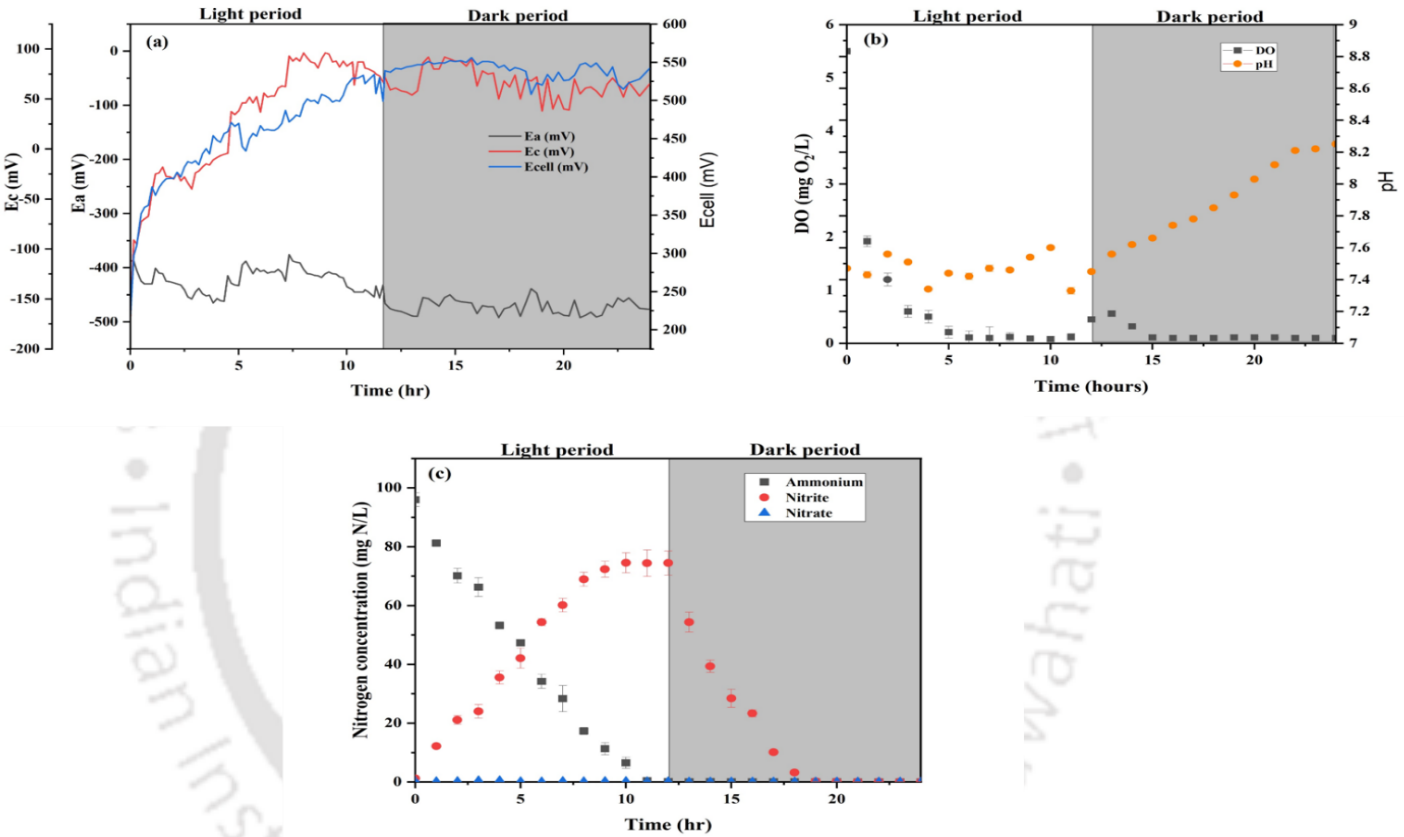


**Fig. 6.3** Results of batch tests at the cathode compartment of the MPMFC in open circuit. (a). cathodic potential. (b) Variation in pH and DO concentration. and (c). Changes in ammonium, nitrite and nitrate concentration

$NO_2^-$ concentrations were 74.22 mg $NO_2^-$/L and 74.12 mg/L, respectively (Fig. 6.2b), which are 1.92 times higher than the value reported in a previous study (Li et al., 2016). These results indicate inhibition of NOB activity at low DO concentration (<0.1 mg/L) and at high $NH_4^+$ concentration during the light period.

Furthermore, the oxidation of $NH_4^+$ was quicker at open circuit than at short circuit (Fig. 6.3b). It is reported that $NO_2^-$ production accounted for 77% due to $NH_4^+$ oxidation for 100 mg $NH_4^+$-N/L inlet concentration (Wang et al., 2015; Li et al., 2016). At DO concentration greater than 0.1 mg/L, $NH_4^+$ is directly oxidized to $NO_2^-$ with a low $NO_3^-$ accumulation. High $NH_4^+$ concentration could adversely affect electricity production in MPMFCs due to competition of oxygen between $NH_4^+$ oxidation and oxygen reduction, whereas low $NH_4^+$concentration tends to produce very less oxygen but high electricity; hence $NH_4^+$ concentration in MFCs should be optimized in MFCs to achieve simultaneous electricity production and short-cut nitritation.

In open circuit, $NO_2^-$ concentration gradually increased during the light period due to nitritation, and later reduced sharply during the dark period in the absence of photosynthetically produced oxygen (Fig. 6.2b). In contrast, $NO_2^-$ production rate was slower in the short circuit than in the open circuit (Fig. 6.2b and Fig. 6.3b). DO concentration reached 5.6 mg $O_2$/L at the beginning of the light period which reduced to below 0.1 mg/L at the beginning of dark period without causing any inhibitory effect on DNB. However, due to the reduced availability of the electron acceptor ($O_2$) at the cathode, the electricity production reduced during the dark period. In addition, denitritation ceased upon complete reduction of $NO_2^-$ in MPMFC during the dark period. The results of nitritation and denitritation rates in open circuit was better than the results in short-circuit for achieving SNR within a short time period. In the presence of $NH_4^+$ and $O_2$ (electron acceptor), the electricity production was high during the light period. Maximum power density obtained was 2.809 mW/m$^2$ at 100 mg $NH_4^+$-N/L, which is however lower than the value reported previously using photosynthetic microalgae microbial fuel cells (Strik et al., 2008). The highest current density observed in the study was 0.0265 mA/m$^2$ over the resistance of 10 Ω at 100 mg $NH_4^+$-N/L in this study.

FESEM images (Fig. 6.4), reveals microalgal biofilm growth on the cathode surface of MPMFC, suggesting that microalgae biofilm served as the biocathode to enable oxygen reduction reaction for achieving short-cut nitrogen removal in this study (Fig. 7.1b and c and Fig. 7.4). Formation and uniform morphology of algal biofilm on the cathode surface was clearly observed in the FESEM image (Fig. 6.4.).

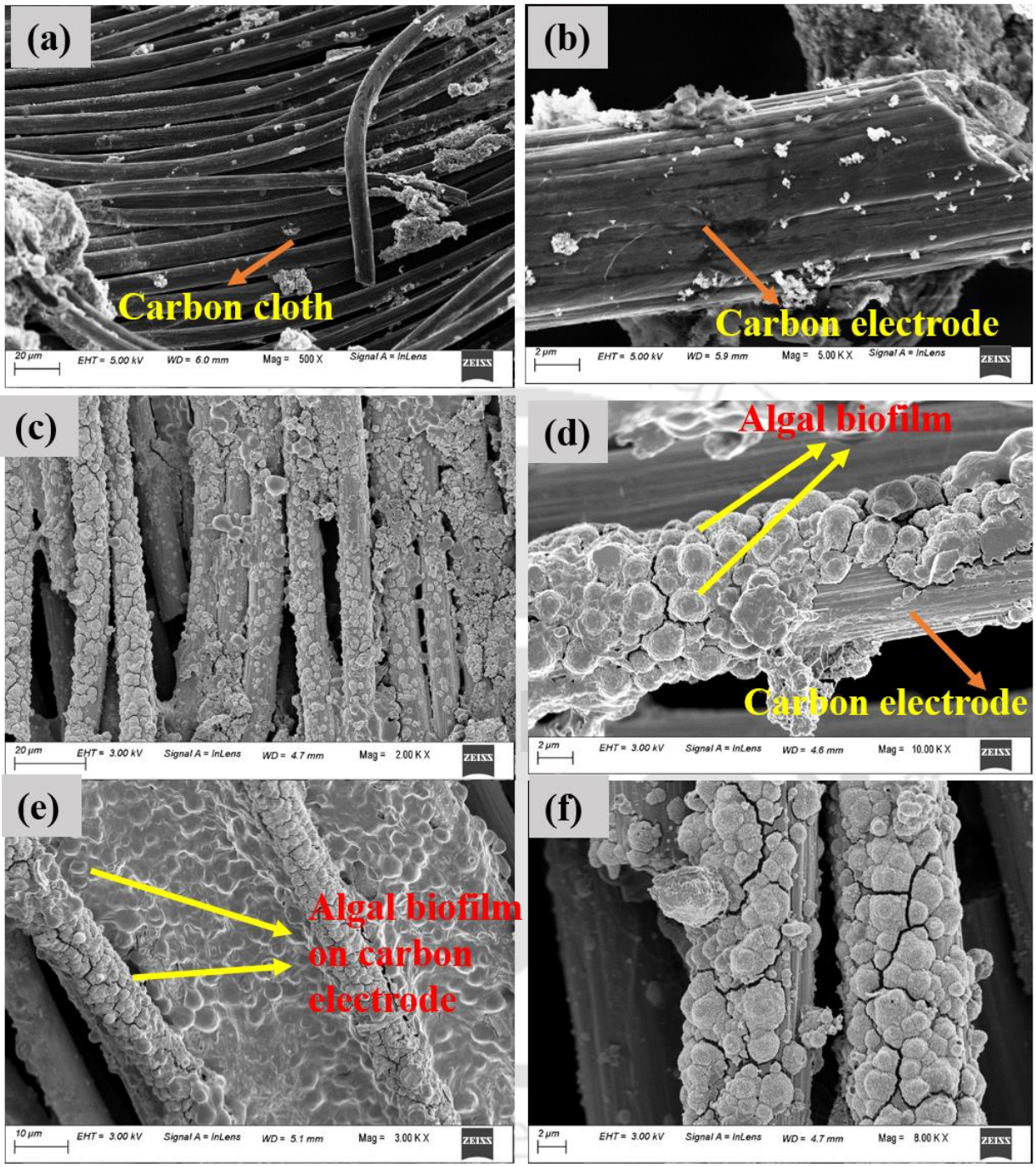


**Fig. 6.4** FESEM images (a and b) of cathode before use in MPMFC. FESEM images of the cathode with algal biofilm during the MPMFC operation are shown in c, d, e and f.

DO and pH are the main factors affecting short-cut nitrogen removal in the MPMFC cathode. DO decreased drastically during the light period from 5.6 to 0.1 mg $O_2$/L and remained almost the

same (0.1 mg $O_2$/L), following which denitritation stopped at the end of the dark period (Fig. 7.2a). Based on these results, it could be inferred that $O_2$ is consumed by AOB for $NH_4^+$ oxidation as per the equation 7.2 and oxygen reduction as per the reaction ($O_2 + 2H_2O + 4e^- \rightarrow 4OH^-$) in the MPMFC cathode, which yielded a constant DO level by inhibiting NOB (Wang et al. 2015). In the case of pH, its value decreased during the light period from 7.47 to 7.32 (Fig. 6.2b) and later increased during the dark period from 7.32 to 7.92 (Fig.6.2b). These results suggest that $H^+$ ions were produced by AOB for $NH_4^+$ oxidation reaction, $OH^-$ ions were produced by the afore mentioned oxygen reduction reaction and ammonium uptake by microalgae (Equation 7.1) in the MPMFC cathode.

The balance between $NH_4^+$ uptake by microalgae, $NH_4^+$ oxidation by AOB and oxygen reduction reaction yielded a constant pH 7.5. Wang et al. (2015) reported decrease in pH from 7.8 to 7.1 in a PSBR during the light period due to $NH_4^+$ oxidation by AOB. However, increase in pH from 7.1 to 7.8 was observed due to denitrification during the dark period. The open circuit showed pH drop owing to the $H^+$ production by $NH_4^+$ oxidation, whereas pH of the short circuit remained constant at 7.5 (Fig. 6.2b and 3b).

### 6.3.2 MPMFC performance under continuous operation mode with effluent recycle

#### 6.3.2.1 Effect of ammonium concentration in the cathode compartment

The results obtained at the cathode under continuous feeding mode with different ammonium concentration (50, 100, 150 and 200 mg $NH_4^+$-N) are presented in Table 6.1. Production of oxygen, nitrite in the catholyte via microalgal photosynthesis and nitritation as well as the additional electron acceptor from the combined feed and recycled effluent significantly increased

**Table 6.1** Results of MPMFC performance during continuous feeding mode under different ammonium concentration at the cathode (12 hr light/12 hr dark period). Effluent from the cathode was recycled to separate $H^+$ ions and biomass. BDL: Below Detection Limit

| **Parameters** | **Ammonium (mg $NH_4^+$- N/L )** | | | |
|---|---|---|---|---|
| | **50** | **100** | **150** | **200** |
| Ammonium loading rate (mg/L.d) | 96±0.01 | 192±0.02 | 292±0.012 | 400±0.021 |
| Conductivity (m.S) | | | | |
| Without recycle (Initial) | 0.400±0.001 | 0.769±0.001 | 1.145±0.004 | 1.506±0.006 |
| Feed | 0.410±0.012 | 2.882±0.011 | 3.524±0.08 | 2.423±0.034 |
| Cathode effluent | 1.754±0.022 | 3.394±0.022 | 1.943±0.011 | 2.509±0.02 |
| DO (mg/L) | | | | |
| Feed | 5.64±0.05 | 1.17±0.02 | 0.78±0.01 | 0.08±0.01 |
| Cathode effluent | 1.20±0.01 | 0.89±0.01 | 0.1±0.002 | 0.1±0.001 |
| $NH_4^+$ (mg/L) | | | | |
| Feed | 48.12±2.4 | 96±4.3 | 146±3.30 | 200±4.5 |
| Cathode effluent | 0.1±0.012 | 0.12±0.012 | 13±1.1 | 29±1.6 |
| $NO_2^-$ (mg/L) | | | | |
| Feed | BDL | 0.02±0.015 | 0.31±0.012 | 0.57±0.01 |
| Cathode effluent | 0.02±0.014 | 0.34±0.01 | 0.43±0.01 | 0.51±0.01 |
| $NO_3^-$ (mg/L) | | | | |
| Feed | 0.123±0.014 | 0.1±0.011 | 0.04±0.014 | 0.01±0.01 |
| Cathode effluent | 0.1±0.011 | 0.04±0.014 | 0.01±0.015 | 0.01±0.013 |
| COD/N ratio | 3.1±0.02 | 3.12±0.02 | 3.2±0.01 | 3.3±0.01 |
| I (mA) | 43±0.01 | 32.8±0.02 | 20.5±0.01 | 56±0.01 |
| P (mW) | 18.49±0.001 | 10.75±0.001 | 4.20±0.001 | 31.36±0.001 |
| $E_{anode}$ (V Vs Ag/AgCl) | -0.473±0.00 | -0.340±0.00 | -0.453±0.00 | -0.486±0.00 |
| $E_{cathode}$ (V VsAg/AgCl) | -0.043±0.00 | +0.163±0.00 | -0.021±0.00 | +0.074±0.00 |
| Coulombic efficiency (%) | 53.75±0.6 | 41.00±1.2 | 25.64±1.7 | 70.00±2.3 |
| Carbon removal rate (mg/L. h) | 66 | 64.2 | 64.34 | 67.44 |
| Ammonium removal rate (mg/L. h) | 7.42 | 8.02 | 11.8 | 14.25 |
| C removal (%) | 100±0.00 | 100±0.00 | 100±0.00 | 100±0.00 |
| N removal (%) | 99.74±0.6 | 99.52±1.5 | 90.80±1.1 | 85.24±1.3 |

the electron acceptor levels in the cathode compartment, and the same was confirmed by a maximum current production of 56±0.1 mA.

Ammonium was supplied to the cathode at average flow rates of 96±0.01, 192±0.01, 292±0.012 and 400±0.021 mg/L·d, which corresponded to inlet concentrations of 50, 100, 150 and 200 mg $NH_4^+$ -N/L, respectively. Whereas the effluent concentration was less than 0.12 mg $L^{-1}$ for the inlet concentrations of 50, 100 and 150 mg $NH_4^+$ -N/L, the value was high (29±1.6 mg $L^{-1}$) for the inlet ammonium concentration of 200 mg $L^{-1}$. The nitrite produced at the cathode compartment was further reduced during the dark period, resulting in effluent nitrite concentration below 0.02±0.014 mg $NO_2^-$-N $L^{-1}$ for an inlet ammonium concentration of 100 mg $NH_4^+$-N $L^{-1}$. These results suggest that the ammonium removal rates are not same for all the inlet concentrations. A high ammonium concentration in the influent generated high current (56±0.01 mA), whereas only 43±0.01 and 32.8±0.02 mA were produced at an ammonium concentration of 50 and 100 mg/L. respectively. No significant ammonium oxidation was observed in the anodic compartment as revealed by $NO_2^-$ and $NO_3^-$ concentration.

Complete removal of total N was also examined at the cathode compartment. During the continuous feeding at an inlet ammonium concentration of 50 mg $NH_4^+$-N/L, nitrogen present in the effluent was very low (0.02±0.014-0.1±0.012 mg $NH_4^+$-N/L), thus showing maximum nitrogen removal efficiency of 99.74±0.6% and a removal rate of 7.42 mg/L h (Table 6.1). At a high ammonium concentration of 200 mg $NH_4^+$-N $L^{-1}$, electricity generation was also high (due to recirculation of 150 mg $NH_4^+$-N/L containing effluent), but the N removal efficiency was only 85.24±1.3% due to insufficient oxygen which was confirmed by a low DO concentration in the cathode compartment (0.1±0.001 mg $L^{-1}$). At 200 mg $NH_4^+$-N $L^{-1}$, the effluent ammonium concentration was very high (29±1.61 mg $L^{-1}$of $NH_4^+$-N), but nitrite was as low as 0.51± 0.017

mg $NO_2^-$ N $L^{-1}$. Besides, negligible concentrations of $NO_3^-$ were observed under all the conditions. Thus, for achieving high current production in MPMFC, high concentration of oxygen and recycle of $H^+$ ions from cathode effluent are important factors (Virdis et al., 2010; Nguyen et al., 2017). In the present work, $O_2$ was produced via microalgal photosynthesis using ammonium and nitrite as nitrogen source, and maximum current generation of 56±0.1 mA was observed for 200 mg $NH_4^+$-N/L ammonium concentration (Table 6.1).

It is recognized that high ammonium concentration enhances current production during simultaneous nitrification and denitrification in microalgae based MFC (Virdis et al., 2010; Nguyen et al., 2017). However, further increase of ammonium concentration leads to reduction in nitrogen removal efficiency in the cathode compartment. Pei et al. (2018) used ammonium rich wastewater for bioelectricity production in cathode compartment and reported a maximum algal biomass production of 0.94 g/L in PMFC. In addition to ammonium, nitrate and nitrite as efficient nitrogen source for the production of oxygen via algal photosynthesis (Pei et al., 2018; Yadav et al., 2020**).** Kakarla and Min. (2019) reported 95.5% ammonium removal by algae in the cathode part of the MFC with a maximum output voltage of 0.35 V in dark period.

#### 6.3.2.2 Effect of COD/N ratio in the cathode

The results for different COD/N ratios in the wastewater under continuous feeding mode are presented in Table 7.2. Glucose was supplied at an average loading rate of 100 mg COD $L^{-1}$ $d^{-1}$, whereas $NH_4^+$ loading rates were 100, 50, 33.3 and 25 mg $NH_4^+$-N $L^{-1}$ $d^{-1}$, which corresponded to COD/N ratios of 1, 2, 3 and 4, respectively. High power and current output values were obtained for a low COD/N ratio (Table 7.2). These results with the results of complete glucose consumption at all the conditions, whereas residual ammonium was observed at all the conditions.

Analysis of the recycle stream from cathode further revealed that the glucose was below detection limit under all conditions, thereby contributing to 100% COD removal. Similar, to the results from

**Table 6.2.** Results of MPMFC performance during continuous feeding regime under different COD/N ratios in the feed (12 hr light/12 hr dark period). (The effluent of the cathode was recycled to the cathode to provide the recycle of $H^+$ ions and biomass. BDL: Below Detection Limit).

| **Parameters** | **COD/N ratio** | | | |
|---|---|---|---|---|
| | **1** | **2** | **3** | **4** |
| Ammonium loading rate (mg/L.d) | 200±0.6 | 400±1.2 | 600±2.3 | 800±2.6 |
| Conductivity (mS) | | | | |
| Without recycle (Initial) | 0.796±0.5 | 0.414±0.3 | 0.259±0.2 | 0.183±0.1 |
| Feed | 0.723±0.06 | 2.676±0.012 | 1.121±0.012 | 1.955±0.01 |
| Cathode effluent | 2.403±0.14 | 0.956±0.012 | 1.892±0.034 | 0.734±0.01 |
| DO (mg/L) | | | | |
| Feed | 5.64±0.02 | 5.62±0.01 | 5.43±0.01 | 6.46±0.02 |
| Cathode effluent | 0.01±0.001 | 0.01±0.0012 | 0.01±0.001 | 0.012±0.001 |
| $NH_4^+$ (mg/L) | | | | |
| Feed | 97±2.5 | 49±4.6 | 32.3±4.4 | 23±1.2 |
| Cathode effluent | 28±3.2 | 5.6±2.1 | 2.1±1.1 | 1.12±0.76 |
| $NO_2^-$ (mg/L) | | | | |
| Feed | BDL | BDL | BDL | BDL |
| Cathode effluent | BDL | BDL | BDL | BDL |
| $NO_3^-$ (mg | | | | |
| Feed | BDL | BDL | BDL | BDL |
| Cathode effluent | BDL | BDL | BDL | BDL |
| I (mA) | 6.3± 0.2 | 30.1± 0.3 | 19.5± 0.12 | 25.9± 0.2 |
| P (mW) | 0.396± 0.001 | 9.06± 0.3 | 3.80± 0.002 | 6.70± 0.1 |
| $E_{anode}$ (V vs Ag/AgCl) | -0.419±0.00 | -0.420±0.00 | -0.411±0.00 | -0.424±0.00 |
| $E_{cathode}$ (V vs Ag/AgCl) | -0.356±0.00 | -118±0.00 | -195±0.00 | -165±0.00 |
| Coulombic efficiency (%) | 7.87 | 37.62 | 24.37 | 32.37 |
| Glucose removal rate (mg/L. d) | 63.4 | 65.55 | 63.24 | 67.67 |
| N removal rate (mg/L. d) | 5.75±0.02 | 3.61±0.012 | 2.51±0.01 | 1.81±0.02 |
| C removal (%) | 100 | 100 | 100 | 100 |
| N removal (%) | 71.13±1.1 | 88.57±1.87 | 93.78±2.2 | 93.91±2.4 |

the previous experiments, negligible amounts of $NO_2^-$ and $NO_3^-$ were observed in the effluent from anode compartment, whereas the $NH_4^+$ concentration was in the range from 30 ± 0.2 to 3.4 ±0.01 mg $L^{-1}$ of $NH_4^+$-N at different COD/N ratios.

In addition to the above, ammonium oxidation in the cathode compartment was very high even during the light period (Table 6.2), $NO_3^-$ and $NO_2^-$ did not accumulate due to its reduction at the cathode compartment. Thus, a maximum N removal efficiency was 93.91± 2.4% at COD/N ratio of 4, along with ammonium removal rate of 1.81± 0.02 mg $NH_4^+$-N $L^{-1}h^{-1}$. The residual ammonium and nitrite in the effluent are 73 ±0.2 mg $NH_4^+$-N $L^{-1}$ and 0.1 mg $NO_2^-$N $L^{-1}$, respectively. In general, ammonium rich wastewater such as anaerobic digestion liquor has a COD/N ratio of 1-3 for nitrogen removal by nitritation–denitrification process (Manser et al, 2016). Wang et al. (2015) revealed that high COD/N ratio resulted in balanced nitrification/denitrification rates, whereas low COD/N ratio limits the denitrification process in microalgae-AOB-DNB consortia (Wang et al., 2015).

In this study, high N removal efficiencies were obtained during the dark period with the addition of an external carbon source. Even at a COD/N ratio of 4, which is very close to the minimum COD needed for DNB, the N removal efficiency was 93.91±2.4% and the effluent contained 1.12±0.76 mg N/L. However, at the low COD/N ratio, N removal was 71.13±1.1% but the $NH_4^+$ oxidation was efficiency very low.

One of the main benefits of PMFC for BNR process is that it can utilize nitrite or nitrate as the nitrogen source under ammonium limiting conditions. Nitritation coupled with denitritation created an anoxic zone for microalgae-AOB-DNB consortium which in turn favored for denitritation by minimum use of carbon source for an efficient N removal along with bioelectricity

production. It also reduced the additional step of recycling algal biomass, which is common among biofuel cells containing suspended biomass of microalgae.

### 6.3.4 Effect of nitrogen source on MPMFC performance

The effect of ammonium, nitrite and nitrate on the performances of MPMFC during the light and dark periods was studied. Cathodic half-cell potential during the light period is shown in Fig. 6.5a, in which maximum peaks at -120 mV for $NH_4^+$, 74 mV for $NO_2^-$ and 70 mV for $NO_3^-$ were observed against Ag/AgCl electrode. The maximum current production of 16.25 mA with $NH_4^+$, 21.05 mA with $NO_2^-$ and 21.12 mA with $NO_3^-$(Fig. 6.5b) were achieved. These values are higher than the previously reported values using microalgae assisted cathode. For instance, He et al. (2009) obtained a maximum current production value of 0.054±0.002 mA, whereas Kakarla and Min (2014) and Wang et al. (2013) reported current values of 0.47 mA and 0.61 mA, respectively. Similarly, Gouveia et al. (2014) reported only 0.28 mA of current production using an algal photosynthetic MFC

Figure 6.5 b depicts that ammonium, nitrite and nitrate were consumed in the experiments. Power curves shown in Figure. 6.5c emphasize that a maximum power density of 9.6 W/ $m^3$ TWV is obtained at the current density of 62 A/ $m^3$ TWV with nitrate. The value is, however, 5.08% and 5.02% lower than nitrite or ammonium, respectively. But the power density obtained in this study is notably higher than the previously reported value of 9 W/ $m^3$ using PMFC (Cui et al., 2014). Nitrite or nitrate as the nitrogen source enhanced the activity of microalgae in terms of $O_2$ production by photosynthesis.

Figure. 6.5d shows the profiles of cyclic voltammetry with the different electron acceptors during the light period.

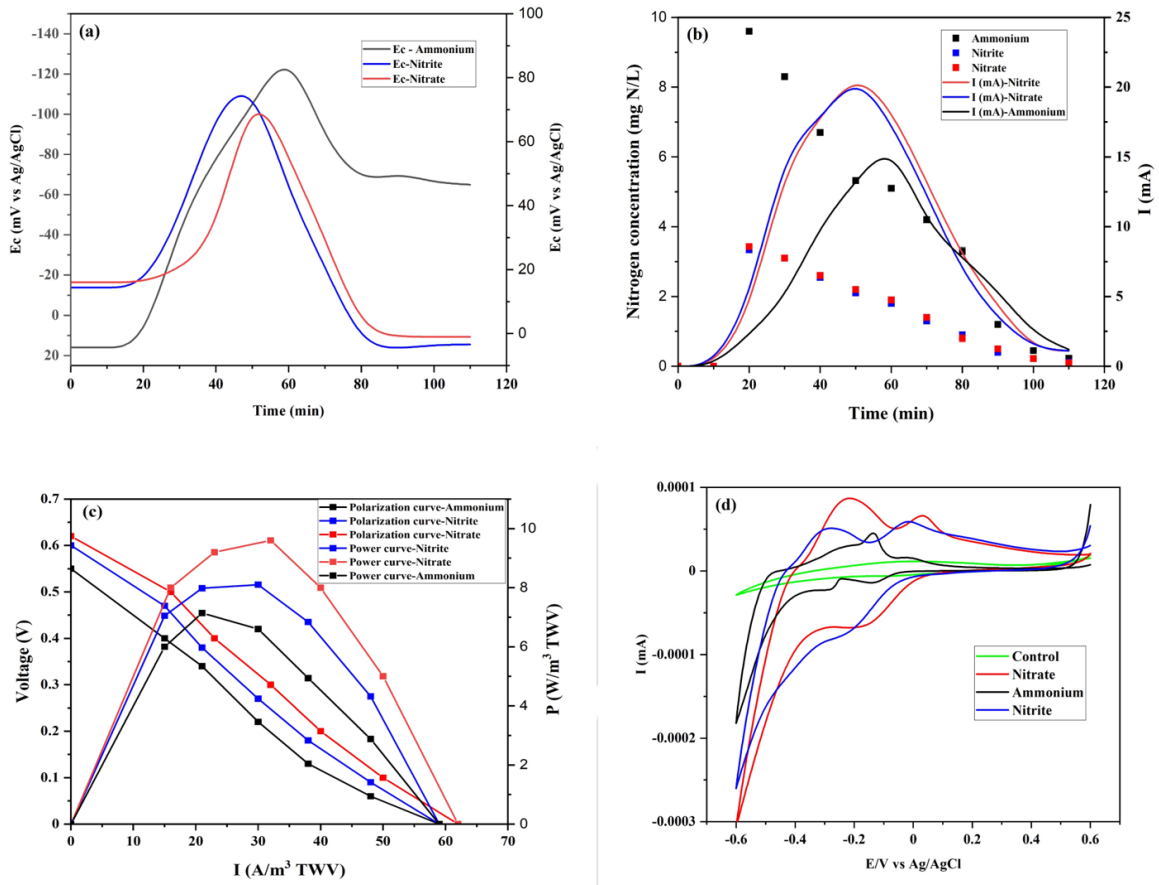


**Fig. 6.5** Batch results of MPMFC at the cathode compartment during the light period supplied with 10 mg $NH_4^+$-N/L or 4 mg $NO_2^-$-N/L or 4 mg $NO_3^-$-N; (a) cathodic half-cell potentials, (b) current production and consumption of ammonium, nitrite and (C). polarization and power curves and (d) cyclic voltammetry

Reduction in peaks for ammonium, nitrite and nitrate are observed at -0.140 mV, -0.241 mV and -0.164 mV, respectively. Kakarla and Min, (2020) used *Scenedesmus obliquus* for oxygen supply in PMFC and observed reduction in peak at −119 mV with a very low reduction in current of −9.3 mA. Reduction in peaks for the different nitrogen source indicate their contribution as reducing electron acceptor in the reduction reaction. With nitrate or nitrite, the electrochemical activity was very high, but with ammonium significant activity was observed during the light period.

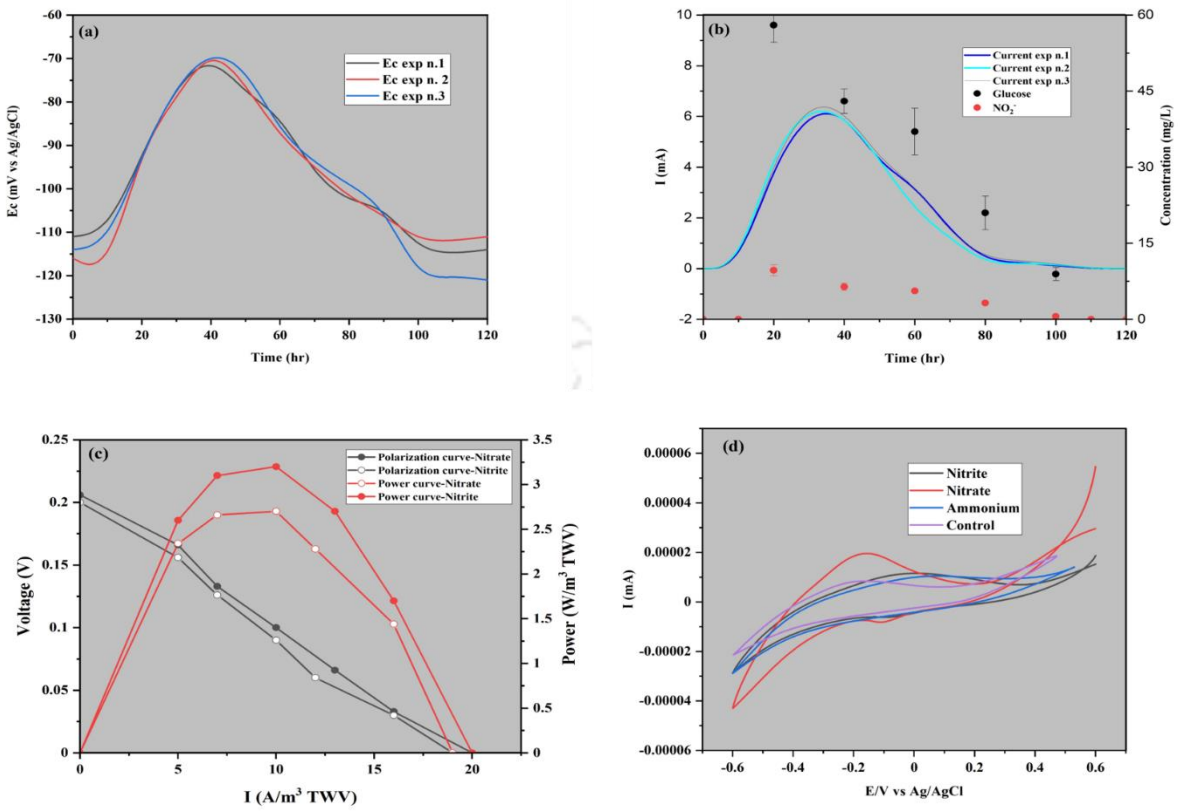


**Fig. 6.6** Results of batch experiments at the cathode compartment of MPAMFC supplied with 64 mg glucose and 10 mg $NaNO_2$ during the dark period. (a) Cathodic half-cell potentials. (b) Profiles of current, glucose and nitrite. (c) Polarization, power curves and cyclic voltammetry and (d) Current production.

The electrochemical activity observed is attributed to the algal biofilm on the surface of the electrode surface, which is however absent in suspended microalgae systems (Kim et al., 2002

Cathodic potential during the dark period peaked at -88 mV vs. Ag/AgCl for $NO_2^-$ as shown in Fig. 6.6a. A maximum current production of 6.3 mA for $NO_2$ was observed (Fig. 6.6b), which is higher than 4.94 ± 0.28 mA reported for simultaneous nitrification and denitrification in MFCs using nitrate as the electron acceptor (Virdis et al., 2010). Figure. 6.6b also reveals that nitrite and glucose were consumed in all the three experiments. From the power curves shown in Fig. 6c, it

evident that a maximum power density of 3.2 W/ $m^3$ TWV (total working volume) is achieved at the current density of 62 A/ $m^3$ TWV with nitrite as the nitrogen source. However, this value is 0.15% lower than that with nitrate. The maximum power density value is also significantly higher than the reported value of 2.8 W/ $m^3$ using a MFC for simultaneous nitrification and denitrification (Virdis et al., 2010). Cyclic voltammetry profile obtained with the different nitrogen compounds (Fig. 6.6d) as the electron acceptor during the dark period reveals no significant reduction in the peak with nitrite or nitrate. These results strongly suggest absence of DNB activity in the cathode of MPMFC.

### 6.3.5 Nitrogen and oxygen mass balance in cathode compartment

The results of nitrogen mass balance and oxygen mass balance in the cathode compartment at the end of the 24 h experiment are presented in Table 6.3 and Table 6.4, respectively. Complete $NH_4^+$removal was achieved in both open circuit and short circuit and the removal efficiency remained constant due to sufficient $O_2$ supply from microalgal photosynthesis. Regression analysis of the data on $NH_4^+$ vs oxygen supplied by microalgae was performed to calculate the oxygen supplied by microalgal photosynthesis during the open circuit and short circuit (Table 6.4), which revealed that oxygen produced by photosynthesis was consumed for nitritation and oxygen

**Table 6.3** Results of nitrogen balance in the cathode compartment

| Operating condition | Initial ($NH_4^+$-N mg/L) | $NO_2^-$-N formed (mg/L) | $NH_3$-N volatilization (mg/L) | $NH_4^+$-N uptake by algae (mg/L) | $NH_4^+$-N uptake by AOB (mg/L) | Denitritation (mg/L) | % $NH_4^+$-N removed by | | | |
|---|---|---|---|---|---|---|---|---|---|---|
| | | | | | | | Nitritation (%) | Uptake by AOB (%) | Uptake by algae (%) | $NH_3$ volatilization (%) |
| Open circuit | 96 | 74.12 | 0.8 | 20.28 | 0.8 | 74.1 | 77.20 | 0.83 | 21.12 | 0.83 |
| Short circuit | 96 | 74.22 | 0.8 | 20.18 | 0.8 | 74.08 | 77.31 | 0.83 | 21.02 | 0.83 |

**Table 6.4** Estimated oxygen supply rate by microalgae and oxygen consumption rate by nitritation under different operational condition at the $NH_4^+$ loading rate of 100 mg-N $L^{-1}$ $d^{-1}$ in the MPMFC.

| Operating condition | $NH_4^+$-N initial (mg/L) | Relative contribution to $NH_4^+$ removal (%)[a] | | $NH_4^+$-N uptake rate by microalgae (mg-N $L^{-1}$ $d^{-1}$ )[a] | $O_2$ supply rate microalgae (mg-$O_2$ $L^{-1}$ $d^{-1}$)[b] | $NH_4^+$ oxidation rate by nitritation (mg-N $L^{-1}$ $d^{-1}$)[a] | $NO_2^-$ reduction rate by denitritation (mg-N $L^{-1}$ $d^{-1}$)[a] | $O_2$ consumption rate by nitritation (mg-$O_2$ $L^{-1}$ $d^{-1}$)[c] |
|---|---|---|---|---|---|---|---|---|
| | | Microalgae uptake | Nitritation | | | | | |
| Open circuit | 96 | 21.12 | 77.20 | 20.28 | 337 | 74.12 | 74.1 | 254.23 |
| Short circuit | 96 | 21.02 | 77.31 | 20.18 | 337 | 74.22 | 74.08 | 254.57 |

a: Based on the assumption that $NH_4^+$ in the feed is completely removed by microalgae and/or nitritation; b: values were calculated from the slope of linear regression between daily $NH_4^+$ (x) consumption and $O_2$ produced by microalgae (y) ($y = 3.7062x-18.289$; $R^2=0.98$); c: values were calculated according to stoichiometric equations of $O_2$ requirements for nitritation (Akizuki et al., 2020)

reduction reaction. The results of nitrogen mass balance revealed significant microalgal uptake of $NH_4^+$ (19.9 mg N $L^{-1}$, corresponding to 20.72%) in open circuit. In PSBR with microalgae and AOB, high $NH_4^+$ concentration (132.7 mg $NH_4^+$-N/L) enhanced $O_2$ production by microalgae (193 mg $O_2$/ L. d) for nitritation as well as for denitritation (Wang et al., 2015). Therefore, optimum $NH_4^+$ concentration is key to its successful removal from wastewater owing to the availability of sufficient $O_2$ supply for AOB activity and cathodic reaction.

It has been suggested that optimum $NH_4^+$ concentration for nitritation/nitrification can vary for different microalgae-AOB consortium or microalgae-partial nitrifying granules (Wang et al., 2015; Akizuki et al., 2020). Kakarla and Min, (2019) observed 90 mg $NH_4^+$-N/L as the optimal ammonium concentration for microalgae to produce electricity in a PMFC. Another study reported that microalgae yielded a high power output (4.13 kWh/$m^3$) with 99% $NH_4^+$ removal with wastewater containing 1550 ± 20 mg $NH_4^+$-N/L (Pei et al., 2018).

It has been reported that PMFC favor $NH_4^+$ uptake by microalgae rather than $NH_4^+$ oxidation by AOB due to competition between AOB and cathodic reaction for oxygen. For example, Pei et al. (2018) reported that a microalgae-bacterial consortium removed $NH_4^+$ by oxidation (84.4%-89.9%) due to AOB than by $NH_4^+$ uptake (9.1%-14.6%) due to microalgae. Microalgae-AOB consortium contribute to both ammonium volatilization and nitrification (approximately 79% of the total nitrogen removal) (Cui et al.,2014). As microalgae require $NH_4^+$ for $O_2$ production and AOB are tolerant to high $NH_4^+$ concentration, the growth of microalgae and AOB in this work probably enhanced its removal even at a high $NH_4^+$ concentration (>50 mg $NH_4^+$-N/L), leading to efficient removal of $NH_4^+$. However, $NH_4^+$ concentration in wastewater such as anaerobic digestate often exceeds 300 mg $NH_4^+$-N/L, other approaches, such as optimization of pH (Akizuki et al.,

2020) or light intensity (Akizuki et al., 2019), may be considered prior to large scale MFC application for treating ammonium rich wastewater.

### 6.3.6 Energy production and consumption in PMFC

From Table 6.5, values of energy produced (output) and energy consumed (input) in the MPMFC were compared with the literature. The total energy produced during the short-cut nitrogen removal in this study was 0.66 kWh/$m^3$ (microalgal photosynthesis), which is obtained by treating 500 mL of ammonium rich wastewater (100 mg $NH_4^+$-N/L). This result is comparable with that of a previous PMFC work on nitrogen removal assisted by microalgal photosynthesis (0.57 kWh/$m^3$, (Pei et al., 2018), Table 6.6), higher than other MFC system with external aeration (0.0079 kW h/$m^3$, (Li et al., 2016), Table 6.6). The high energy production observed in this MPMFC is attributed to its low volume- 500 ml and different geometry- rectangular, large surface area and spacing of electrodes (Pei et al., 2018; Yang et al., 2019). In PMFCs treating ammonium rich wastewater, ($NH_4^+$-N: 1550 mg/L) or domestic wastewater (e.g. kitchen waste and swine waste), energy production is reported was in the range of 0.088–1.8 kW h/$m^3$ (Ma et al., 2017; Pei et al., 2018; Li et al., 2019; Yang et al., 2019).

The energy utilized by BNR in the cathode compartment of the PMFC was evaluated based on the $O_2$ transfer efficiency and oxygen balance (1.24 kg $O_2$/kWh) (Virdis et al., 2010). Energy cost related to pumping of ammonium rich wastewater was calculated based on the literature (Virdis et al., 2010; Li et al., 2016). The energy saved (0.406–kW h/$m^3$) in this study is much higher than that reported in the literature on previous shortcut nitrification using MFC's (0.0009–0.0013 kW h/$m^3$, Table 6.6), (Li et al., 2016), which is due to algal photosynthesis and shortcut nitritation with less oxygen (Li et al., 2016; Pei et al., 2018; Nguyen and Min., 2020). These results clearly

demonstrate that the present PMFC used in this study is highly efficient for both electricity production and nitrogen removal.

**Table 6.5** Comparison of energy input, energy output and net energy in the MPMFC with SNR with the values reported in the literature on different PMFCs

| **Energy ($kWh/m^3$)** | | **This study** | **PMFC [Li et al., 2019]** | | **MFCs with shortcut nitrogen removal [Li et al., 2016]** | **MFC with ammonium removal [Zhang et al., 2012]** |
|---|---|---|---|---|---|---|
| | | | **With aeration** | **Without aeration** | | |
| Input | Aeration/microalgal photosynthesis | 0 | -0.060 | - | -0.0026 | -0.0252 |
| Output | Energy production | 0.66 | 0.169 | 0.077 | 0.079 | 0.032 |
| Net | Total | 0.66 | 0.109 | 0.077 | 0.0764 | 0.0068 |

**Table 6.6** Comparison of energy production and consumption values in the MPMFC with the literature on different PMFC and MFC systems

| **Energy ($kWh/m^3$)** | **This study** | **PMFC [Li et al., 2019 ]** | **PMFC with ammonium removal [Yang et al., 2019; Pei et al., 2018]** | **MFC with ammonium removal [Li et al., 2016]** |
|---|---|---|---|---|
| Production | 0.66 | 0.088-0.109 | 0.57-1.8 | 0.0079 |
| Consumption | - | - | - | 0.0018 |
| Balance | 0.66 | 0.088-0.109 | 0.57-1.8 | 0.0061 |
| Saving by BNR | 0.406 | - | - | 0.0009-0.0013 |

### 6.4 Significant findings

Performance toward MPMFC with effluent recycle at the cathode compartment showed high treating synthetic wastewater containing different ammonium concentrations and COD/N ratio. Algal photosynthesis in the cathode compartment enhanced the shortcut nitrogen removal of ammonium. This study successfully demonstrated shortcut nitrogen removal in PMFC technology by integrating nitritation into the cathodic compartment, which can overcome the issues related to aeration cost and NOB activity. Moreover, microalgal-AOB-DMB consortium is capable of shortcut nitrogen removal and COD removal in the MFC setup by minimal consumption of organic carbon source for denitrification. In addition, the $H^+$ produced at the cathode compartment during nitritation avoided pH increase through cathodic reduction which resulted in significantly high bioelectricity generation in the system.

# Chapter 7

# Summary and conclusions

Treatment of ammonium rich domestic and industrial wastewater using microalgae and ammonia oxidizing bacteria (AOB) is attractive as it serves as an excellent substrate/nitrogen source for such microorganism. The conventional activated sludge process for ammonium removal relies on mechanical aeration. In addition to very high operating cost due to mechanical aeration, ASP requires addition of external carbon source for nitrification and denitrification. On the other hand, microalgae-bacteria consortia are not only able to grow autotrophically on ammonium but also offer advantages, such as high N affinity, anoxic zone for denitrification, algal photosynthesis, shortcut nitrogen removal, biomass with good settling characteristics and energy production. However, application of ammonium removal by microalgae-bacterial consortia to produce useful commodities e.g. biofuels, pigments, biopolymer, is less known. Hence, this work was aimed at treatment and value addition to ammonium rich wastewater by using microalgae-bacterial consortia.

The capability of microalga-bacterial biomass from three different wastewater treatment facilities to use ammonium as the sole substrate and nitrogen source was examined. The different microalgae-bacterial biomass was screened for their ability to remove ammonium at a high concentration of 200 mg/L. The results showed that among the three different sources the microalgae-bacterial consortium from IITG wastewater treatment plant treating sewage was highly efficient in oxidizing ammonium to nitrogen gas along with a small amount of carbon dioxide. Addition of organic carbon source in a photosequencing batch reactor (PSBR) during the dark period enhanced the activity of denitrifying bacteria in the microalgae-bacterial consortium, which resulted in nitrogen gas as the main end products. The effect of initial ammonium concentration, pH, DO concentration, and light intensity on ammonium removal using the microalgae-bacterial

consortium was studied to achieve maximum ammonium removal. Based on 3S rRNA sequence analysis of the microalgae, it was identified as *C. sorokiniana* which is well known for ammonium removal.

Detailed bio-kinetics of ammonium removal by the microalgae-bacterial consortium revealed an active role played by microalgae, AOB, NOB and DNB for achieving an efficient removal of ammonium. However, with an increase in initial ammonium concentration the ammonium removal by AOB decreased, whereas, its removal due to microalgae was high. Both the ammonium and nitrogen gas production were best described by using the microalgae-AOB-MUD based bio-kinetic models. Also, the profiles of ammonium, nitrite, nitrate and DO in this study were accurately predicted by the microalgae-AOB-MUD bio-kinetic models. However, NOB growth was inhibited at a high ammonium concentration. Estimated values of the bio-kinetic model parameters further supported the shortcut nitrogen removal without nitrate formation by microalgae, AOB and DNB in the consortium. In addition, this bio-kinetic study revealed that nitrate produced by NOB could be utilized by microalgae as the sole nitrogen source, thus minimizing nitrate accumulation in the photobioreactor.

Light intensity significantly affected the ammonium removal by microalgae-AOB-NOB consortium. The empirical model as mentioned earlier showed that light intensity below 40 μmol photons $m^{-2}$ $s^{-1}$ was ineffective towards nitrification due to oxygen limitation condition. Light intensity in the range, 40-160 μmol photons $m^{-2}$ $s^{-1}$ was found suitable for complete nitrification, whereas above 100 μmol photons $m^{-2}$ $s^{-1}$ light intensity caused inhibition of microalgal-AOB-NOB consortium, thus causing a low nitrification efficiency.

The effect of different nitrogen source competition using microalgae-bacterial consortia on ammonium removal was further studied and the values $NH_4^+$ removal rates were similar at 50 and 100 mg $NH_4^+$-N/L respectively, indicating enhancement in ammonium removal by both nitrification and microalgae uptake. By comparing the results from this work with a previous study, $O_2$ supplied by microalgae through $NH_4^+$ uptake was found to strongly influence the overall $NH_4^+$ removal by consortium. An ASM-AB model was developed, considering that microalgal growth on $NH_4^+$, $NO_2^-$and $NO_3^-$, which revealed that (a) $NH_4^+$ concentrations at 150-200 mg $NH_4^+$-N/L led to insufficient $O_2$ production, (b) 50 mg $NH_4^+$-N/L is effective for microalgal photosynthesis and nitrification with excess of production and (c) 100 mg $NH_4^+$-N/L is suitable for complete nitrification $O_2$ limitation in the system.

Finally, ammonium removal by algae-AOB-DNB consortium was integrated in a MFC system, which was referred as an integrated shortcut nitrogen removal-microbial fuel cell. In this study, A MPMFC with effluent recycle at the cathode compartment was fed with synthetic wastewater containing at different ammonium concentrations and COD/N ratios. Algal photosynthesis in the cathode compartment enhanced the shortcut removal of ammonium. This study provided direct evidence of shortcut nitrogen removal in MPMFC by integrating nitritation into the cathodic compartment, which has the capability to overcome issues related to high aeration cost and NOB activity (due to high requirement of dissolved oxygen for nitritation and cathodic reaction). Moreover, as the microalgae-AOB consortium capable of shortcut nitrogen removal and carbon are separated in the MFC setup, the organic carbon source requirement for denitrification is minimized as compared with that required for other systems containing such microalgae-bacterial consortium. In addition, the $H^+$ ions produced at the cathode compartment during nitritation resulted in a low pH of the system as well as a high current production in the MPMFC.

Large scale application of such microalgae-bacterial consortia for ammonium removal has not been demonstrated yet, and therefore, it could be implemented by industries such as food processing, tannery, dairy and fertilizer industries for treating ammonium rich wastewater. Moreover, the aeration costs involved could be greatly reduced by microalgal photosynthesis using microalgae-bacterial consortia, thus minimizing the operation costs in the wastewater treatment process involved. Fig. 7.1 shows a proposed scheme of process outline for biological nitrogen removal by microalgae-bacterial consortia in such wastewater treatment process.

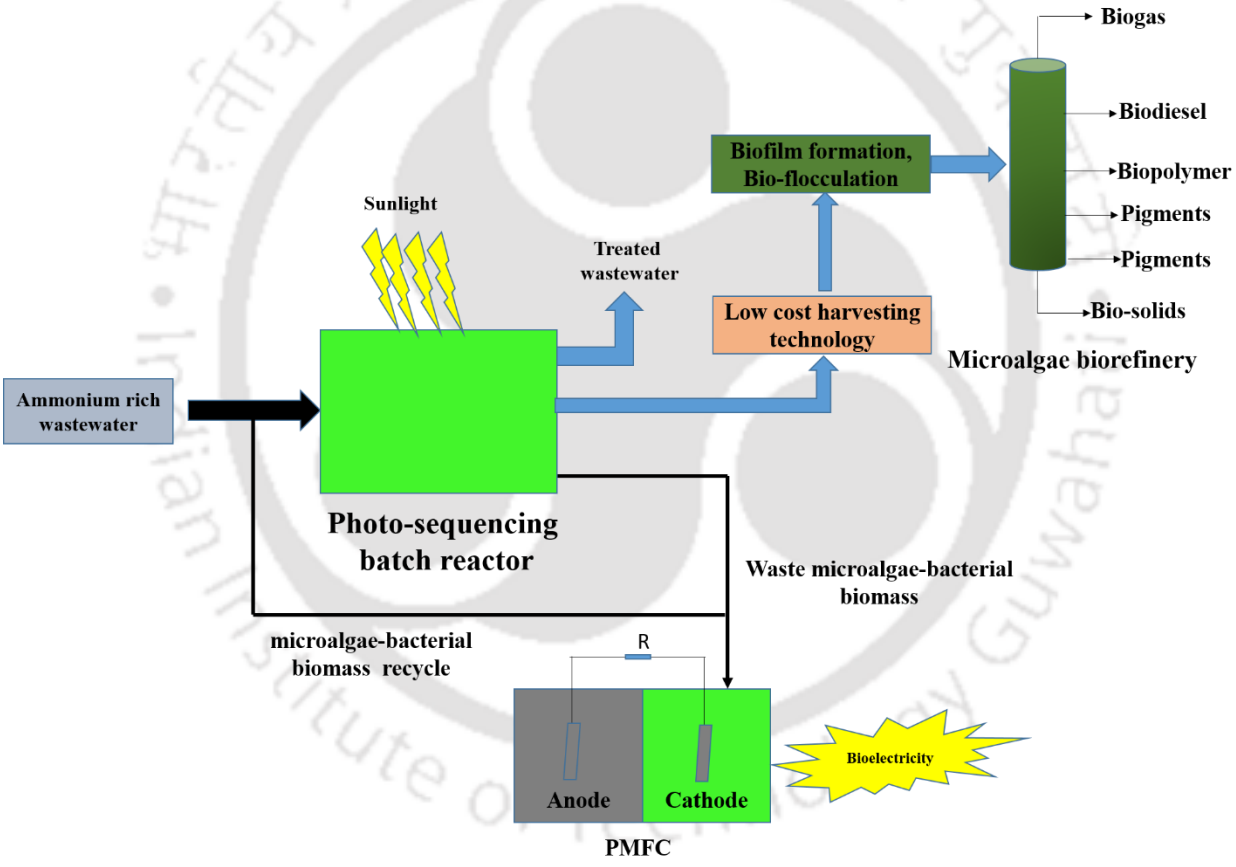


**Fig. 7.1** Schematic showing a proposed process outline for biological nitrogen removal using microalgae-bacterial consortia.

In addition to the above, following are some more suggestions for future work based on this thesis:

1. Long term process stability of microalgae-bacterial consortia for efficient ammonium removal

2. Scale up of the PSBR system to treat ammonium rich wastewater using microalgae-bacterial consortia
3. Effect of sun light on ammonium removal by microalgae-bacterial consortia for real time application on outdoor open environment
4. Mass transfer effect on kinetics of microalgal-bacterial floc for ammonium removal in a PSBR

# Bibliography

- Akizuki, S., Cuevas-Rodríguez, G. and Toda, T., 2019. Microalgal-nitrifying bacterial consortium for energy-saving ammonia removal from anaerobic digestate of slaughterhouse wastewater. J. Water Process Eng. 31, 100753.

- Akizuki, S., Kishi, M., Cuevas-Rodríguez, G. and Toda, T., 2020. Effects of different light conditions on ammonium removal in a consortium of microalgae and partial nitrifying granules. Water Res. 171, 115445.
- Akizuki, S., Kishi, M., Cuevas-Rodríguez, G. and Toda, T., 2020. Effects of different light conditions on ammonium removal in a consortium of microalgae and partial nitrifying granules. Water Res.171, 115445.
- American Public Health Association, American Water Works Association and Water Environment Federation, Standard methods for the examination of water and wastewater. American Public Health Association (2017).
- Andreotti, V., Solimeno, A., Rossi, S., Ficara, E., Marazzi, F., Mezzanotte, V., & García, J. 2020. Bioremediation of aquaculture wastewater with the microalgae Tetraselmis suecica: Semi-continuous experiments, simulation and photo-respirometric tests. Sci. Total Environ. 738, 139859.
- Ananyev, G., Gates, C., Kaplan, A. and Dismukes, G.C., 2017. Photosystem II-cyclic electron flow powers exceptional photoprotection and record growth in the microalga Chlorella ohadii. Biochimica et Biophysica Acta (BBA)-Bioenergetics, 1858, 873-883.
- Azov, Y. and Goldman, J.C., 1982. Free ammonia inhibition of algal photosynthesis in intensive cultures. Appl. Environ. Microbiol. 43, 735-739.

- Cao, X., Huang, X., Liang, P., Boon, N., Fan, M., Zhang, L. and Zhang, X., A completely anoxic microbial fuel cell using a photo-biocathode for cathodic carbon dioxide reduction, Energy Environ Sci. 2 (2009) 498-501.

- Chen, X., Goh, Q.Y., Tan, W., Hossain, I., Chen, W.N. and Lau, R., 2011. Lumostatic strategy for microalgae cultivation utilizing image analysis and chlorophyll a content as design parameters. Bioresour. Technol. 102, 6005-6012.
- Clauwaert, P., Rabaey, K., Aelterman, P., De Schamphelaire, L., Pham, T.H., Boeckx, P., Boon, N. and Verstraete, W., Biological denitrification in microbial fuel cells, Environ. Sci. Technol. 41 (2007) 3354-3360.
- Cui, Y., Rashid, N., Hu, N., Rehman, M.S.U. and Han, J.I., 2014. Electricity generation and microalgae cultivation in microbial fuel cell using microalgae-enriched anode and bio-cathode. Energy convers. and manage. 79, 674-680.
- del Campo, A.G., Cañizares, P., Rodrigo, M.A., Fernández, F.J., and Lobato, J., Microbial fuel cell with an algae-assisted cathode: a preliminary assessment, J. Power Sources, 242 (2013) 638-645.
- Ding, Y., Song, X., Wang, W. and Wang, Y., 2018. Effects of Influent Algae Concentrations and Seasonal Variations on Pollutant Removal Performance in High-Rate Algae Ponds. Polish Journal of Environmental Studies, 27.
- El Ouarghi, H., Praet, E., Jupsin, H. and Vasel, J.L., 2003. Comparison of oxygen and carbon dioxide balances in HRAP (high-rate algal ponds). Water Sci. Technol. 48, 277-281.
- Gajda, I., Greenman, J., Melhuish, C. and Ieropoulos, I., Self-sustainable electricity production from algae grown in a microbial fuel cell system, Biomass Bioenergy. 82 (2015) 87-93.
- Gong, W., Xie, B., Deng, S., Fan, Y., Tang, X. and Liang, H., 2019. Enhancement of anaerobic digestion effluent treatment by microalgae immobilization: characterized by

fluorescence excitation-emission matrix coupled with parallel factor analysis in the photobioreactor. Sci. Total Environ. 678, 105-113.

- González, C., Marciniak, J., Villaverde, S., García-Encina, P.A. and Muñoz, R., 2008. Microalgae-based processes for the biodegradation of pretreated piggery wastewaters. Appl. Microbiol. Biotechnol. 80, 891-898.
- González-Camejo, J., Montero, P., Aparicio, S., Ruano, M.V., Borrás, L., Seco, A. and Barat, R., 2020. Nitrite inhibition of microalgae induced by the competition between microalgae and nitrifying bacteria. Water Res. 172, 115499.
- González-Fernández, C., Molinuevo-Salces, B. and García-González, M.C., 2011. Nitrogen transformations under different conditions in open ponds by means of microalgae–bacteria consortium treating pig slurry. Bioresour. Technol. 102, 960-966.
- Gouveia, L., Neves, C., Sebastião, D., Nobre, B.P. and Matos, C.T., 2014. Effect of light on the production of bioelectricity and added-value microalgae biomass in a photosynthetic alga microbial fuel cell. Bioresour. Technol.154, 171-177.
- He, Q., Yang, H., Wu, L. and Hu, C., 2015. Effect of light intensity on physiological changes, carbon allocation and neutral lipid accumulation in oleaginous microalgae. Bioresour. Technol. 191, 219-228.
- He, Z., Kan, J., Mansfeld, F., Angenent, L.T. and Nealson, K.H., 2009. Self-sustained phototrophic microbial fuel cells based on the synergistic cooperation between photosynthetic microorganisms and heterotrophic bacteria. Environ. Sci. Technol. 43, 1648-1654.

- Huang, C., Xiong, L., Guo, H.J., Li, H.L., Wang, C., Chen, X.F., Zhao, C. and Chen, X.D., 2019. Anaerobic digestion of elephant grass hydrolysate: Biogas production, substrate metabolism and outlet effluent treatment. Bioresour. Technol. 283, 191-197.

- Kakarla, R. and Min, B., 2014. Photoautotrophic microalgae Scenedesmus obliquus attached on a cathode as oxygen producers for microbial fuel cell (MFC) operation. Int. J. Hydrogen Energy, 39, 10275-10283.

- Kakarla, R. and Min, B., Sustainable electricity generation and ammonium removal by microbial fuel cell with a microalgae assisted cathode at various environmental conditions, Bioresour. Technol. 284 (2019) 161-167.

- Karya, N.G.A.I., Van der Steen, N.P. and Lens, P.N.L., 2013. Photo-oxygenation to support nitrification in an algal–bacterial consortium treating artificial wastewater. Bioresour. Technol. 134, 244-250.

- Karya, N.G.A.I., Van der Steen, N.P. and Lens, P.N.L., Photo-oxygenation to support nitrification in an algal–bacterial consortium treating artificial wastewater, Bioresour. Technol. 134 (2013) 244-250.

- Kim, H.,J., Park, H.S., Hyun, M.S., Chang, I.S., Kim, M. and Kim, B.H., 2002. A mediator-less microbial fuel cell using a metal reducing bacterium, Shewanella putrefaciens. Enzyme Microbial Technol. 30 (2002) 145-152.

- Kondaveeti, S., Choi, KS., Kakarla, R. and Min, B., Microalgae Scenedesmus obliquus as renewable biomass feedstock for electricity generation in microbial fuel cells (MFCs), Front Environ Sci Eng. 8 (2014) 784-791.

- Kondaveeti, S., Lee, S.H., Park, H.D. and Min, B., Bacterial communities in a bioelectrochemical denitrification system: the effects of supplemental electron acceptor, Water Res. 51 (2014) 25-36.

- Lan, J.C.W., Raman, K., Huang, C.M. and Chang, C.M., The impact of monochromatic blue and red LED light upon performance of photo microbial fuel cells (PAMFCs) using Chlamydomonas reinhardtii transformation F5 as biocatalyst, Biochem. Eng. J. 78 (2013) 39-43.

- Lang, Z., Zhou, M., Zhang, Q., Yin, X., & Li, Y. 2020. Comprehensive treatment of marine aquaculture wastewater by a cost-effective flow-through electro-oxidation process. Sci. Total Environ. 722, 137812.

- Li, M., Zhou, M., Luo, J., Tan, C., Tian, X., Su, P. and Gu, T., 2019. Carbon dioxide sequestration accompanied by bioenergy generation using a bubbling-type photosynthetic algae microbial fuel cell. Bioresour. Technol. 280, 95-103.

- Li, Y., Williams, I., Xu, Z., Li, B. and Li, B., 2016. Energy-positive nitrogen removal using the integrated short-cut nitrification and autotrophic denitrification microbial fuel cells (MFCs). Appl. Energy, 163, 352-360.

- Logan, B.E., Hamelers, B., Rozendal, R., Schröder, U., Keller, J., Freguia, S., Aelterman, P., Verstraete, W. and Rabaey, K., 2006. Microbial fuel cells: methodology and technology. Environ. Sci. Technol. 40, 5181-5192.

- Ma, J., Wang, Z., Zhang, J., Waite, TD. and Wu, Z., Cost-effective Chlorella biomass production from dilute wastewater using a novel photosynthetic microbial fuel cell (PAMFC). Water Res. 108 (2017) 356-364.

- Manser, N.D., Wang, M., Ergas, S.J., Mihelcic, J.R., Mulder, A., Van De Vossenberg, J., Van Lier, J.B. and Van Der Steen, P., 2016. Biological nitrogen removal in a photosequencing batch reactor with an algal-nitrifying bacterial consortium and Anammox granules. Environ. Sci. Technol. Lett. 3, 175-179.
- Manser, N.D., Wang, M., Ergas, S.J., Mihelcic, J.R., Mulder, A., Van De Vossenberg, J., Van Lier, J.B. and Van Der Steen, P., Biological nitrogen removal in a photosequencing batch reactor with an algal-nitrifying bacterial consortium and Anammox granules, Environ. Sci. Technol. Lett. 3 (2016) 175-179.
- Mendoza, J.L., Granados, M.R., De Godos, I., Acién, F.G., Molina, E., Heaven, S. and Banks, C.J., 2013. Oxygen transfer and evolution in microalgal culture in open raceways. Bioresour. Technol. 137, 188-195.
- Nguyen, H.T. and Min, B., 2020. Leachate treatment and electricity generation using an algae-cathode microbial fuel cell with continuous flow through the chambers in series. Sci. Total Environ. 723, 138054.
- Nguyen, H.T., Kakarla, R. and Min, B., Algae cathode microbial fuel cells for electricity generation and nutrient removal from landfill leachate wastewater. Int. J. Hydrogen Energy, 42 (2017) 29433-29442.
- Pei, H., Yang, Z., Nie, C., Hou, Q., Zhang, L., Wang, Y. and Zhang, S., Using a tubular photosynthetic microbial fuel cell to treat anaerobically digested effluent from kitchen waste: Mechanisms of organics and ammonium removal. Bioresour. Technol. 256 (2018) 11-16.
- Perrine, Z., Negi, S. and Sayre, R.T., 2012. Optimization of photosynthetic light energy utilization by microalgae. Algal Research, 1, 134-142.

- Pizzera, A., Scaglione, D., Bellucci, M., Marazzi, F., Mezzanotte, V., Parati, K. and Ficara, E., 2019. Digestate treatment with algae-bacteria consortia: A field pilot-scale experimentation in a sub-optimal climate area. Bioresour. Technol. 274, 232-243.

- Powell, EE., Mapiour, ML., Evitts, RW. And Hill, GA., Growth kinetics of Chlorella vulgaris and its use as a cathodic half cell, Bioresour Technol. 100 (2009) 269-274.

- Qian, W., Peng, Y., Li, X., Zhang, Q. and Ma, B., 2017. The inhibitory effects of free ammonia on ammonia oxidizing bacteria and nitrite oxidizing bacteria under anaerobic condition. Bioresour. Technol. 243, 1247-1250

- Rada-Ariza, A.M., Lopez-Vazquez, C.M., Van der Steen, N.P. and Lens, P.N.L., 2017. Nitrification by microalgal-bacterial consortia for ammonium removal in flat panel sequencing batch photo-bioreactors. Bioresour. Technol. 245, 81-89.

- Rashid, N., Cui, YF., Rehman, MSU. and Han, JI., Enhanced electricity generation by using algae biomass and activated sludge in microbial fuel cell, Sci Total Environ. 456 (2013) 91-94.

- Sarvajith, M., Reddy, G.K.K. and Nancharaiah, Y.V., 2018. Textile dye biodecolourization and ammonium removal over nitrite in aerobic granular sludge sequencing batch reactors. J. Hazard. Mater. 342, pp.536-543.

- Sinharoy, A., Manikandan, NA, and Pakshirajan, K., A novel biological sulfate reduction method using hydrogenogenic carboxydotrophic mesophilic bacteria, Bioresour. Technol. 192, (2015) 494-500.

- Strik, D.P., Terlouw, H., Hamelers, H.V. and Buisman, C.J., 2008. Renewable sustainable biocatalyzed electricity production in a photosynthetic algal microbial fuel cell (PAMFC). Appl. Microbiol. Biotechnol.81, 659-668

- Strik, DP., Terlouw, H., Hamelers, HV. and Buisman, CJ., Renewable sustainable biocatalyzed electricity production in a photosynthetic algal microbial fuel cell (PAMFC), Appl Microbiol Biotechnol. 81 (2008) 659-668.

- Thomas, P.K., Dunn, G.P., Passero, M. and Feris, K.P., 2017. Free ammonia offers algal crop protection from predators in dairy wastewater and ammonium-rich media. Bioresour. Technol. 243, pp.724-730.

- Van Dongen, U.G.J.M., Jetten, M.S. and Van Loosdrecht, M.C.M., 2001. The SHARON®-Anammox® process for treatment of ammonium rich wastewater. Water Sci. and Technol. 44(1), 153-160.

- Vargas, G., Donoso-Bravo, A., Vergara, C. and Ruiz-Filippi, G., 2016. Assessment of microalgae and nitrifiers activity in a consortium in a continuous operation and the effect of oxygen depletion. Electron. J. Biotechnol. 23, 63-68.

- Vergara, C., Muñoz, R., Campos, J.L., Seeger, M. and Jeison, D., 2016. Influence of light intensity on bacterial nitrifying activity in algal-bacterial photobioreactors and its implications for microalgae-based wastewater treatment. Int. Biodeterior. Biodegrad, 114, 116-121.

- Virdis, B., Rabaey, K., Rozendal, R.A., Yuan, Z. and Keller, J., Simultaneous nitrification, denitrification and carbon removal in microbial fuel cells, Water Res. 44 (2010) 2970-2980.

- Wang, M., Yang, H., Ergas, S.J. and van der Steen, P., 2015. A novel shortcut nitrogen removal process using an algal-bacterial consortium in a photo-sequencing batch reactor (PSBR). Water Res. 87, 38-48.
- Wang, M., Yang, H., Ergas, S.J. and van der Steen, P., A novel shortcut nitrogen removal process using an algal-bacterial consortium in a photo-sequencing batch reactor (PSBR), Water Res. 87 (2015) 38-48.
- Wang, X., Feng, Y., Liu, J., Lee, H., Li, C., Li, N. and Ren, N., Sequestration of $CO_2$ discharged from anode by algal cathode in microbial carbon capture cells (MCCs), Biosens Bioelectron. 25 (2010) 2639-2643.
- Wang, Y., Ho, S.H., Cheng, C.L., Guo, W.Q., Nagarajan, D., Ren, N.Q., Lee, D.J. and Chang, J.S., 2016. Perspectives on the feasibility of using microalgae for industrial wastewater treatment. Bioresour. Technol. 222, 485-497.
- Wu, YC., Wang, ZJ., Zheng, Y., Xiao, Y., Yang, ZH. and Zhao, F.,Light intensity affects the performance of photo microbial fuel cells with Desmodesmus sp. A8 as cathodic microorganism, Appl Energy. 116 (2014) 86-90.
- Xiao, L., Young, EB., Berges, JA. and He, Z., Integrated photo-bioelectrochemical system for contaminants removal and bioenergy production, Environ Sci Technol. 46 (2012) 11459-11466.
- Xie, B., Gong, W., Tang, X., Bai, L., Guo, Y., Wang, J., Zhao, J., Fan, Y., Li, G. and Liang, H., 2019. Blending high concentration of anaerobic digestion effluent and rainwater for cost-effective Chlorella vulgaris cultivation in the photobioreactor. Chem. Eng. J, 360, 861-865.

- Yadav, G., Sharma, I., Ghangrekar, M. and Sen, A., live bio-cathode to enhance power output steered by bacteria-microalgae synergistic metabolism in microbial fuel cell. J. Power Sources. 449 (2020) 227560.
- Yan, Z., Liu, K., Yu, H., Liang, H., Xie, B., Li, G., Qu, F. and van der Bruggen, B., 2019. Treatment of anaerobic digestion effluent using membrane distillation: Effects of feed acidification on pollutant removal, nutrient concentration and membrane fouling. Desalination, 449, 6-15.
- Yang, Y., Li, X., Yang, X. and He, Z., Enhanced nitrogen removal by membrane-aerated nitritation-anammox in a bioelectrochemical system, Bioresour. Technol. 238 (2017) 22-29.
- Yang, Z., Nie, C., Hou, Q., Zhang, L., Zhang, S., Yu, Z. and Pei, H., 2019. Coupling a photosynthetic microbial fuel cell (PMFC) with photobioreactors (PBRs) for pollutant removal and bioenergy recovery from anaerobically digested effluent. Chem. Eng J. 359, 402-408.
- Zhang, F. and He, Z., 2012. Integrated organic and nitrogen removal with electricity generation in a tubular dual-cathode microbial fuel cell. Process Biochem. 47(12), 2146-2151.
- Zhu, C., Wang, H., Yan, Q., He, R. and Zhang, G., Enhanced denitrification at biocathode facilitated with biohydrogen production in a three-chambered bioelectrochemical system (BES) reactor, Chem. Eng. J. 312 (2017) 360-366.
- Zheng, X., Wu, R. and Chen, Y., Effects of ZnO nanoparticles on wastewater biological nitrogen and phosphorus removal. Environ. Sci. Technol. 45 (2011) 2826-2832

.

# List of publications

- **Book chapters**

1. Ramasamy, S., Arun, S. and Pakshirajan K., An overview of algal photobioreactors for resource recovery from waste. In Bioreactors (pp. 215-248). Elsevier.

- **Publications in international journals**

1. Arun, S., Manikandan, N.A., Pakshirajan, K. and Pugazhenthi, G., 2019. Novel shortcut biological nitrogen removal method using an algae-bacterial consortium in a photo-sequencing batch reactor: Process optimization and kinetic modelling. Journal of environmental management, 250, p.109401.
2. Arun, S., Sinharoy, A., Pakshirajan, K. and P.N.L. Lens., 2020.Algae based microbial fuel cells for wastewater treatment and recovery of value added products. Journal of renewable and sustainable reviews,132, p.110041.
3. Arun, S., Ramasamy, S., Pakshirajan, K. and Pugazhenthi G., 2020. Shortcut nitrogen removal and bioelectricity production by microalgae-bacterial consortia using an integrated membrane photosynthetic microbial fuel cell. Journal of environmental management. Under revision.
4. Arun, S., Ramasamy, S., and Pakshirajan, K., Nitrogen source competition among nitrification by microalgae-bacterial consortia in photo-sequencing batch reactor. Science of the Total Environment. Submitted.
5. Arun, S. and Pakshirajan, K., Effect of different light intensity on ammonium removal by microalgae-nitrifying consortia in photo-sequencing batch reactor, Journal of Cleaner Production. Under revision.

- **Presentation in international/national conferences**

1. Arun, S. and Pakshirajan, K., 'Photo-oxygenation for biological nitrogen removal from ammonium rich wastewater using algae-bacterial consortium' Reflux 2016, 25-27th March, IIT Guwahati.

2. Arun, S. and Pakshirajan, K., 'Algae based photo-activated sludge system for nitrogen removal from ammonium rich wastewater using photo sequencing bioreactor.' RACEEE-2017, 27-28 February, SSN college of engineering.

3. Arun, S. and Pakshirajan K., 'Enhanced Algae based biological nitrogen removal in a photosequencing batch reactor with an algae enriched ammonium oxidizing bacteria and methanol utilizing denitrifiers.' ICBFC-2019, 12-13 September, Annamalai university.

4. Arun, S. and Pakshirajan, K., 'Enhanced microalgae-bacterial consortium for biological nitrogen removal in a photosequencing batch reactor.' ICBFC-2018, 15-17 March, VIT vellore.

5. Arun, S. and Pakshirajan, K., 'Novel shortcut biological nitrogen removal method using an algae-bacterial consortium in a photo-sequencing batch reactor: Process optimization and kinetic modelling.' CESE-2018, 4-8 November, Bangkok, Thailand.

- **Manuscripts under preparation**

1. Arun, S., Sinharoy, A., Pakshirajan, K., Pugazhenthi, G. and P.N.L. Lens., 2020. Microalgae-bacterial consortia for advanced nitrogen removal: A review

# Appendix A

**Determination of $NH_4^+$-N metabolism:**

A nitrogen mass balance was utilized to determine the metabolism of $NH_4^+$ during the start phase and BNR phase, as described in **Figure A1**. The input rate of N($N_{influent}$) was based on the influent flow rate and $NH_4^+$-N concentration. N removal is based on :1) uptake due to algae, AOB and MUD ($N_{uptake}$); 2) volatilization of $HNO_2$, $NH_3$and $HNO_3$ ($N_v$); 3) denitritation products ($N_2O$ and $N_2$; $N_d$) and 4) effluent N ($N_{effluent}$). Denitritation products were determined by the following equation (A1)

$$N_d = N_{influent} - N_{uptake} - N_v - N_{effluent} \quad (A1)$$

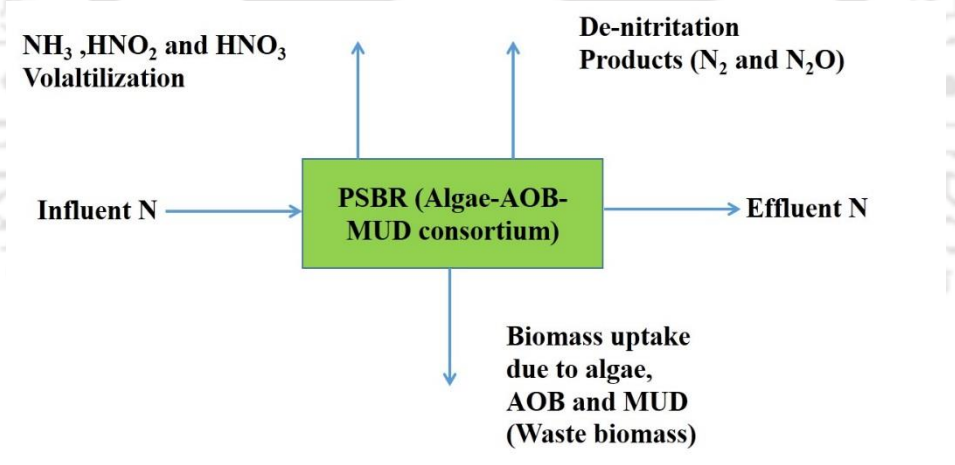


**Fig. A1-** Nitrogen mass balance due to algae-AOB-MUD consortium in the PSBR

**Determination of various input parameters**

$N_{influent}$ and effluent $N_{effluent}$

$N_{influent}$wascalculated based on the product of $NH_4^+$-N in the feed and the influent flow rate. $N_{effluent}$ was calculated from the product of concentrations of $NH_4^+$-N, $NO_3^-$-N and $NO_2^-$-N in the effluent and the effluent flow rate.

**Biomass uptake ($N_{uptake}$)**

Daily N uptake by biomass comprising of algae, AOB and MUD was determined by multiplying the daily volume of wasted liquor, total suspended solids (TSS) concentration and measured nitrogen/TSS ratio:

$$N_{uptake} = V_{wL} \cdot TSS_R \cdot f_N \qquad (A2)$$

where $V_w$ is the daily volume of wasted mixed liquor ($0.10\ L\ d^{-1}$); $TSS_R$ is the total suspended solids concentration of the mixed liquor ($mg\ L^{-1}$); $f_N$ is the measured nitrogen/TSS ratio (dimensionless).

**Ammonia volatilization ($N_a$)**

The equilibrium between ammonium and ammonia is significantly affected by pH and it is expressed in the following equation (A3)

$$NH_4^+ + OH^- \rightleftharpoons NH_3 + H_2O \quad K_{i\ (ammonia)}\ (30°C)\ (A3)$$

$$K_i = \frac{[NH_4^+][OH^-]}{[NH_3]} = 1.810 \times 10^{-5}\ (A4)$$

where, $K_i$ is the ionic equilibrium constant for ammonia.

Mass transfer coefficient of ammonia in liquid anaerobically digested swine manure was reported by Wang et al. (2015) as follows (equation A4)

$$\frac{d\,M_{TAN}}{d\,t} = K_{OL}A_0([NH_3]_L - [NH_3]_{Air})\ (A5)$$

Where $M_{TAN}$ is the mass of total dissolved ammonia (mg); $K_{OL}$ is the overall mass transfer coefficient of dissolved ammonia ($1.5 \times 10^{-4} m\ s^{-1}$); $A_0$ is the interfacial surface area

($2.83 \times 10^{-3} m^2$); $[NH_3]_L$ is the concentration of dissolved ammonia in the liquid (mg $L^{-1}$) and $[NH_3]_{Air}$ is the concentration of ammonia in the air (assumed to be 0 mg $L^{-1}$). Integration of Eq. 4 yields the overall quantity of ammonia volatilized as given by equation (A5):

$$N_a = \int K_{OL}\, A_0([NH_3]_L - [NH_3]_{Air})\, dt \qquad (A5)$$

The calculation was carried out for 81 days time period i.e when ammonium pH of 7.51 was observed during the start-up phase of PSBR. Based on this calculation, the free ammonia nitrogen volatilization rate was estimated to be less than 0.014 mg $d^{-1}$, which was negligible compared with other nitrogen conversion pathways in this study and hence, the free ammonia nitrogen volatilization was neglected for this study.

**Nitric acid and nitrous acid volatilization**

The equilibrium between nitrite anion and nitrous acid is also affected by pH as depicted in equation (A7)

$$NO_2^- + H^+ \rightleftharpoons HNO_2 K_a\ (30°C \quad (A7)$$

$$K_a = \frac{[NO_2^-][H^+]}{[HNO_2]} = 4.5 \cdot 10^{-4} \qquad (A8)$$

where, $K_a$ is the ionic equilibrium constant for nitrous acid.

Using extreme values of the parameters pH=7.51 and $NO_2^-$-N concentration 200 mg $L^{-1}$, maximum $HNO_2$-N concentration in the PSBR was found to be 0.015 mg $L^{-1}$. Although the mass transfer coefficient is unknown and given the low amount concentration of $HNO_2$ formed in this study, its volatilization rate was neglected.

**Metabolism of ammonium**

Based on the nitrogen balance equations detailed earlier, the nitrogen input and output averaged over each phase of the PSBR are presented in Table A1. Percentages are shown in Table 3 of the chapter 3.

**Table A1.** Nitrogen mass balance in the start-up and BNR phase (mg N $d^{-1}$)

| Phase | Nitrogen Input (mg N $d^{-1}$) | Nitrogen Output (mg N $d^{-1}$) | | | | |
|---|---|---|---|---|---|---|
| | | Effluent-$NH_4^+$-N | Effluent-$NO_2^-$-N | Effluent-$NO_3^-$-N | Biomass uptake | Denitritation |
| **Start-up phase** | 71.9 | 2.15 | 54.7 | 1.02 | 12.14 | 0.89 |
| **BNR phase** | 112.26 | BDL | BDL | BDL | 20.43 | 92.18 |

**Bio-kinetic modeling of nitrogen removal**

Four metabolic models, model 1, model 2, model 3 and model 4 were implemented in Aquasim (Switzerland) (Reichert,1998) 2.1 to understand on interaction of algae-AOB, algae-AOB-NOB, algae-AOB-MUD and algae-AOB-MUD with methanol addition at the beginning of the light period for BNR in the PSBR. Fig.A2 shows schematic of different pathways involved in $NH_4^+$oxidation, $NO_2^-$ oxidation and $NO_2^-$ reduction in the algae-bacterial consortium which formed the basis of the different models formulated in this study for describing the kinetics of nitrogen removal in this study.

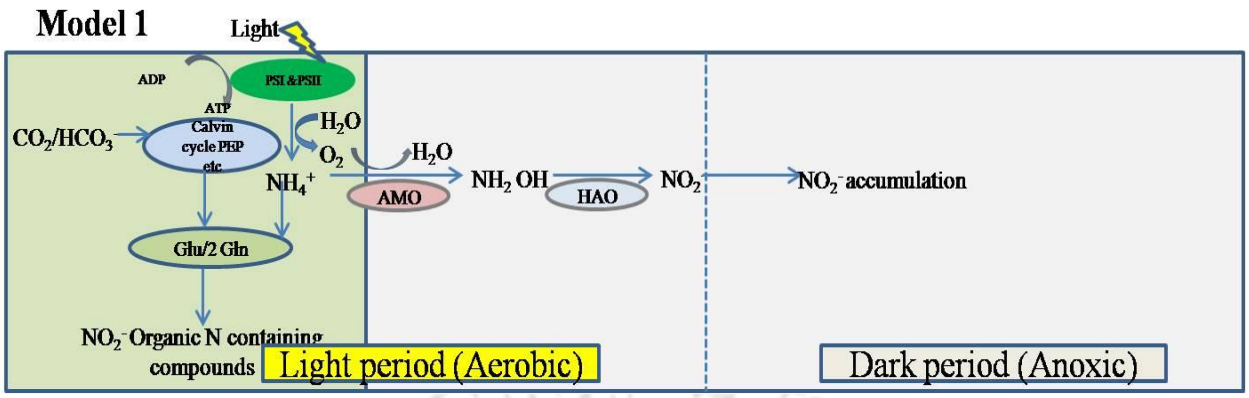


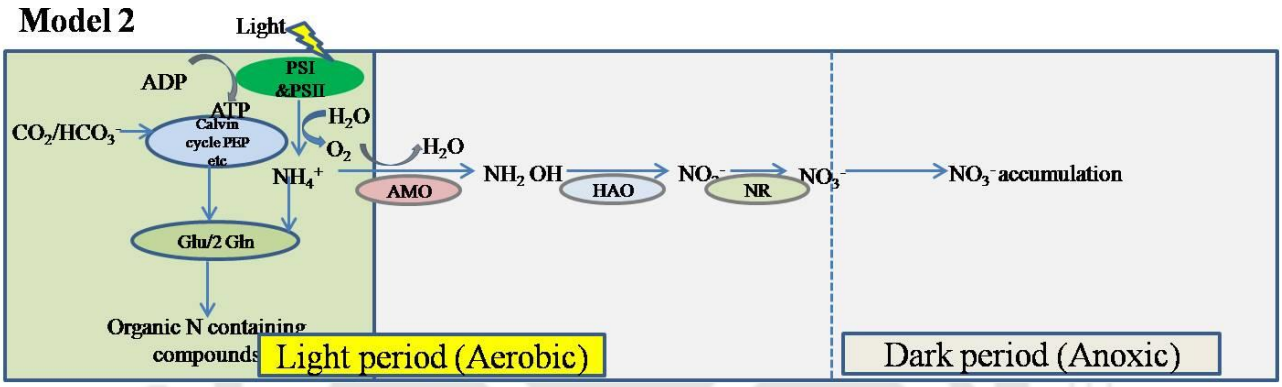


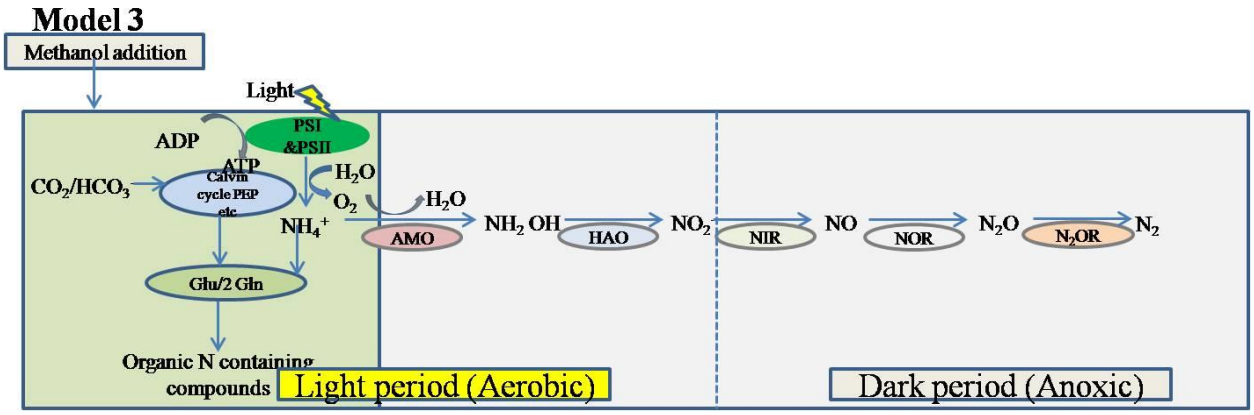

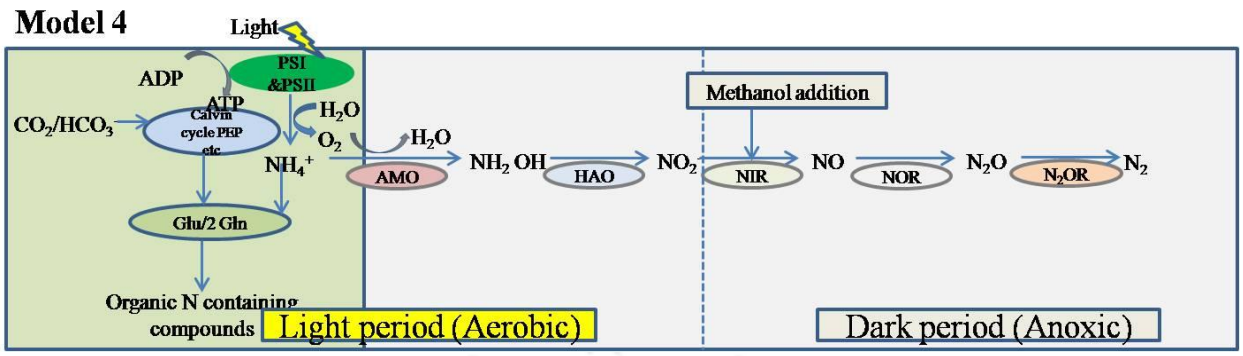


**Fig. A2-**Reaction schemes used in the four algae-bacterial models evaluated in this study: (1) Model 1-algae-AOB pathway; (2) Model 2-algae-AOB-NOB pathway; (3) Model 3-algae-AOB-MUD pathway; (4) Model 3-algae-AOB-MUD pathway with methanol addition at the beginning of the light period.

Components of Model 4, presented in Table A2, are based on the production of $O_2$, uptake of $NH_4^+$, oxidation of $NH_4^+$, reduction of $NO_2^-$. The main features of Model 4 are 1) $NH_4^+$ and $HCO_3^-$ uptake by algae in the presence of light, 2) oxidation of $NH_4^+$into $NO_2^-$ by AOB, 3) reduction of $NO_2^-$ into $N_2$ gas by MUD. This differentiates model 4 from the other models (1, 2 and 3) do not consider $NO_2^-$ reduction by MUD. Model 1 and 3 estimate $NO_2^-$ production from enzymatic oxidation of $NH_4^+$ whereas model 2 estimates $NO_3^-$ production from enzymatic oxidation of $NH_4^+$ and $NO_2^-$.

**Table A2.** Process matrices for the four metabolic models evaluated in this study

**Model 1**

| Model component | 1 | 2 | 3 | 4 | 5 | 6 | 7 | Process rate |
|---|---|---|---|---|---|---|---|---|
| | $X_A$ g COD / $m^3$ | $X_{AOB}$ g COD/ $m^3$ | $S_{HCO_3}$ g $HCO_3^-/m^3$ | $S_{PO_4}$ g $PO^-_4$−P / $m^3$ | $S_{NH_4}$ g $NH^+_4$ − N/ $m^3$ | $S_{NO_2}$ g $NO^-_2$ − N/ $m^3$ | $S_{O_2}$ g $O_2$ /$m^3$ | |
| 1.Algae growth on $NH_4$ and $HCO_3$ and $PO_4$ and light intensity | 1 | | $-\frac{1}{Y_{HCO_3}}$ | $-\frac{1}{Y_{PO_4}}$ | $-\frac{1}{Y_{NH_4}}$ | | $Y_{O_2}$ | $\mu_{max,A}\left(\frac{S_{NH_4}}{K_{NH_4,A}+S_{NH_4}}\right)\left(\frac{S_{HCO_3}}{K_{HCO_3,A}+S_{HCO_3}}\right)\left(\frac{S_{PO_4}}{K_{PO_4,A}+S_{PO_4}}\right)\left(\frac{I}{K_I+I}\right)X_A$ |
| 2. Algae decay | -1 | | | | | | | $b_A X_A$ |
| 3.AOB growth | | | | | $-i_{N,BM}-\frac{1}{Y_{AOB}}$ | $\frac{1}{Y_{AOB}}$ | $-\frac{3.43-Y_{AOB}}{Y_{AOB}}$ | $\mu_{max,AOB}\frac{S_{O_2}}{K_{O_2,AOB}+S_{O_2}}\frac{S_{NH_4}}{K_{NH_4,AOB}+S_{NH_4}}X_{AOB}$ |
| 4. Bacteria decay of AOB | | | | | $-i_{Xbac}$ | | | $b_{AOB}X_{AOB}$ |
| 5.Transfer $O_2$ | | | | | | | 1 | $K_{\mathrm{L}}a_{o2}(S_{o2^*-S_{o2}})$ |

**Model 2**

| Model component | 1 | 2 | 3 | 4 | 5 | 6 | 7 | 8 | 9 | Process rate |
|---|---|---|---|---|---|---|---|---|---|---|
| | $X_A$ g COD / $m^3$ | $X_{AOB}$ g COD / $m^3$ | $X_{NOB}$ g COD / $m^3$ | $S_{HCO_3}$ g $HCO_3^-$ /$m^3$ | $S_{PO_4}$ g$PO^-_4$−P /$m^3$ | $S_{NH_4}$ g $NH^+_4$ − N/ $m^3$ | $S_{NO_2}$ g $NO^-_2$ − N/$m^3$ | $S_{NO_3}$ g $NO^-_3$ − N/$m^3$ | $S_{O_2}$ g $O_2$ /$m^3$ | |
| 1.Algae growth on $NH_4$ and,$HCO_3$ and $PO_4$ and light intensity | 1 | | | $-\frac{1}{Y_{HCO_3}}$ | $-\frac{1}{Y_{PO_4}}$ | $-\frac{1}{Y_{NH_4}}$ | | | $Y_{O_2}$ | $\mu_{max,A}\left(\frac{S_{NH_4}}{K_{NH_4,A}+S_{NH_4}}\right)\left(\frac{S_{HCO_3}}{K_{HCO_3,A}+S_{HCO_3}}\right)\left(\frac{S_{PO_4}}{K_{PO_4,A}+S_{PO_4}}\right)\left(\frac{I}{K_I+I}\right)X_A$ |
| 2. Algae decay | -1 | | | | | | | | | $b_A X_A$ |

| | | | | | | | | | | |
|---|---|---|---|---|---|---|---|---|---|---|
| **3.AOB growth** | | | | | $-i_{N,BM}$ $-\frac{1}{Y_{AOB}}$ | $\frac{1}{Y_{AOB}}$ | | $-\frac{3.43-Y_{AOB}}{Y_{AOB}}$ | $\mu_{max,AOB}\frac{S_{O_2}}{K_{O_2,AOB}+S_{O_2}}\frac{S_{NH_4}}{K_{NH_4,AOB}+S_{NH_4}}X_{AOB}$ |
| **4. Bacteria decay of AOB** | | −1 | | | $-i_{X,AOB}$ | | | | $b_{AOB}X_{AOB}$ |
| **4.NOB growth** | | | | | $-i_{N,BM}$ | $-\frac{1}{Y_{NOB}}$ | $\frac{1}{Y_{NOB}}$ | $-\frac{1.14-Y_{NOB}}{Y_{NOB}}$ | $\mu_{max,NOB}\frac{S_{O_2}}{K_{O_2,NOB}+S_{O_2}}\frac{S_{NO_2}}{K_{NO_2,AOB}+S_{NO_2}}\frac{K_{I,NH_4}}{K_{I,NH_4}+S_{NH_4}}X_{NOB}$ |
| **4. Bacteria decay of NOB** | | | −1 | | | | | | $b_{NOB}X_{NOB}$ |
| **5.Transfer $O_2$** | | | | | | | | 1 | $K_{\mathrm{L}}a_{o2}(S_{o2^*-S_{o2}})$ |

**Models 3 and 4**

| **Model component** | **1** | **2** | **3** | **4** | **5** | **6** | **7** | **8** | **9** | **Process rate** |
|---|---|---|---|---|---|---|---|---|---|---|
| **Process** | $\mathbf{X_A}$ **g COD / m³** | $\mathbf{X_{AOB}}$ **g COD /m³** | $\mathbf{X_H}$ **g COD / m³** | $\mathbf{S_{HCO_3}}$ **g $HCO_3^-$ /m³** | $S_{PO_4}$ **g$PO^-{}_4$−P / m³** | $\mathbf{S_{NH_4}}$ **g $NH^+{}_4$ − N/ m³** | $\mathbf{S_{NO_2}}$ **g $NO^-{}_2$ − N /m³** | $\mathbf{S_{O_2}}$ **g $O_2$ /m³** | $\mathbf{S_{N_2}}$ **g $N_2$/m³** | |
| **1.Algae growth on $NH_4$ and,$HCO_3$,$PO_4$ and light intensity** | 1 | | | $-\frac{1}{Y_{HCO_3}}$ | $-\frac{1}{Y_{PO_4}}$ | $-\frac{1}{Y_{NH_4}}$ | | $Y_{O_2}$ | | $\mu_{max,A}\left(\frac{S_{NH_4}}{K_{NH_4,A}+S_{NH_4}}\right)\left(\frac{S_{HCO_3}}{K_{HCO_3,A}+S_{HCO_3}}\right)\left(\frac{S_{PO_4}}{K_{PO_4,A}+S_{PO_4}}\right)\left(\frac{I}{K_I+I}\right)X_A$ |
| **2. Algae decay** | -1 | | | | | | | | | $b_AX_A$ |
| **3.AOB growth** | | | | | | $-i_{N,BM}-\frac{1}{Y_{AOB}}$ | $\frac{1}{Y_{AOB}}$ | $-\frac{3.43-Y_{AOB}}{Y_{AOB}}$ | | $\mu_{max,AOB}\frac{S_{O_2}}{K_{O_2,AOB}+S_{O_2}}\frac{S_{NH_4}}{K_{NH_4,AOB}+S_{NH_4}}X_{AOB}$ |
| **4. Bacteria decay of AOB** | | −1 | | | | $-i_{X,AOB}$ | | | | $b_{AOB}X_{AOB}$ |
| **5.Anoxic growth on nitrite** | | | | | | $-i_{N,BM}$ | $-\frac{1-Y_{H,NOx}}{1.71\cdot Y_{H,NOx}}$ | | $\frac{1-Y_{H,NOx}}{1.71\cdot Y_{H,NOx}}$ | $\mu_{max,H}\eta_H\frac{K_{I,O_2}}{K_{I,O_2}+S_{O_2}}\frac{S_{NH_4}}{K_{NH_4,H}+S_{NH_4}}\frac{X_{STO}/X_H}{K_{STO}+(X_{STO}/X_H)}\frac{S_{NO_2}}{K_{NO_2,H}+S_{NO_2}}X_H$ |
| **6. Bacteria decay of heterotrophs** | | | −1 | | | | | | | |
| **7.Transfer $O_2$** | | | | | | | 1 | | | $K_{\mathrm{L}}a_{o2}(S_{o2^*-S_{o2}})$ |

# Appendix B

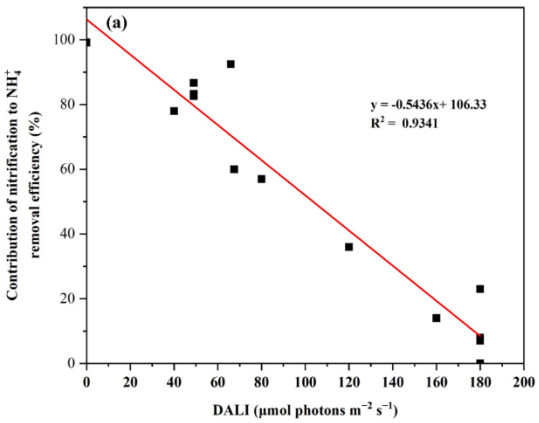


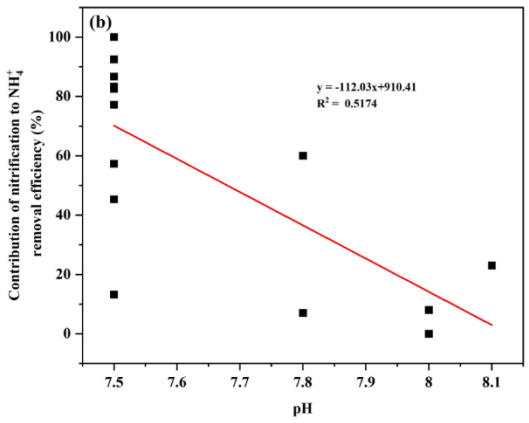


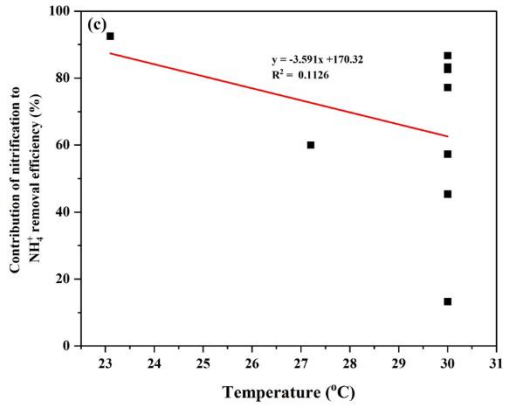


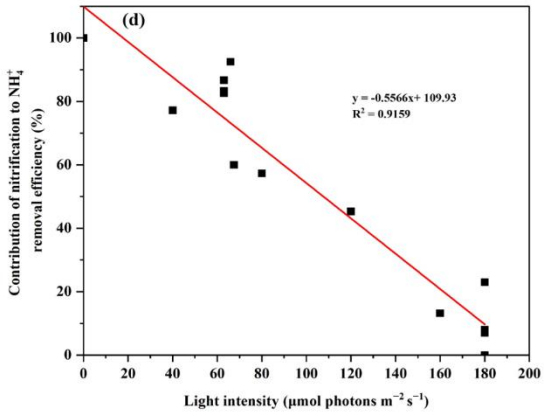


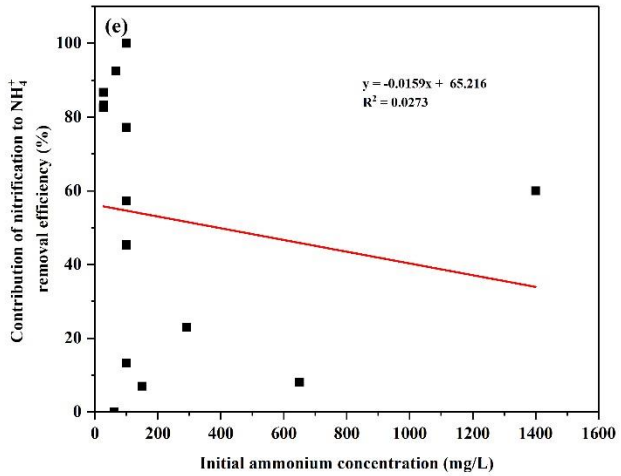

**Fig. B1.** Relationship between ammonium removal and possible parameters controlling the ammonium removal: (a) DALI, (b) pH, (c) temperature, (d) light intensity, and (e) initial ammonium concentration

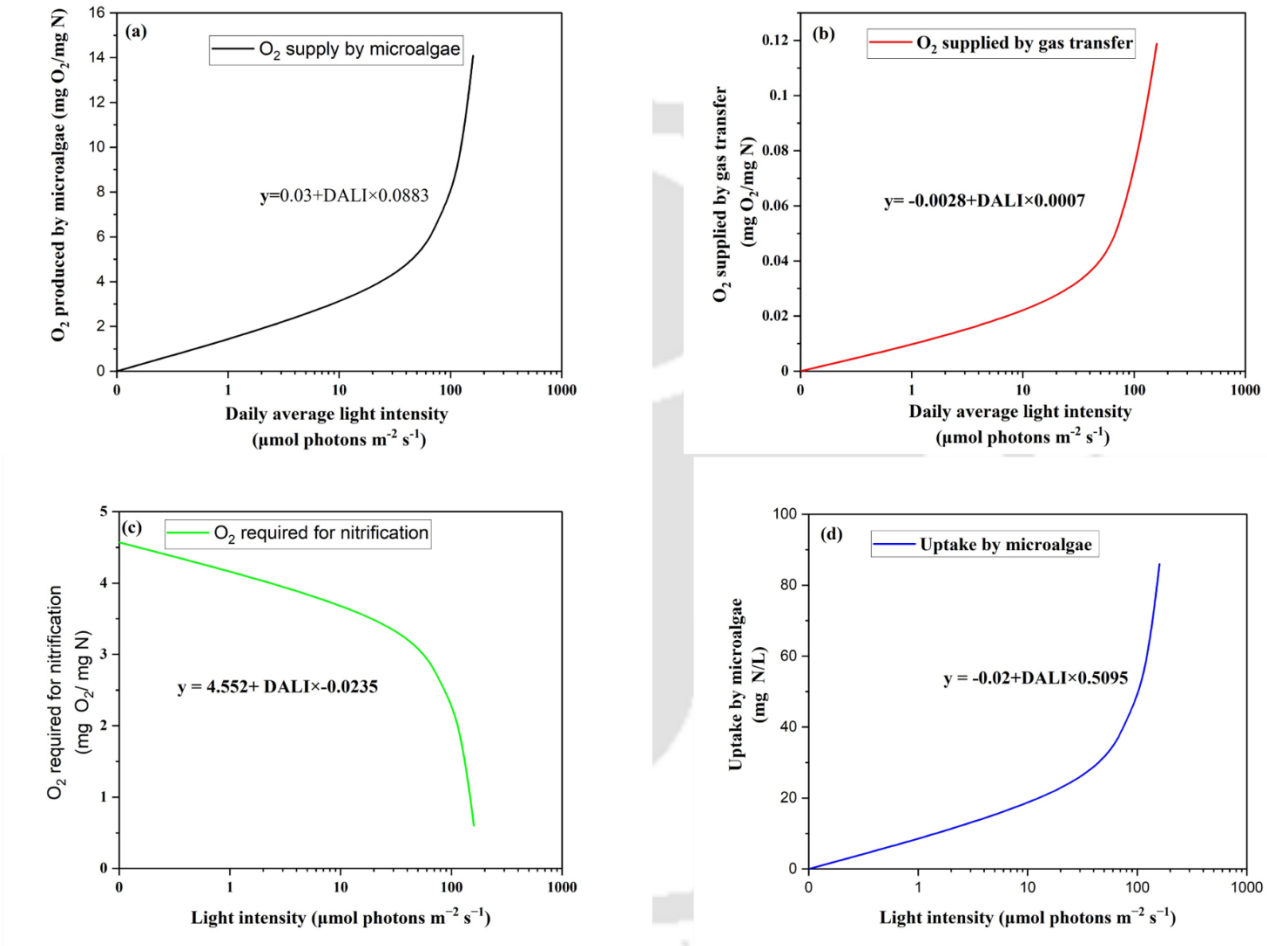


**Figure B2.** Relationship between total $O_2$ required for nitrification, oxygen produced by microalgae, oxygen supplied by gas transfer and microalgal uptake

**Table B1.** Simple cost estimation of the microalgae-bacteria based bioprocess system developed in this work for ammonium removal and its comparison with microalgae system

| **Items** | **Cost** | |
|---|---|---|
| **Amortization cost (a)** | **Microalgae system** | **Microalgae-bacterial system** |
| Construction (US$) | 97333 | 97333 |
| Piping and fittings (US$) | 14291 | 14291 |
| Electrical (US$) | 11232 | 6178 |
| Mechanical (US$) | 91606 | 50384 |
| Footprint (US$) | 35358 | 35358 |
| **Operation and maintenance costs (b)** | | |
| Reagent (US$/year) | 5813 | 5813 |
| Electricity consumption (US$/year) | 9216 | 5069 |
| Pump and mixing (US$/year) | 9104 | 6373 |
| Staff (US$/year) | 1821 | 1871 |
| Maintenance cost (US$/year) | 3747 | 1799 |
| **Total (a+b)** | ~$**279521** | ~$**224469** |